INFORMATION TO USERS

This manuscript has been reproduced from the microfilm master. UMI films the text directly from the original or copy submitted. Thus, some thesis and dissertation copies are in typewriter face, while others may be from any type of computer printer.

The quality of this reproduction is dependent upon the quality of the copy submitted. Broken or indistinct print, colored or poor quality illustrations and photographs, print bleedthrough, substandard margins, and improper alignment can adversely affect reproduction.

In the unlikely event that the author did not send UMI a complete manuscript and there are missing pages, these will be noted. Also, if unauthorized copyright material had to be removed, a note will indicate the deletion.

Oversize materials (e.g., maps, drawings, charts) are reproduced by sectioning the original, beginning at the upper left-hand corner and continuing from left to right in equal sections with small overlaps. Each original is also photographed in one exposure and is included in reduced form at the back of the book.

Photographs included in the original manuscript have been reproduced xerographically in this copy. Higher quality 6" x 9" black and white photographic prints are available for any photographs or illustrations appearing in this copy for an additional charge. Contact UMI directly to order.

UMI

A Bell & Howell Information Company
300 North Zeeb Road, Ann Arbor MI 48106-1346 USA
313/761-4700 800/521-0600

Université d'Ottawa · University of Ottawa

Buckling of Broad, Anchored, Cylindrical Liquid-Storage Tanks Subjected to Horizontal Ground Motion

by

Tony Boutros

Thesis submitted to the School of Graduate Studies
as partial fulfillment of the requirements
for the degree of M.A.Sc. in
Mechanical Engineering

University of Ottawa

ABSTRACT

The study of the seismic response of broad, anchored, cylindrical liquid-storage tanks has large practical significance because these structures are used in many critical engineering applications (petroleum industries, nuclear power stations, municipal water supply systems, wine industries...). The performance of such tanks during recent earthquakes and in experiments has indicated that the existing codes for designing tanks are in need of improvement.

Due to the complexity of the dynamic analysis, several researchers have used a static approach to predict the dynamic buckling load. It has been demonstrated that such a static analysis yields useful information. On the basis of this finding, an approximate analytical method is developed to study the buckling of broad, anchored, cylindrical liquid-storage tanks subjected to horizontal ground motion. The solution is based on the linearized Donnell's shell stability equations and Galerkin's approach. The smallest buckling load (or the critical load factor) is calculated using the inverse iteration method. Theoretical results are then determined for two cases of broad tanks presented as examples. The validity of the findings of the present work is checked through comparison with results obtained by the numerical Finite Element Method (FEM).

ACKNOWLEDGMENT

The author wishes to express his gratitude to Dr. D. Redekop for his continuous encouragement, invaluable suggestions, and patient guidance throughout the research.

Special thanks to the author's family and fiancée for their moral support and encouragement during the study.

The financial support received from the University of Ottawa is gratefully acknowledged.

Contents

List of Figures

List of Tables

Nomenclature

D	bending stiffness parameter =
E	Young's modulus of elasticity
F	stress function
G	pseudo-acceleration
g	gravity acceleration
K	stiffness matrix
L	length of the cylinder
M	mass matrix
M_x, M_φ, $M_{x\varphi}$, $M_{\varphi x}$	bending and twisting moment
N_x, N_φ, $N_{x\varphi}$, $N_{\varphi x}$	normal and shearing force intensities
Q_x, Q_φ	transverse shear force intensities
r	radius of the cylinder
t	thickness of the cylinder
u, v, w	displacement components in the x, φ, z directions respectively
x, φ, z	coordinate system (analytical solution)
X, Y, Z	Cartesian coordinates (FEM)
ε_x, ε_φ, $\gamma_{x\varphi}$	strain components
ν	Poisson ratio
ς	$=\frac{x}{r}$
ρ_l	density of the liquid
λ	load factor

$$\frac{\partial(\ )}{\partial \varsigma} = (\ )'$$

$$\frac{\partial(\ )}{\partial \varphi} = (\ )^{\bullet}$$

Chapter 1

Introduction

1.1 Shell Types in Structural Engineering

Shells may be divided into different groups according to the shape of their middle surface [1]. One can distinguish between shells of revolution, translational shells, skew shells, rectangular shells, and cylindrical shells.

Circular cylindrical shells are used extensively as liquid-storage tanks in the petroleum industry as well as in municipal water supply systems. These structures are efficient because they carry the hydrostatic pressure caused by their contents mostly through membrane stresses.

Liquid-filled cylindrical tanks can be characterized by their height-to-radius ratio. For a ratio less or greater than 1.5, a tank is named broad or tall respectively. Also, depending on its base fixity, a tank is classified as anchored (fixed base) (Fig 1.1) or unanchored (free base) [2]. In the present study broad, anchored, cylindrical liquid-storage tanks are examined.

1.2 Definition of Problem

Any structural member has two kinds of stiffness: membrane stiffness and bending stiffness. The membrane stiffness is in general "several orders of magnitude greater" than the bending stiffness. A thin shell can absorb a great deal of membrane strain energy without deforming excessively. It must deform much more in order to absorb an equivalent amount of bending strain energy. If the shell is loaded in such a way that most of its strain energy is in the form of membrane compression, and if there is a way that this stored-up membrane energy can be converted into bending energy, the shell may fail in a process called *buckling* [3].

Broad, anchored, cylindrical liquid-filled storage tanks have been damaged during recent earthquakes [4,5,6]. This may lead to loss of contents, which apart from the economical losses can result in dangerous consequences. Therefore, existing codes for designing tanks [7] are in need of improvement.

Buckling of such tanks is suspected to be due primarily to the horizontal component of the ground motion [8]. Under normal conditions, the stresses in the tank wall are dominated by the hoop stress due to the hydrostatic pressure (Fig. 1.2). During ground motion, an additional fluid pressure is caused by the motion of the tank. This hydrodynamic pressure can be expressed according to Veletsos and Malhotra [2] by the sum of two components:

1. "an impulsive component which represents the effect of the part of the liquid that may be considered to move in synchronism with the tank wall as a rigid mass" and,
2. "a convective component which represents the effects of the part of contained liquid undergoing a sloshing motion".

Further, the contribution of the convective component of the response is usually small and can be neglected. Also, for relatively broad tanks the contribution of higher impulsive modes of vibration to the response can also be ignored [9]. Under these conditions, the dynamic pressure depends on the amplitude of the horizontal ground acceleration and varies along the length of the tank as well as in the circumferential direction. In the latter case the pressure varies as $\cos\theta$ [10] (Fig. 1.3). Consequently, at a critical acceleration it happens that the tank buckles as it exchanges its membrane strain energy for bending strain energy.

1.3 Methods of Solution

Several authors have studied experimentally and theoretically the buckling of broad, anchored, cylindrical liquid-filled storage tanks under earthquake motion. Experimental studies are very expensive and have shown some weakness in characterizing accurately the buckling of such tanks. But on the other hand, they are very useful to verify some engineering concepts and to improve design criteria.

Theoretical studies are divided into two groups: numerical and analytical. Due to the cost and time consumption of the numerical study, an analytical solution is preferable. However, a numerical solution is very effective when complicated geometries and boundary conditions are involved.

Static and dynamic buckling of liquid-storage tanks have been examined analytically. Dynamic analyses have shown a high degree of complexity due to several factors such as liquid sloshing, shell flexibility, soil/structure interaction, ... [11]. For these reasons, several researchers (e.g. Natsiavas and Babcock [12]) have analyzed the buckling behavior of liquid-

filled tank models using a static approach. In this approach the maximum value of pressure induced by dynamic and static loading was considered. The practical validity of this method was confirmed experimentally by Nagashima et al. [13], who have shown that a static buckling evaluation can be applied to predict buckling caused by horizontal (or vertical) excitation.

The objective of this work is to develop an approximate static, analytical method to study the buckling of broad, anchored, cylindrical liquid-storage tanks subjected to horizontal ground motion.

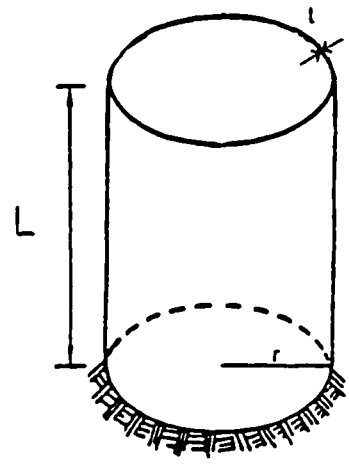

Figure 1.1: Geometry of a cylindrical anchored tank.

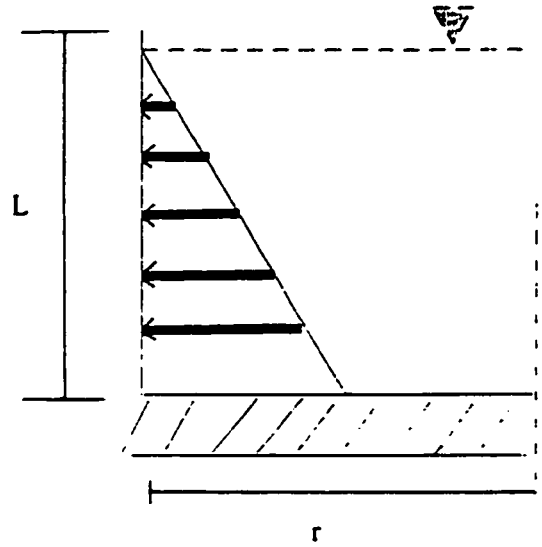

Figure 1.2: Variation of the hydrostatic pressure in the axial direction.

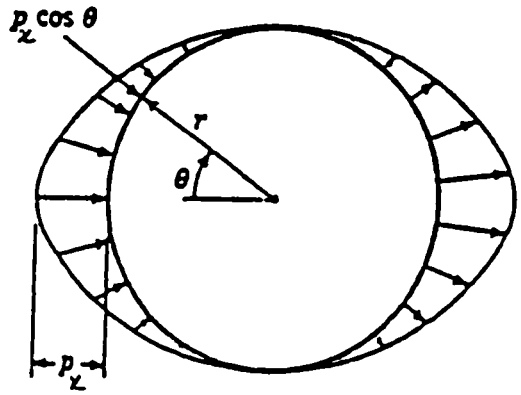

Figure 1.3: Variation of the hydrodynamic pressure in the circumferential direction.

Chapter 2

Literature Survey

2.1 Previous Work

Anchored, broad, cylindrical tanks subjected to lateral loads can buckle in two modes: shear and bending. Not many researchers were aware at first that shear buckling exists. Many studies have been conducted to verify this fact in recent years. Studies have been performed theoretically and experimentally to understand how and why buckling occurs in such structures.

Several researchers (e.g. Niwa and Clough [14]) have used the shaking table test (Figs. 2.1-2.4) to simulate the ground motion and to study different factors affecting the buckling of some chosen tanks. Broad (anchored and unanchored) tanks have been examined under horizontal and vertical accelerations. Bending buckling damage has been observed to be of two types: elephant-foot buckling and diamond-shaped buckling. The bending buckling modes have been observed at the bottom of the tank. Niwa and Clough have found also that the rocking motion in the unanchored tanks can generate large axial compressive stresses in the shell over the narrow contact zone; these cyclic dynamic stresses induce the bending buckle pattern in the tank wall. They have demonstrated that the elephant-foot buckle

mechanism for broad tanks can result from two motions: uplifting and rocking. An extensive experimental evaluation of tank buckling with ground excitation has also been conducted by Shih and Babcock [15]. It basically confirmed the important role of the $\cos\theta$ mode in tank failure. Manos [16] has evaluated the performance of anchored wine tanks during the San Juan, Argentina earthquake. He has shown the effect of the overturning moment on the anchors: "anchors may yield, fracture, or be pulled out". He has explained that the transformation of anchored tanks to unanchored ones induces uplifting and rocking in the system. As a result the possibility of buckling increases. He has discussed the importance of making a good design for the anchors in order to prevent any possible failure.

Buckling and dynamic response of broad, anchored liquid-storage cylindrical tanks subjected to horizontal ground motion have also been studied theoretically by many researchers. Zhou et al. [8] have used Sanders nonlinear thin shell theory and an idealized fluid model to study the elephant-foot buckling failure of anchored, broad tanks under horizontal excitation. Natsiavas and Babcock [12] have used an energy type method to study the shear buckling observed at the top of a fluid-filled anchored tank during base excitation. They have found that energy methods compared with the FEM provide a better insight into the coupling of the various modes during the whole procedure of developing and solving the system equations. Veletsos et al. [2] have shown that the hydrodynamic pressure of an anchored tank subjected to horizontal excitation can be expressed by the sum of two components: "impulsive" and "convective". The contribution of the convective component of the response is usually small and can be neglected [2,10]. For relatively broad tanks, the

contribution of higher impulsive modes of vibration of the response can also be ignored [9]. Hydrodynamic pressures on the wall and base of a broad, anchored tank have been determined [2,10]. Ishida and Kobayashi [17] presented a four degree-of-freedom model for analyzing the rocking response of tanks. Auli et al. [18] presented another approach in which the interaction between the bottom plate, foundation and shell was modeled by placing axial springs around the lower edge of the shell. Several analytical works have also been conducted by Fujita [19], Fisher and Seeber [20], Veletsos and Tang [10], to study the soil effect in the seismic response of anchored tanks. It has been found that the foundation flexibility has significant effects on the impulsive components of the response. Also, it has been shown that the interaction of the liquid with the elastic shell and with the elastic ground yields a system of vibration quite different from those systems which neglect ground elasticity.

Numerical analyses have been used often to provide accurate solutions to buckling problems. Geometrical imperfections can have a major effect on the behavior and buckling of cylindrical liquid storage tanks under lateral seismic action. Such imperfections can not be examined accurately by experimental or analytical studies. Considering that, Kokubo et al. [21] have developed a special purpose FEM program. They have used 8-node isoparametric shell elements to study the effects of four types of geometrical imperfections and combined loading on buckling loads and postbuckling behavior. For short cylindrical shells they have found that shear buckling is dominant. Liu et al. [22] have also analyzed the effect of geometrical imperfection on the dynamic buckling of liquid-filled shell subjected to seismic motion. They have chosen a simple circumferential imperfection pattern to explain the

additional buckling modes encountered in some experiments. The FEM has been used to obtain accurate results. Yi and Natsiavas [23] have presented a FEM model to study the seismic response of liquid-filled tanks. They have discretized the shell structure using cylindrical finite elements. They have included in their study the formulation of the nonlinear base uplift problem and effects due to shell and ground flexibility. Nishino et al. [24] have used the FEM code 'FINAS' (Finite Element Nonlinear Structure Analysis System) to study the dynamic buckling behavior of liquid-filled thin-walled cylindrical tanks. This FEM code was unable to carry out the dynamic buckling analysis at each time step of transient response employing direct integration method. Therefore, they have obtained a static solution for the eigenvalue problem at the time step defining the maximum bending moment and shearing force on bottom end of the shell. The solution has included the fluid-structure interaction. Wunderlich et al. [25] have studied the dynamic behavior of liquid-filled shells of revolution. They have modeled the shell using shell ring elements including non-linear behavior, coupled with isoparametric continuum ring elements and special infinite elements for the soil and isoparametric pressure ring elements for the fluid. They have found that non-linear effects in the soil have lead to different stress distributions in the shell and influenced the plastic collapse of the structure.

Due to the complexity of the dynamic analysis (nonlinearities, soil / structure interaction, sloshing motion, ...) some researchers have used a static approach to obtain an acceptable solution for this dynamic problem. Nagashima et al. [13] have explained three methods for converting seismic loads to static loads: namely, "lateral load buckling tests" [26], in which a

horizontal force is applied on the tank wall; "tilt buckling test", in which buckling is caused by injecting liquids into cylinders in an inclined state; and "centrifugal force buckling tests", which permit liquid-containing cylinders to rotate or swing around. Several researchers (Clough, Niwa, Lundquist, Shih, Babcock,...etc..) have used these methods. They have referred to some earlier studies where buckling of a cantilever shell under a transverse load has been analyzed. The following discussion sheds light on the most well-known static analyses.

Lu [26] studied the buckling of a cantilever shell under transverse end load. He used the prebuckling membrane stresses obtained by beam theory, but he disregarded boundary conditions. This solution has considered only cylinders of moderate or large length (L/R>4). Schroeder [27] presented a solution for the elastic buckling of a perfect cantilever cylinder under a transverse shear. The linearized Donnell's equations, in conjunction with Galerkin's method were used to obtain an approximate solution to the problem. Boundary conditions were not completely satisfied. Galletly and Bachut [28] have shown in their report how buckling occurs in a cantilever cylindrical shell subjected to a transverse shearing force at its tip.

Referring to above studies, Nagashima et al. [13] have used the "lateral load buckling test" in their experimental study. Two types of buckling modes were created: local buckling mode and diamond-shaped mode. The first type was caused by shear and the second by bending (Figs. 2.5, 2.6). Experimental and FEM results have shown good agreement between the two methods for a medium range of frequency. Galletly and Bachut [29] have used the same approach to predict the buckling of a nuclear reactor vessel under horizontal ground motion.

Experimental and theoretical results on the plastic buckling of short, steel cantilevered cylindrical shells subjected to transverse edge shearing loads have shown a good agreement between the two methods [29].

2.2 Donnell Linearized Stability Equations

Stability equations for cylindrical shells have been available in the literature since the late 1800s. The earliest solutions for cylinders subjected to axial compression were presented by Lorenz in 1911 [30]. Solutions for buckling under uniform lateral pressure were given by Southwell [31] in 1913 and by von Mises [32] in 1914. In 1932 Flügge [33] presented a "comprehensive treatment" of cylindrical shell stability, including combined loading and cylinders subjected to bending. Results for cylinders subjected to torsional loading were given by Donnell [34] in 1933.

The Donnell equations form the basis for more stability analyses in the literature than any other set of cylindrical shell equations. Accurate results can be obtained, by the use of these equations, for cylindrical panels and for complete cylindrical shells [35]. Due to their simplicity, Donnell's stability equations have been used by a number of researchers. Tooth and Fernandez [36] have studied the buckling of horizontal vessels under internal pressure. They have used Donnell's linear stability equations. Results obtained from analytical studies have been compared with those obtained by some experimental investigations. Comparison has shown good agreement between the two methods. Huang et al. [37] have used Donnell's stability equations to study the instability of a cylindrical shell under three-point bending. Analytical results agree with those obtained by the FEM. Yamaki [38] has used also

Donnell's stability equations to study the buckling of shells under several kinds of loading (uniform pressure, hydrostatic pressure, bending...). Studies have been carried out for two types of boundary conditions: simply-simply and clamped-clamped. He has compared results obtained from Donnell's theory with those derived from the Sanders and Flügge theories. The three theories produced approximately similar results.

2.3 Approximate Solutions of Differential Equations

Approximate solutions of differential equations are ones which satisfy only some of the conditions of the problem; for example the differential equations may be satisfied only at a few positions, rather than at each point. An approximate solution can be expanded in a set of known functions with arbitrary parameters. These parameters can be determined by two ways: the method of Weighted Residuals and the Variational Method.

In the method of weighted residuals one can work directly with the differential equation and boundary conditions whereas in the variational method one must use a functional related to the differential equation and boundary conditions. There are two strategies in both methods: (1) a first approximation may be sufficient; its validity is assessed using experience and intuition, and (2) a sequence of approximations can be calculated in order to demonstrate convergence to the correct solution. In the second strategy the calculations must be sent to a computer: successive approximations must be calculated without any reformulation or intervention by the analyst [39].

The method of weighted residuals encompasses several methods (collocation, Galerkin, integral,...). The Galerkin method is the most known and powerful method [39,40].

Variational methods are not applicable to all problems, and thus "suffer a lack of generality". They require a lot of mathematical manipulations. On the other hand, the method of weighted residuals is simple and easy to apply. In the present study, the first strategy is applied to the Galerkin approach.

2.4 Outline of Present Investigation

In the present study an approximate analytical method is developed to study the buckling of broad, anchored, cylindrical liquid-storage tanks subjected to horizontal ground motion. A static approximation is used to represent the actual dynamic situation.

The solution is based on the linearized Donnell's stability equations and Galerkin's approach. Hydrodynamic pressure [2] chosen at a constant acceleration, and hydrostatic pressure are the only loadings considered. The boundary conditions are completely satisfied. The smallest buckling load (or the critical load factor) is calculated using the inverse iteration method. This theory is incorporated in the FORTRAN computer code BUCBAN. Theoretical results are then determined for two cases of broad tanks (L/r = 0.5 and L/r = 1.0) presented as examples. The general structural FEM analysis program ADINA is also used to determine the critical load factor and the corresponding mode shapes. Results from the two programs are compared and discussed in detail.

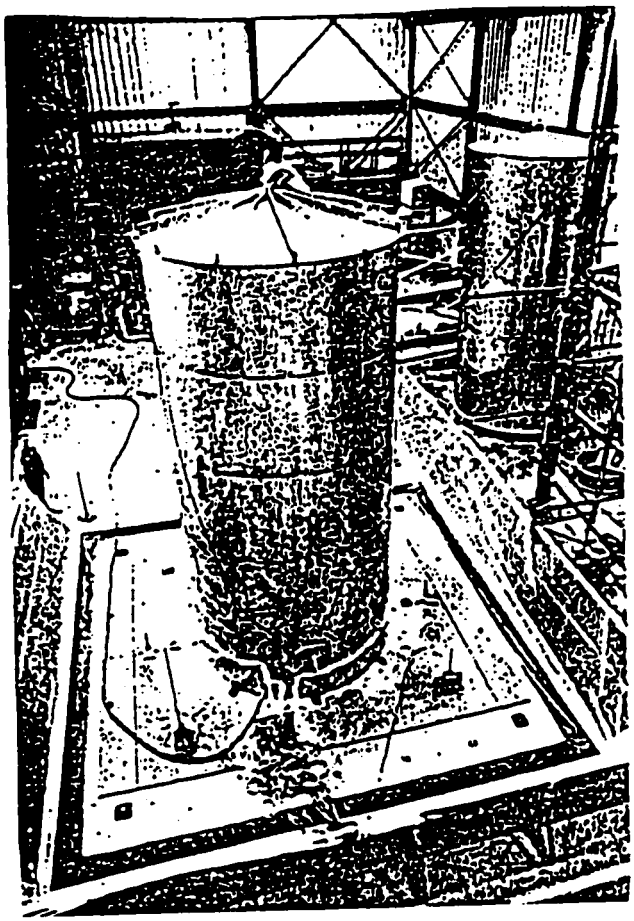

Figure 2.1: 2.9m x 6.1m tank on shaking table [14].

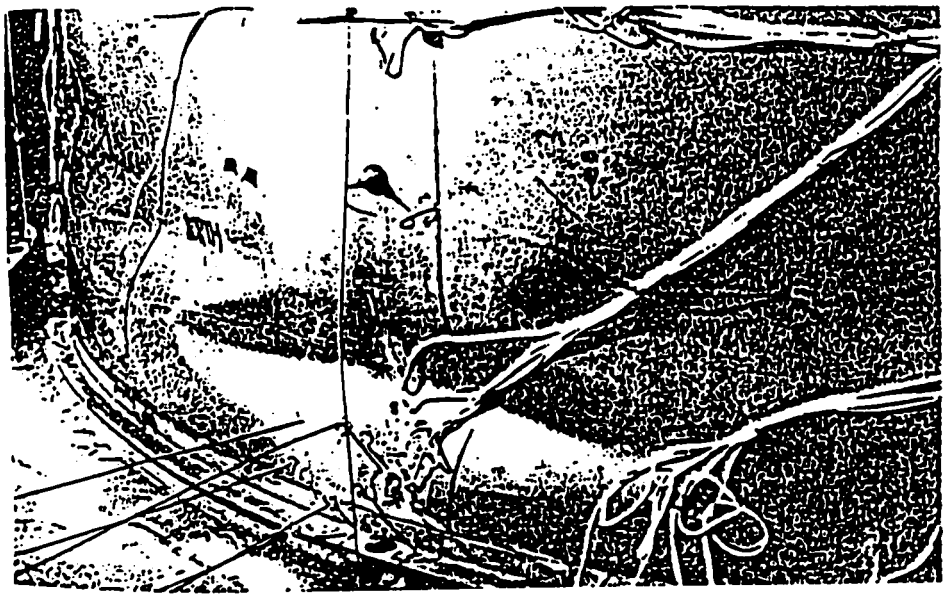

Figure 2.2: Buckling damage obtained during the shaking table test (free base) [14].

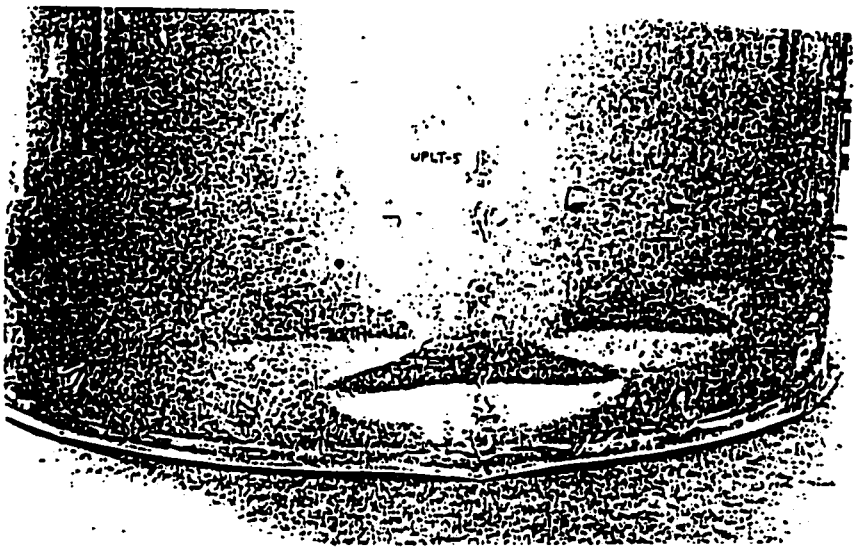

Figure 2.3: Buckling damage obtained during the shaking table test (fixed base) [14].

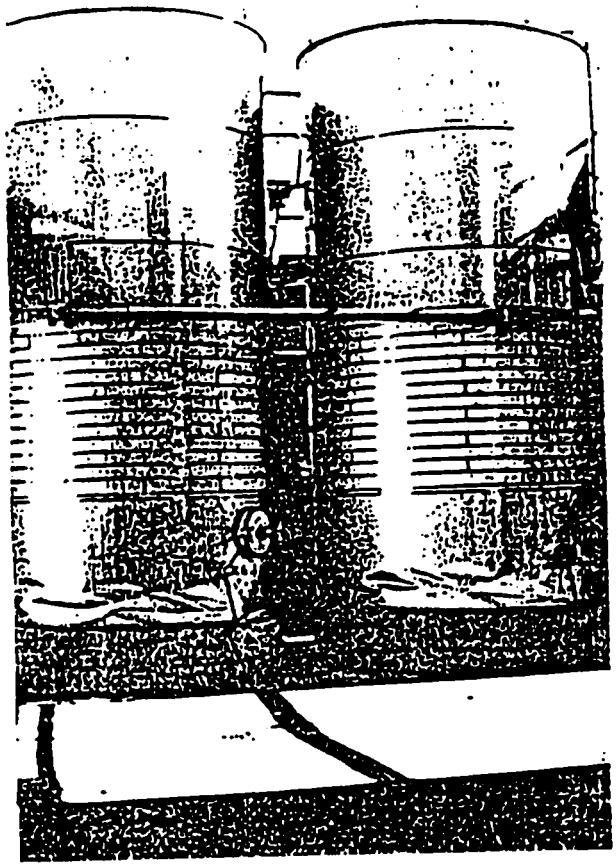

Figure 2.4: Diamond-shaped buckle in a Wente 'tall' tank (Wente Bros. winery) [14].

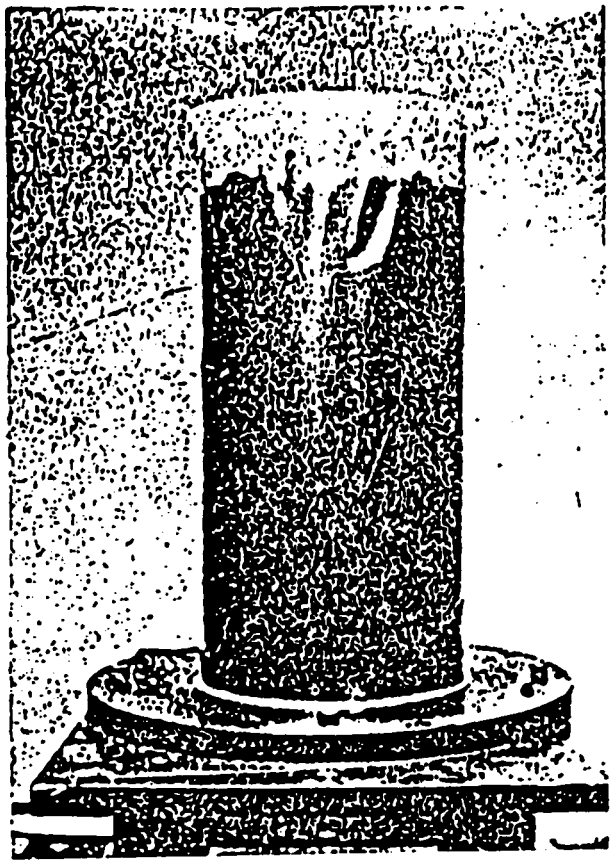

Figure 2.5: Buckling at the top of the model tank [15].

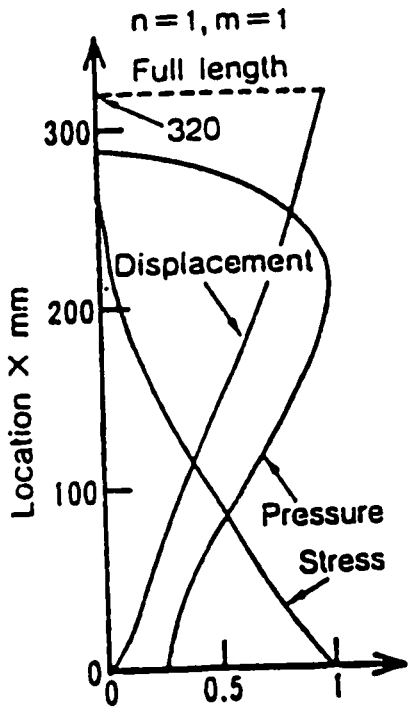

Figure 2.6: An example of displacement distribution, pressure and axial membrane stress obtained during a lateral load buckling test [13].

Chapter 3

Analytical Solution

3.1 Introduction

The circular cylindrical shell constitutes a fundamental element in light-weight structures and the determination of the buckling load has been one of the most crucial problems for the design and development of these structures. Hence, a number of studies were conducted on this subject since the basic equations were established by Flügge and Donnell in the 1930s.

In the early stage of the development, approximate solutions were obtained by applying the Ritz or Galerkin procedure with a few unknown parameters, under the assumption of the membrane prebuckling state. Only the classical "simple support" conditions were considered, for which relatively simple expressions can be used to represent incremental buckling displacements. In the second stage of the development following the rapid spreading of computers, solutions were obtained for more complicated boundary conditions. Linear and nonlinear theories of circular cylindrical shells, such as those of Donnell, Flügge and Sanders were used for wide ranges of geometries and boundary conditions.

In this chapter an approximate analytical method is developed to study the buckling of broad, anchored, cylindrical liquid-storage tanks subjected to horizontal ground motion. The

solution is based on the linearized Donnell's shell stability equations and Galerkin's approach.

3.2 Geometry and Loading

The cylindrical tank has a radius r, a thickness t and a length L (Fig. 3.1) A point on the shell midsurface is defined by axial and circumferencial coordinates x and φ. For convenience a non-dimensional axial coordinate is defined as $\varsigma = \frac{x}{r}$. The cartesian frame in Fig. 3.1 refers in the following to the development of the analytical solution.

This study covers two sizes of broad tanks; $\frac{L}{r} = 0.5$ and $\frac{L}{r} = 1.0$. The loading is considered to stem from two types of lateral pressure; hydrostatic and "hydrodynamic". The hydrostatic pressure arises due to fluid pressure on the tank wall. This pressure, varying linearly from the top to the bottom of the tank, is given by :

$$P_{st} = \rho_l g x \tag{3.1}$$

where ρ_l is the density of water and g is the acceleration of gravity. For the validation study described in Chap. 5 the hydrostatic pressure is considered as external, while for the analysis of practical tanks described in Chap. 6 this pressure is considered as internal.

The "hydrodynamic" pressure is arising from the fluid motion. This pressure at a constant pseudo-acceleration (peak) is expressed [2] by:

$$P_d = \alpha(x)\,\rho_l r G \cos\varphi \tag{3.2}$$

where $\alpha(x)$ is a dimensionless function which defines the heightwise variation (Fig. 3.2) of the pressure, and G is the assumed pseudo-acceleration.

Interaction between the base plate and the tank is not considered here. Auli et al. [18] have shown that the consideration of this interaction leads to a nonlinear problem which complicates the solution greatly.

The tank is rigidly anchored at the base and is without a roof or ring beam at the top. Consequently, the first edge (top) is assumed free, while the second is clamped. Thus the following boundary conditions are enforced at the shell ends:

$$\text{at } x = 0 \qquad N_x = N_{x\varphi} = M_x = Q_x = 0$$

$$\text{at } x = L \qquad w = w_{,x} = u = v = 0 \tag{3.3}$$

where N_x, $N_{x\varphi}$ are respectively the normal and shearing force intensities, M_x is the bending moment with respect to the x axis, Q_x is the transverse shearing force intensity in the radial direction and u, v, w are the displacement components in the x, φ, z directions respectively. The sign convention for the displacement components and stress resultants is given in Fig. 3.3.

Grossi [41,42] has shown that for the free edge the following equations can be used to give a good approximation in the satisfying of the M_x and Q_x requirements respectively:

$$\frac{\partial^2 w}{\partial x^2} = 0 \qquad (\text{at } x = 0)$$

$$\frac{\partial^3 w}{\partial x^3} = 0 \qquad (\text{at } x = 0) \tag{3.4}$$

3.3 Governing Equation

Stability equations for cylindrical shells have been available in the literature since the late 1880. The linearized Donnell equations have been used by several authors (see Sect. 2.2). The major steps used to obtain the governing equation are presented in the following.

The stress resultants for elastic isotropic cylindrical shells are [36]:

$$
\begin{aligned}
N_x &= C(\varepsilon_x + \nu\varepsilon_\varphi) \\
N_\varphi &= C(\varepsilon_\varphi + \nu\varepsilon_x) \\
N_{x\varphi} &= N_{\varphi x} = C\frac{(1-\nu)}{2}\gamma_{x\varphi} \\
M_x &= -\frac{D}{r^2}(w'' + \nu\ddot{w}) \\
M_\varphi &= -\frac{D}{r^2}(\ddot{w} + \nu w'') \\
M_{x\varphi} &= M_{\varphi x} = \frac{D}{r^2}(1-\nu)\dot{w}' \\
Q_x &= -\frac{D}{r^3}(w''' + \dot{w}'') \\
Q_\varphi &= -\frac{D}{r^3}(\dot{w}'' + w''' + \dot{w}')
\end{aligned}
\tag{3.5}
$$

where

$$
C = \frac{Et}{(1-\nu^2)}\ ;\ D = \frac{Et^3}{12(1-\nu^2)}\ ;\ (\ )' = \frac{\partial(\ )}{\partial\zeta}\ ;\ (\ )^{\cdot} = \frac{\partial(\ )}{\partial\varphi}
$$

and the strain components ε_x, ε_φ, and $\gamma_{x\varphi}$ are defined as:

$$\varepsilon_x = \frac{u'}{r} + \frac{w'^2}{2r^2}$$
$$\varepsilon_\varphi = \frac{(v^{\cdot} - w)}{r} + \frac{\dot{w}^2}{2r^2} \qquad (3.6)$$
$$\gamma_{x\varphi} = \frac{(\dot{u} + v')}{r} + \frac{w'\dot{w}}{r^2}$$

E is the Young's modulus and ν is the Poisson ratio.

Setting the radial pressure to zero, the equilibrium equations can be defined as [36]:

$$N_x' + N_{\varphi x}^{\cdot} = 0$$
$$N_\varphi^{\cdot} + N_{x\varphi}' = 0$$
$$Q_x' + Q_\varphi^{\cdot} + \frac{N_x w''}{r} + N_\varphi(1 + \frac{\ddot{w}}{r}) + (N_{\varphi x} + N_{x\varphi})\frac{\dot{w}}{r} = 0 \qquad (3.7)$$
$$M_{x\varphi}' + M_\varphi^{\cdot} + rQ_\varphi = 0$$
$$M_{\varphi x}^{\cdot} + M_x' - rQ_x = 0$$

A stress function F is introduced, satisfying

$$F'' = N_\varphi;\ \ddot{F} = N_x;\ F'^{\cdot} = -N_{x\varphi} = -N_{\varphi x} \qquad (3.8)$$

In order to obtain equations which relate the stress function F to the radial displacement w the following manipulations are required. The operators ∇^2, ∇^4, and ∇^8 are defined as:

$$\nabla^8(\ldots) = \nabla^4\nabla^4(\ldots)$$
$$\nabla^4(\ldots) = \nabla^2\nabla^2(\ldots) \qquad (3.9)$$

$$\nabla^2(\ldots) = (\frac{\partial^2}{\partial\varsigma^2} + \frac{\partial^2}{\partial\varphi^2})(\ldots) = (\ldots)_{,\varsigma\varsigma} + (\ldots)_{,\varphi\varphi}$$

Thus

$$\nabla^4(F) = F^{''''} + 2F^{''\cdot\cdot} + F^{\cdot\cdot\cdot\cdot} \tag{3.10}$$

Since $F^{''\cdot\cdot} = F^{\cdot\cdot''}$ one can introduce the following:

$$\begin{aligned} \nabla^4(F) &= F^{''''} + 2F^{''\cdot\cdot} + F^{\cdot\cdot\cdot\cdot} - \nu(F^{''''} + F^{''\cdot\cdot} - 2F^{''}) \\ \nabla^4(F) &= (N_\varphi - \nu N_x)^{''} + (N_x - \nu N_\varphi)^{\cdot\cdot} - 2(1+\nu)N_{x\varphi}^{\cdot\cdot} \end{aligned} \tag{3.11}$$

Substituting first (3.5.a - 3.5.c) into (3.11) and then substituting (3.6) into the resulting equation, one obtains:

$$\nabla^4(F) = \frac{-Et}{r^2}(rw^{''} + w^{''}w^{\cdot\cdot} - w^{\cdot 2}) \tag{3.12}$$

The second equation is obtained from (3.7) by eliminating Q_x and Q_φ, and then combining (3.5.d - 3.5.f) together with (3.8). The result is

$$\nabla^4(w) = \frac{r^2}{D}(rF^{''} + F^{''}w^{\cdot\cdot} + F^{\cdot\cdot}w^{''} - 2F^{'\cdot}w^{\cdot}) \tag{3.13}$$

Equations (3.12) and (3.13) are the two non-linear equations relevant to the large deflection range.

In order to find the stability equation one can investigate the possible existence of adjacent equilibrium configurations. For this purpose a small increment represented by w_1 is given to w_0, the prebuckling deformation, to reach an adjacent equilibrium configuration w called the buckling mode, which is very close to the original one. Linearizing the procedure one can have

$$w \rightarrow w_0 + w_1 \tag{3.14}$$

Assuming the stress resultants change in the same way,

$$F \rightarrow F_0 + F_1 \tag{3.15}$$

Substituting (3.14) and (3.15) into (3.12) and (3.13), neglecting the prebuckling rotation terms and confining the equations to linear terms, the following equations are found

$$\nabla^4(F_1) = -\frac{Et}{r} w_1''$$
$$\nabla^4(w_1) = \frac{r^2}{D}(rF_1'' + F_0'' w_1 + F_0 w_1'' - 2F_0' w_1') \tag{3.16}$$

These two equations can be combined into a single equation by applying the ∇^4 operator to both equations and adding them. The resulting equation is :

$$\frac{D}{r^2}\nabla^8 w_1 + Et w_{1,\varsigma\varsigma\varsigma\varsigma} - \lambda\nabla^4(N_{x_0} w_{1,\varsigma\varsigma} + N_{\varphi_0} w_{1,\varphi\varphi} + 2N_{\varphi x_0} w_{1,\varsigma\varphi}) = 0 \tag{3.17}$$

where $N_{x_0}, N_{\varphi_0}, N_{\varphi x_0}$ are the membrane stress resultants and λ is the buckling load parameter. In fact, Eq. (3.17) is the Donnell linear stability equation valid for any load condition corresponding to the original state, where the deformation w_1 corresponds to an increment beyond this equilibrium position.

3.4 Membrane stresses

The initial bending stresses are not taken into consideration. Previous studies conducted by Tooth et al. [36], Huang et al. [37], and Yamaki [38] have shown the validity of this approximation for a number of different loadings. All approximations inherent in the Donnell shell theory are embedded in Eq. (3.17).

Using the Donnell equations, membrane stresses can be obtained for hydrostatic and "hydrodynamic" pressures. N_{x_0}, N_{φ_0}, and $N_{\varphi x_0}$ are expanded in a Fourier series as:

$$N_{x_0} = \sum_{m=1,3}^{\bar{m}_h} \sum_{n=0,1}^{\bar{n}_h} A_{\bar{m}n} \cos \bar{n}\varphi \sin \mu_{\bar{m}} \varsigma$$

$$N_{\varphi_0} = \sum_{m=1,3}^{\bar{m}_h} \sum_{n=0,1}^{\bar{n}_h} B_{\bar{m}n} \cos \bar{n}\varphi \sin \mu_{\bar{m}} \varsigma \qquad (3.18)$$

$$N_{\varphi x_0} = \sum_{m=1,3}^{\bar{m}_h} \sum_{n=0,1}^{\bar{n}_h} C_{\bar{m}n} \sin \bar{n}\varphi \sin \mu_{\bar{m}} \varsigma$$

where $\mu_{\bar{m}} = \dfrac{\bar{m}\pi r}{2L}$ and the coefficients $A_{\bar{m}n}$, $B_{\bar{m}n}$, and $C_{\bar{m}n}$ are calculated using the Normal Fitting Method. The expansions (3.18) satisfy the end boundary conditions (3.3).

3.5 Approximate Displacement Function

Yamaki [38] has given theoretical solutions for a number of cylindrical shell buckling problems involving different kinds of loading (uniform pressure, hydrostatic pressure...) and boundary conditions. He has presented both exact and approximate solutions. The exact solutions are algebraically complex requiring the solution of a hierarchy of eigenvalue problems. Simpler approximate solutions are obtained by using assumed displacement functions and satisfying governing equations in the mean. The displacement functions must satisfy the boundary conditions exactly. Several terms (in the axial and circumferential directions) containing free constants are generally employed in the functions to improve the

approximation. Yamaki has reported also that the Donnell stability solutions are practically accurate so long as the corresponding circumferential buckling wave number ***n*** exceeds 4.

In the present study an approximate solution is formulated. Thus the expression for w_1 is taken as:

$$w_1 = \sum_{m=m_i, m_{i+2}\ldots}^{m_h} \sum_{n=n_i, n_{i+1}\ldots}^{n_h} a_{mn}(X_1 \sin \mu_m \varsigma - X_2 \sin 2\mu_m \varsigma + X_3 \sin 3\mu_m \varsigma - X_4 \sin 4\mu_m \varsigma$$

$$-X_5 \sin \frac{m\pi}{2}) \cos n\varphi \qquad (3.19)$$

where $\mu_m = \frac{m\pi r}{2L}$, a_{mn} are constant coefficients and X_1, X_2, X_3, X_4 and X_5 are real numbers coupled together in order to satisfy boundary conditions (3.3,3.4). Consequently,

$$X_1 - X_3 = X_5 \qquad (w_1 = 0 \quad \text{at } x = L) \qquad (3.20.a)$$

$$X_2 = 2X_4 \qquad (w_{1,x} = 0 \quad \text{at } x = L) \qquad (3.20.b) \qquad (3.20)$$

$$X_1 + 27X_3 = 8X_2 + 64X_4 \qquad (w_{1,xxx} = 0 \quad \text{at } x = L) \qquad (3.20.c)$$

Boundary conditions significantly affect the number of terms used to compose the displacement function. In other words, when boundary conditions are simple and similar at all edges, one can obtain easily the displacement function. Yamaki has given approximate displacement functions for simply-simply and clamped-clamped supported shells.

In this study the presence of the free edge complicates the problem. This is due to the free edge motion described by X_5. If X_5 is equal to zero then (using 3.20.a and 3.20.c)

$$X_1 = X_3 = (\frac{8X_2 + 64X_4}{28}) \qquad (3.20.d)$$

But in reality the free edge motion does exist and X_5 is not zero. This is verified by the FEM solution. For this reason X_5 can be approximately determined using some experimental and numerical results [13,43]. It was found that X_5 depends on the kind of loading. Consequently using Eqs. (3.20.a-3.20.d) and by trial and error X_3 (or X_1) can be obtained as:

$$X_3 = 1.0675\left(\frac{8X_2 + 64X_4}{28}\right) \quad \text{(for hydrostatic pressure)} \tag{3.20.e}$$

$$X_3 = 1.0965\left(\frac{8X_2 + 64X_4}{28}\right) \quad \text{(for "hydrodynamic" pressure)}$$

Considering the above conditions, it is seen that once one of the constants has been selected, the rest of X_i may be determined.

The series parameters m_i, m_h, n_i and n_h can be varied in the search for the mode corresponding to the smallest buckling pressure. As a double series is involved selectivity must be exercised in the choice of trial buckling modes to keep the numerical problem of a practical size.

3.6 Method of Approach

Substitution of the expansions (3.18) and (3.19) into the governing equation (3.17) and application of trigonometric identities lead to the requirement (3.21):

$$\sum_{m=m_i,m_{i+2}\cdots}^{m_h}\sum_{n=n_i,n_{i+1}\cdots}^{n_h} a_{mn}\{(\overline{H_1}\sin\mu_m\varsigma+\overline{H_2}\sin 2\mu_m\varsigma+\overline{H_3}\sin 3\mu_m\varsigma+\overline{H_4}\sin 4\mu_m\varsigma+\overline{H_5})\cos n\varphi$$

$$-\lambda\sum_{\bar{m}=1,3\cdots}^{\bar{m}_h}\sum_{\bar{n}=0,1\cdots}^{\bar{n}_h}[D_{11}\cos(\mu_{\bar{m}}-\mu_m)\varsigma\cos(\bar{n}-n)\varphi+D_{12}\cos(\mu_{\bar{m}}-\mu_m)\varsigma\cos(\bar{n}+n)\varphi+$$

$$D_{13}\cos(\mu_{\bar{m}}+\mu_m)\varsigma\cos(\bar{n}-n)\varphi+D_{14}\cos(\mu_{\bar{m}}+\mu_m)\varsigma\cos(\bar{n}+n)\varphi+$$

$$D_{21}\cos(\mu_{\bar{m}}-2\mu_m)\varsigma\cos(\bar{n}-n)\varphi+D_{22}\cos(\mu_{\bar{m}}-2\mu_m)\varsigma\cos(\bar{n}+n)\varphi+$$

$$D_{23}\cos(\mu_{\bar{m}}+2\mu_m)\varsigma\cos(\bar{n}-n)\varphi+D_{24}\cos(\mu_{\bar{m}}+2\mu_m)\varsigma\cos(\bar{n}+n)\varphi+$$

$$D_{31}\cos(\mu_{\bar{m}}-3\mu_m)\varsigma\cos(\bar{n}-n)\varphi+D_{32}\cos(\mu_{\bar{m}}-3\mu_m)\varsigma\cos(\bar{n}+n)\varphi+$$

$$D_{33}\cos(\mu_{\bar{m}}+3\mu_m)\varsigma\cos(\bar{n}-n)\varphi+D_{34}\cos(\mu_{\bar{m}}+3\mu_m)\varsigma\cos(\bar{n}+n)\varphi+$$

$$D_{41}\cos(\mu_{\bar{m}}-4\mu_m)\varsigma\cos(\bar{n}-n)\varphi+D_{42}\cos(\mu_{\bar{m}}-4\mu_m)\varsigma\cos(\bar{n}+n)\varphi+$$

$$D_{43}\cos(\mu_{\bar{m}}+4\mu_m)\varsigma\cos(\bar{n}-n)\varphi+D_{43}\cos(\mu_{\bar{m}}+4\mu_m)\varsigma\cos(\bar{n}+n)\varphi+$$

$$D_{51}\sin\mu_{\bar{m}}\varsigma\cos(\bar{n}-n)\varphi+D_{52}\sin\mu_{\bar{m}}\varsigma\cos(\bar{n}+n)\varphi+$$

$$D_{61}\sin(\mu_{\bar{m}}-\mu_m)\varsigma\cos(\bar{n}-n)\varphi+D_{62}\sin(\mu_{\bar{m}}-\mu_m)\varsigma\cos(\bar{n}+n)\varphi+$$

$$D_{63}\sin(\mu_{\bar{m}}+\mu_m)\varsigma\cos(\bar{n}-n)\varphi+D_{64}\sin(\mu_{\bar{m}}+\mu_m)\varsigma\cos(\bar{n}+n)\varphi+$$

$$D_{71}\sin(\mu_{\bar{m}}-2\mu_m)\varsigma\cos(\bar{n}-n)\varphi+D_{72}\sin(\mu_{\bar{m}}-2\mu_m)\varsigma\cos(\bar{n}+n)\varphi+$$

$$D_{73}\sin(\mu_{\bar{m}}+2\mu_m)\varsigma\cos(\bar{n}-n)\varphi+D_{74}\sin(\mu_{\bar{m}}+2\mu_m)\varsigma\cos(\bar{n}+n)\varphi+$$

$$D_{81}\sin(\mu_{\bar{m}}-3\mu_m)\varsigma\cos(\bar{n}-n)\varphi+D_{82}\sin(\mu_{\bar{m}}-3\mu_m)\varsigma\cos(\bar{n}+n)\varphi+$$

$$D_{83}\sin(\mu_{\bar{m}}+3\mu_m)\varsigma\cos(\bar{n}-n)\varphi+D_{84}\sin(\mu_{\bar{m}}+3\mu_m)\varsigma\cos(\bar{n}+n)\varphi+$$

$$D_{91}\sin(\mu_{\bar{m}}-4\mu_m)\varsigma\cos(\bar{n}-n)\varphi+D_{92}\sin(\mu_{\bar{m}}-4\mu_m)\varsigma\cos(\bar{n}+n)\varphi+$$

$$D_{93}\sin(\mu_{\bar{m}}+4\mu_m)\varsigma\cos(\bar{n}-n)\varphi+D_{94}\sin(\mu_{\bar{m}}+4\mu_m)\varsigma\cos(\bar{n}+n)\varphi]\}=0$$

where

$$\overline{H_1}=X_1(\frac{D}{r^2}(\mu_m^2+n^2)^4+Et\mu_m^4)$$

$$\overline{H_2}=-X_2(\frac{D}{r^2}(4\mu_m^2+n^2)^4+16Et\mu_m^4)$$

$$\overline{H_3}=X_3(\frac{D}{r^2}(9\mu_m^2+n^2)^4+81Et\mu_m^4)$$

$$\overline{H_4}=-X_4(\frac{D}{r^2}(16\mu_m^2+n^2)^4+256Et\mu_m^4)$$

$$\overline{H_5} = -X_5 \frac{D}{r^2} n^8 \sin\frac{m\pi}{2}$$

$$D_{11} = \frac{\overline{D_1}}{4}((\mu_{\bar{m}} - \mu_m)^2 + (\bar{n} - n)^2)^2 \qquad (3.22)$$

$$D_{12} = \frac{\overline{D_1}}{4}((\mu_{\bar{m}} - \mu_m)^2 + (\bar{n} + n)^2)^2$$

$$D_{13} = -\frac{\overline{D_1}}{4}((\mu_{\bar{m}} + \mu_m)^2 + (\bar{n} - n)^2)^2$$

$$D_{14} = -\frac{\overline{D_1}}{4}((\mu_{\bar{m}} + \mu_m)^2 + (\bar{n} + n)^2)^2$$

$$D_{21} = \frac{\overline{D_2}}{4}((\mu_{\bar{m}} - 2\mu_m)^2 + (\bar{n} - n)^2)^2$$

$$D_{22} = \frac{\overline{D_2}}{4}((\mu_{\bar{m}} - 2\mu_m)^2 + (\bar{n} + n)^2)^2$$

$$D_{23} = -\frac{\overline{D_2}}{4}((\mu_{\bar{m}} + 2\mu_m)^2 + (\bar{n} - n)^2)^2$$

$$D_{24} = -\frac{\overline{D_2}}{4}((\mu_{\bar{m}} + 2\mu_m)^2 + (\bar{n} + n)^2)^2$$

$$D_{31} = \frac{\overline{D_3}}{4}((\mu_{\bar{m}} - 3\mu_m)^2 + (\bar{n} - n)^2)^2$$

$$D_{32} = \frac{\overline{D_3}}{4}((\mu_{\bar{m}} - 3\mu_m)^2 + (\bar{n} + n)^2)^2$$

$$D_{33} = -\frac{\overline{D_3}}{4}((\mu_{\bar{m}} + 3\mu_m)^2 + (\bar{n} - n)^2)^2$$

$$D_{34} = -\frac{\overline{D_3}}{4}((\mu_{\bar{m}} + 3\mu_m)^2 + (\bar{n} + n)^2)^2 \qquad (3.22)$$

$$D_{41} = \frac{\overline{D_4}}{4}((\mu_{\bar{m}} - 4\mu_m)^2 + (\bar{n} - n)^2)^2$$

$$D_{42} = \frac{\overline{D_4}}{4}((\mu_{\bar{m}} - 4\mu_m)^2 + (\bar{n} + n)^2)^2$$

$$D_{43} = -\frac{\overline{D_4}}{4}((\mu_{\bar{m}} + 4\mu_m)^2 + (\bar{n} - n)^2)^2$$

$$D_{44} = -\frac{\overline{D_4}}{4}((\mu_{\bar{m}} + 4\mu_m)^2 + (\bar{n} + n)^2)^2$$

$$D_{51} = \frac{\overline{D_5}}{2}(\mu_{\bar{m}}^2 + (\bar{n} - n)^2)^2$$

$$D_{52} = \frac{\overline{D_5}}{2}(\mu_{\bar{m}}^2 + (\bar{n} + n)^2)^2$$

$$D_{61} = \frac{\overline{D_6}}{4}((\mu_{\bar{m}} - \mu_m)^2 + (\bar{n} - n)^2)^2$$

$$D_{62} = -\frac{\overline{D_6}}{4}((\mu_{\bar{m}} - \mu_m)^2 + (\bar{n} + n)^2)^2$$

$$D_{63} = \frac{\overline{D_6}}{4}((\mu_{\bar{m}} + \mu_m)^2 + (\bar{n} - n)^2)^2$$

$$D_{64} = -\frac{\overline{D_6}}{4}((\mu_{\bar{m}} + \mu_m)^2 + (\bar{n} + n)^2)^2$$

$$D_{71} = \frac{\overline{D_7}}{4}((\mu_{\bar{m}} - 2\mu_m)^2 + (\bar{n} - n)^2)^2 \qquad (3.22)$$

$$D_{72} = -\frac{\overline{D_7}}{4}((\mu_{\bar{m}} - 2\mu_m)^2 + (\bar{n} + n)^2)^2$$

$$D_{73} = \frac{\overline{D_7}}{4}((\mu_{\bar{m}} + 2\mu_m)^2 + (\bar{n} - n)^2)^2$$

$$D_{74} = -\frac{\overline{D_7}}{4}((\mu_{\bar{m}} + 2\mu_m)^2 + (\bar{n} + n)^2)^2 \qquad (3.22)$$

$$D_{81} = \frac{\overline{D_8}}{4}((\mu_{\bar{m}} - 3\mu_m)^2 + (\bar{n} - n)^2)^2$$

$$D_{82} = -\frac{\overline{D_8}}{4}((\mu_{\bar{m}} - 3\mu_m)^2 + (\bar{n} + n)^2)^2$$

$$D_{83} = \frac{\overline{D_8}}{4}((\mu_{\bar{m}} + 3\mu_m)^2 + (\bar{n} - n)^2)^2$$

$$D_{84} = -\frac{\overline{D_8}}{4}((\mu_{\bar{m}} + 3\mu_m)^2 + (\bar{n} + n)^2)^2$$

$$D_{91} = \frac{\overline{D_9}}{4}((\mu_{\bar{m}} - 4\mu_m)^2 + (\bar{n} - n)^2)^2$$

$$D_{92} = -\frac{\overline{D_9}}{4}((\mu_{\bar{m}} - 4\mu_m)^2 + (\bar{n} + n)^2)^2$$

$$D_{93} = \frac{\overline{D_9}}{4}((\mu_{\bar{m}} + 4\mu_m)^2 + (\bar{n} - n)^2)^2$$

$$D_{94} = -\frac{\overline{D_9}}{4}((\mu_{\bar{m}} + 4\mu_m)^2 + (\bar{n} + n)^2)^2$$

and

$$\begin{aligned}
\overline{D_1} &= -X_1(n^2 B_{\bar{m}n} + \mu_m{}^2 A_{\bar{m}n}) \\
\overline{D_2} &= X_2(n^2 B_{\bar{m}n} + 4\mu_m{}^2 A_{\bar{m}n}) \\
\overline{D_3} &= -X_3(n^2 B_{\bar{m}n} + 9\mu_m{}^2 A_{\bar{m}n}) \\
\overline{D_4} &= X_4(n^2 B_{\bar{m}n} + 16\mu_m{}^2 A_{\bar{m}n})
\end{aligned} \tag{3.23}$$

$$\begin{aligned}
\overline{D_5} &= X_5 n^2 B_{\bar{m}n} \sin\frac{m\pi}{2} \\
\overline{D_6} &= -2X_1 n\mu_m C_{\bar{m}n} \\
\overline{D_7} &= 4X_2 n\mu_m C_{\bar{m}n} \\
\overline{D_8} &= -6X_3 n\mu_m C_{\bar{m}n} \\
\overline{D_9} &= 8X_4 n\mu_m C_{\bar{m}n}
\end{aligned} \tag{3.23}$$

3.6.1 Galerkin Method

The equation (3.21) has the form:

$$\sum\sum a_{mn}\{f_{mn}(\varsigma,\varphi)\} = 0 \tag{3.24}$$

Using the Galerkin approach, the equation is multiplied by $w_1(\hat{m},\hat{n})$ and integrated over the shell surface. Here $\hat{m}$ and $\hat{n}$ cover the complete set of m,n combinations in the series for w_1. The typical equation may then be reduced to :

$$\sum_{m=m_i,m_{i+2}}^{m_h}\sum_{n=n_i,n_{i+1}}^{n_h} a_{mn}\{\overline{H_1}\, I_{n\hat{n}}(X_1 J_{\hat{m}m} - X_2 J_{2\hat{m}m} + X_3 J_{3\hat{m}m} - X_4 J_{4\hat{m}m} - X_5 S_{\hat{m}} J_m)$$

$$+\overline{H_2}\, I_{n\hat{n}}(X_1 J_{\hat{m}2m} - X_2 J_{2\hat{m}2m} + X_3 J_{3\hat{m}2m} - X_4 J_{4\hat{m}2m} - X_5 S_{\hat{m}} J_{2m})$$

$$+\overline{H_3}\, I_{n\hat{n}}(X_1 J_{\hat{m}3m} - X_2 J_{2\hat{m}3m} + X_3 J_{3\hat{m}3m} - X_4 J_{4\hat{m}3m} - X_5 S_{\hat{m}} J_{3m})$$

$$+\overline{H_4}\, I_{n\hat{n}}(X_1 J_{\hat{m}4m} - X_2 J_{2\hat{m}4m} + X_3 J_{3\hat{m}4m} - X_4 J_{4\hat{m}4m} - X_5 S_{\hat{m}} J_{4m})$$

$$+\overline{H_5}\, I_{n\hat{n}}(X_1 J_{\hat{m}} - X_2 J_{2\hat{m}} + X_3 J_{3\hat{m}} - X_4 J_{4\hat{m}} - X_5 S_{\hat{m}} \mathrm{Xi}) \qquad (3.25)$$

$$-\lambda[\sum_{m=1,3,\ldots}^{\overline{m_h}}\sum_{n=0,1,\ldots}^{\overline{n_h}}[(D_{11} I'_{n\hat{n}\bar{n}} + D_{12} I''_{n\hat{n}\bar{n}})(X_1 J'_{\hat{m}m\bar{m}} - X_2 J'_{2\hat{m}m\bar{m}} + X_3 J'_{3\hat{m}m\bar{m}} - X_4 J'_{4\hat{m}m\bar{m}} - X_5 S_{\hat{m}} J'_{m\bar{m}})$$

$$+(D_{13} I'_{n\hat{n}\bar{n}} + D_{14} I''_{n\hat{n}\bar{n}})(X_1 J''_{\hat{m}m\bar{m}} - X_2 J''_{2\hat{m}m\bar{m}} + X_3 J''_{3\hat{m}m\bar{m}} - X_4 J''_{4\hat{m}m\bar{m}} - X_5 S_{\hat{m}} J''_{m\bar{m}})$$

$$+(D_{21} I'_{n\hat{n}\bar{n}} + D_{22} I''_{n\hat{n}\bar{n}})(X_1 J'_{\hat{m}2m\bar{m}} - X_2 J'_{2\hat{m}2m\bar{m}} + X_3 J'_{3\hat{m}2m\bar{m}} - X_4 J'_{4\hat{m}2m\bar{m}} - X_5 S_{\hat{m}} J'_{2m\bar{m}})$$

$$+(D_{23} I'_{n\hat{n}\bar{n}} + D_{24} I''_{n\hat{n}\bar{n}})(X_1 J''_{\hat{m}2m\bar{m}} - X_2 J''_{2\hat{m}2m\bar{m}} + X_3 J''_{3\hat{m}2m\bar{m}} - X_4 J''_{4\hat{m}2m\bar{m}} - X_5 S_{\hat{m}} J''_{2m\bar{m}})$$

$$+(D_{31} I'_{n\hat{n}\bar{n}} + D_{32} I''_{n\hat{n}\bar{n}})(X_1 J'_{\hat{m}3m\bar{m}} - X_2 J'_{2\hat{m}3m\bar{m}} + X_3 J'_{3\hat{m}3m\bar{m}} - X_4 J'_{4\hat{m}3m\bar{m}} - X_5 S_{\hat{m}} J'_{3m\bar{m}})$$

$$+(D_{33} I'_{n\hat{n}\bar{n}} + D_{34} I''_{n\hat{n}\bar{n}})(X_1 J''_{\hat{m}3m\bar{m}} - X_2 J''_{2\hat{m}3m\bar{m}} + X_3 J''_{3\hat{m}3m\bar{m}} - X_4 J''_{4\hat{m}3m\bar{m}} - X_5 S_{\hat{m}} J''_{3m\bar{m}})$$

$$+(D_{41} I'_{n\hat{n}\bar{n}} + D_{42} I''_{n\hat{n}\bar{n}})(X_1 J'_{\hat{m}4m\bar{m}} - X_2 J'_{2\hat{m}4m\bar{m}} + X_3 J'_{3\hat{m}4m\bar{m}} - X_4 J'_{4\hat{m}4m\bar{m}} - X_5 S_{\hat{m}} J'_{4m\bar{m}})$$

$$+(D_{43} I'_{n\hat{n}\bar{n}} + D_{44} I''_{n\hat{n}\bar{n}})(X_1 J''_{\hat{m}4m\bar{m}} - X_2 J''_{2\hat{m}4m\bar{m}} + X_3 J''_{3\hat{m}4m\bar{m}} - X_4 J''_{4\hat{m}4m\bar{m}} - X_5 S_{\hat{m}} J''_{4m\bar{m}})$$

$$+(D_{51} I'_{n\hat{n}\bar{n}} + D_{52} I''_{n\hat{n}\bar{n}})(X_1 J_{\hat{m}m\bar{m}} - X_2 J_{2\hat{m}m\bar{m}} + X_3 J_{3\hat{m}m\bar{m}} - X_4 J_{4\hat{m}m\bar{m}} - X_5 S_{\hat{m}} J_{m\bar{m}})$$

$$+(D_{61} I'_{n\hat{n}\bar{n}} + D_{62} I''_{n\hat{n}\bar{n}})(X_1 K'_{\hat{m}m\bar{m}} - X_2 K'_{2\hat{m}m\bar{m}} + X_3 K'_{3\hat{m}m\bar{m}} - X_4 K'_{4\hat{m}m\bar{m}} - X_5 S_{\hat{m}} K'_{m\bar{m}})$$

$$+(D_{63} I'_{n\hat{n}\bar{n}} + D_{64} I''_{n\hat{n}\bar{n}})(X_1 K''_{\hat{m}m\bar{m}} - X_2 K''_{2\hat{m}m\bar{m}} + X_3 K''_{3\hat{m}m\bar{m}} - X_4 K''_{4\hat{m}m\bar{m}} - X_5 S_{\hat{m}} K''_{m\bar{m}})$$

$$+(D_{71} I'_{n\hat{n}\bar{n}} + D_{72} I''_{n\hat{n}\bar{n}})(X_1 K'_{\hat{m}2m\bar{m}} - X_2 K'_{2\hat{m}2m\bar{m}} + X_3 K'_{3\hat{m}2m\bar{m}} - X_4 K'_{4\hat{m}2m\bar{m}} - X_5 S_{\hat{m}} K'_{2m\bar{m}})$$

$$+(D_{73} I'_{n\hat{n}\bar{n}} + D_{74} I''_{n\hat{n}\bar{n}})(X_1 K''_{\hat{m}2m\bar{m}} - X_2 K''_{2\hat{m}2m\bar{m}} + X_3 K''_{3\hat{m}2m\bar{m}} - X_4 K''_{4\hat{m}2m\bar{m}} - X_5 S_{\hat{m}} K''_{2m\bar{m}})$$

$$+(D_{81}I'_{n\hat{n}\bar{n}}+D_{82}I''_{n\hat{n}\bar{n}})(X_1K'_{\hat{m}3m\bar{m}}-X_2K'_{2\hat{m}3m\bar{m}}+X_3K'_{3\hat{m}3m\bar{m}}-X_4K'_{4\hat{m}3m\bar{m}}-X_5S_{\hat{m}}K'_{3m\bar{m}})$$

$$+(D_{83}I'_{n\hat{n}\bar{n}}+D_{84}I''_{n\hat{n}\bar{n}})(X_1K''_{\hat{m}3m\bar{m}}-X_2K''_{2\hat{m}3m\bar{m}}+X_3K''_{3\hat{m}3m\bar{m}}-X_4K''_{4\hat{m}3m\bar{m}}-X_5S_{\hat{m}}K''_{3m\bar{m}})$$

$$+(D_{91}I'_{n\hat{n}\bar{n}}+D_{92}I''_{n\hat{n}\bar{n}})(X_1K'_{\hat{m}4m\bar{m}}-X_2K'_{2\hat{m}4m\bar{m}}+X_3K'_{3\hat{m}4m\bar{m}}-X_4K'_{4\hat{m}4m\bar{m}}-X_5S_{\hat{m}}K'_{4m\bar{m}})$$

$$+(D_{93}I'_{n\hat{n}\bar{n}}+D_{94}I''_{n\hat{n}\bar{n}})(X_1K''_{\hat{m}4m\bar{m}}-X_2K''_{2\hat{m}4m\bar{m}}+X_3K''_{3\hat{m}4m\bar{m}}-X_4K''_{4\hat{m}4m\bar{m}}-X_5S_{\hat{m}}K''_{4m\bar{m}})]]\}=0$$

The "*Ks*", "*Js*", and "*Ss*" terms of equation (3.25) are defined in *Appendix A.* They represent integrals which must be evaluated with due regard for the relative values of the arguments of the trigonometric functions involved.

3.6.2 Eigenvalue Problem

The Galerkin approach leads to a matrix equation of the form :

$$[A](a) - \lambda\,[B]\,(a)=0 \qquad (3.26)$$

where (a) represents the array of coefficients a_{mn} and [A] and [B] are two symmetrical matrices. This equation represents a general eigenvalue problem and may be solved for the eigenvalue λ by the use of inverse iteration method [44] described in Chap. 4. The main goal of this work is to predict the critical load factor corresponding to the smallest value of λ.

In Chap. 5 the eigenvalue problem is solved for two kinds of loading (considered separately); external hydrostatic pressure and "hydrodynamic" pressure. In Chap. 6 the combination of internal hydrostatic and "hydrodynamic" pressures are considered. The internal hydrostatic pressure does not cause buckling. Therefore, the critical load factor is

calculated in Chap. 6 with respect to the "hydrodynamic" pressure. The resulting matrix equation describing the general eigenvalue problem in Chap. 6 has the form:

$$[A](a) - [B'](a) - \lambda\,[B''](a) = [A - B'](a) - \lambda\,[B''](a) = 0 \qquad (3.27)$$

where the two matrices [B'] and [B"] contain terms related to the membrane stresses for the hydrostatic and "hydrodynamic" pressures respectively.

The analysis was carried out in two stages. Values were found in the first stage for modes corresponding to a single assumed harmonic in the axial direction. From this set the harmonic with the smallest buckling pressure was identified. In the second stage, a final solution was found using a combination of harmonics in the axial direction starting with the one giving the smallest buckling pressure and identified in the first stage.

The theory presented in the preceding for the smallest buckling load was incorporated in the FORTRAN computer code BUCBAN. Results from this program are discussed in the following chapters.

3.7 Conclusion

An approximate solution scheme based on the linearized Donnell's shell theory and Galerkin's approach has been developed to study the buckling of broad, anchored tanks (free-fixed ends). The specific membrane loading is given through (3.18) upon choice of coefficients $A_{\overline{mn}}$, $B_{\overline{mn}}$, and $C_{\overline{mn}}$. In Chap. 5 this theory is applied to cases of empty tanks subjected to hydrostatic (external) and "hydrodynamic" pressures. In Chap. 6 the same theory is applied to practical cases of full tanks (internal hydrostatic pressure) subjected to "hydrodynamic" pressure. For other kinds of loading the Eq. (3.20.e) must be adjusted.

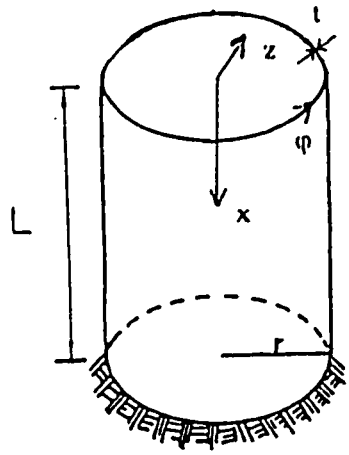

Figure 3.1: System considered.

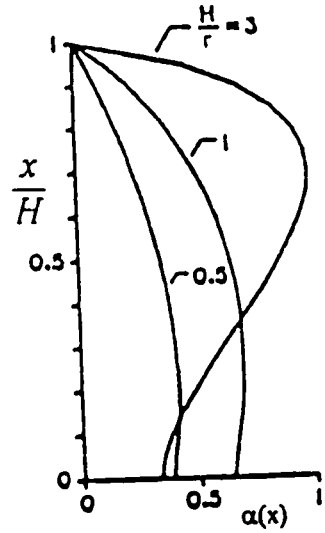

Figure 3.2: Function $\alpha(x)$ for impulsive component of hydrodynamic pressure [2,10] (x axis starts from the bottom).

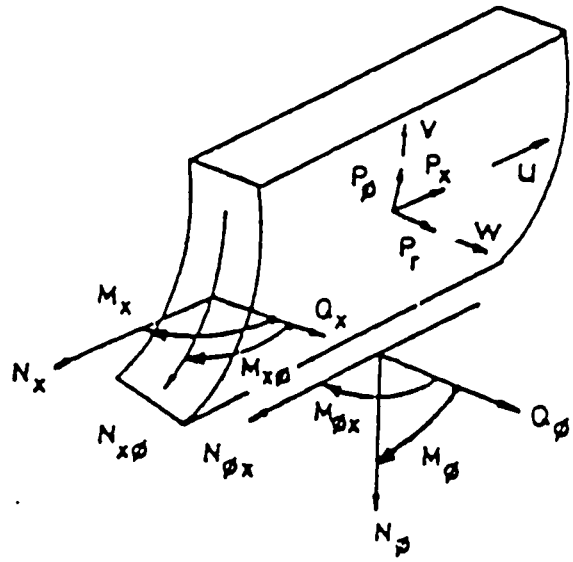

Figure 3.3: Shell theory displacements and stress resultants.

Chapter 4

Finite Element Solution

4.1 Introduction

The FEM is a numerical method for solving problems of engineering and mathematical physics. Typical problem areas of interest in engineering that are solvable by use of the FEM include structural analysis (buckling, vibration, stress analysis,...), heat transfer, fluid flow,...et.

For problems involving complicated geometries, loading, and material properties, it is generally not possible to obtain analytical mathematical solutions. These analytical solutions generally require the solution of ordinary or partial differential equations, which, because of factors listed above, are not usually obtainable. Hence, one needs to rely on numerical methods, such as the FEM for acceptable solutions.

The finite element formulation of the problem results in a system of simultaneous algebraic equations for solution, rather than requiring the solution of differential equations. These numerical methods yield approximate values of the unknowns at discrete numbers of points in the continuum. Hence, this process of modeling a body by dividing it into an "equivalent system of smaller bodies or units" (finite elements) interconnected at points common to two

or more elements and/or boundary lines and/or surfaces is called *discretization*. In the FEM, instead of solving the problem for the entire body in one operation, one formulates the equations for each finite element and combines them to obtain the solution of the whole body. But on the other hand, this solution is expensive in terms of time. For this reason, many researchers prefer to use analytical methods in order to minimize the cost.

4.2 Computer Programs for the Finite Element Method

There are two general approaches to the solution of problems by the FEM. The first is to use large commercial programs called general-purpose programs which are designed to solve many types of problems. The other is to develop small, special-purpose programs to solve specific problems.

The major disadvantage of special-purpose programs is clearly their inability to solve different classes of problems. For this reason, general-purpose programs are oftenly used to solve a large variety of problems. Numerous commercial software packages are available for FEM implementation. A partial list of existing programs includes: ALGOR, ADINA, NASTRAN, ANSYS, GIFTS, IMAGES-3D.

In the present study, the FEM solution is determined using the ADINA program [43]. ADINA (Automatic Dynamic Incremental Non-linear Analysis) was developed at MIT (Massachusetts Institute of Technology) by Bathe. This program provides several advantages for the user. In addition to its capacity to solve dynamic and non-linear problems, this program can read geometry and element data prepared by another mesh/element generator such as another pre-processor or CAD program. The user has also the opportunity to use

several types of elements: truss elements, two-D solid elements, three-D solid elements, beam elements, plate elements, shell elements, pipe elements, general spring elements, fluid elements. This variety in types of elements is not provided in all above listed programs (example: Algor). Depending on the nature and complexity of the problem, one can choose the appropriate type of elements. ADINA has effective data facilities available, including those for mesh generation and for graphically checking the prepared model. To build the input file no particular order of the commands is required. This fact reduces the time consumed to prepare and check the input data especially for a large finite element model.

4.3 Modeling the Problem Using ADINA

Several points should be defined in ADINA in order to solve this linear buckling problem:

- Linear analysis: small strains are used.
- Material: elastic material is chosen.
- Geometry: due to the symmetrical loading and geometry, only one half of the tank is modeled. This point is justified and discussed in detail in Sect. 5.3
- Element: the isoparametric shell element having eight nodes and uniform thickness is chosen. The integration order is taken as 3x3x3 for this specified element.
- Degree of freedom: there are three displacements and two rotations at each node.
- Loading: surface pressure loading is used in this study.
- Mesh: it consists of a number of elements in both circumferential and longitudinal directions. This number of elements is selected to provide convergence. In Chap. 5 a convergence

check is presented for every specific mesh. It has been observed that the number of elements in the circumferential direction has the largest effect on the solution.

The selected mesh for the first tank, having an aspect ratio $\frac{L}{r} = 1.0$, consisted of 60 (20x3) eight-nodded isoparamateric shell elements with a total of 227 nodes (Fig. 4.1). However, for the second tank having an aspect ratio $\frac{L}{r} = 0.5$, the selected mesh consisted of 120 (40x3) eight-nodded isoparametric shell elements with a total of 447 nodes (Fig. 4.2).

- Convergence tolerance: high convergence tolerance is desirable to minimize the physical norm error of the solution (10E-10).
- Boundary conditions: nodes located at the top of the tank have five degrees of freedom, while at the bottom they are completely fixed (clamped edge). Finally at the remaining edges, nodes can have only, due to the symmetry, two displacement and two rotation degrees of freedom.

4.4 Solution Methods for Eigenproblems

One can distinguish between two kinds of eigenproblems: standard and general. The simplest problem encountered is the standard eigenproblem:

$$K\phi = \lambda\phi \tag{4.1}$$

where K is the stiffness matrix for the finite element assemblage, ϕ is the eigenvector and λ is the eigenvalue. There are n eigenvalues and corresponding eigenvectors satisfying (4.1).

The ith eigenpair is denoted as (λ_i, ϕ_i), where the eigenvalues are ordered according to their magnitudes:

$$0 \leq \lambda_1 \leq \lambda_2 \leq \ldots \leq \lambda_{n-1} \leq \lambda_n \tag{4.2}$$

For the general eigenproblem, the equation has the form:

$$K\phi = \lambda M\phi \tag{4.3}$$

where M is the mass matrix . K, λ, and ϕ have the same definitions as before.

The most common eigenproblems that are encountered in general scientific analysis are standard eigenproblems. For this reason, the solution of standard eigenproblems has attracted much attention in numerical analysis, and many solution algorithms are available. However, there are some techniques to transform the general eigenproblem to a standard one [44].

When considering the design of an effective solution method for an eigenproblem, a basic question is wether one should first solve for the eigenvalue λ, and then calculate the eigenvector ϕ, or vice versa, or whether it is most economical to solve for both λ and ϕ simultaneously. The answer to this question depends on the solution requirements. In this study the main goal is to calculate the smallest eigenvalue for a general eigenproblem described in Chap. 3.

The solution methods can be subdivided into four groups: vector iteration methods, transformation methods, polynomial iteration techniques, and the Sturm sequence techniques [44]. All these methods are iterative in nature.

The effectiveness of a solution method depends largely on two factors: first, the possibility of a reliable use of the procedure, and second, the cost of solution. The solution cost is essentially determined by the number of high-speed storage operations and an efficient use of

backup storage devices. However, it is most important that a solution method can be employed in a reliable manner.

A vector iteration technique named *inverse iteration* has been used in the analytical solution. The real justification for using this method derives from the fact that it does work and it can be used economically. The same method is employed also in ADINA. The technique of inverse iteration is very effectively used to calculate an eigenvector and at the same time the corresponding eigenvalue can also be evaluated.

4.4.1 Inverse Iteration Method

The inverse iteration algorithm can be described as follows. Assume that K is positive definite, whereas M may be a diagonal or banded mass matrix. Take a vector for ϕ say x_1. Assume that $y_1 = Mx_1$ then evaluate for k=1,2,....,

$$K\bar{x}_{k+1} = y_k \tag{4.4}$$

$$\bar{y}_{k+1} = M\bar{x}_{k+1} \tag{4.5}$$

$$\rho(\bar{x}_{k+1}) = \frac{\bar{x}_{k+1}^T y_k}{\bar{x}_{k+1}^T \bar{y}_{k+1}} \tag{4.6}$$

$$y_{k+1} = \frac{\bar{y}_{k+1}}{(\bar{x}_{k+1}^T \bar{y}_{k+1})^{1/2}} \tag{4.7}$$

where, provided that $y_1^T \phi_1 \neq 0$,

$$y_{k+1} \to M\phi_1 \quad \text{and} \quad \rho(\bar{x}_{k+1}) \to \lambda_1 \quad \text{as} \quad k \to \infty \tag{4.8}$$

It should be noted that the superscript T denotes the transpose and the vector $\rho(\bar{x}_{k+1})$ is the Rayleigh quotient.

$\rho(\bar{x}_{k+1})$ is an approximation to the eigenvalue λ_1. It is this approximation to λ_1 that is conveniently used to measure convergence in the iteration. Denoting the current approximation to λ_1 by $\lambda_1^{(k+1)}$ [i.e., $\lambda_1^{(k+1)} = \rho(\bar{x}_{k+1})$], one can measure convergence using

$$\frac{\left|\lambda_1^{(k+1)} - \lambda_1^{(k)}\right|}{\lambda_1^{(k+1)}} \leq tol \tag{4.9}$$

The tolerance (tol) should be 10^{-2s} or smaller when the eigenvalue λ_1 is required to 2s-digit accuracy. In this study s has been chosen equal to five.

Finally if l is the last iteration one can calculate λ_1 and ϕ_1;

$$\lambda_1 = \rho(\bar{x}_{l+1}) \tag{4.10}$$

$$\phi_1 = \frac{\bar{x}_{l+1}}{(\bar{x}_{l+1}^T \bar{y}_{l+1})^{1/2}} \tag{4.11}$$

All other eigenpairs (λ_i, ϕ_i) can be calculated by the same iterative cycle.

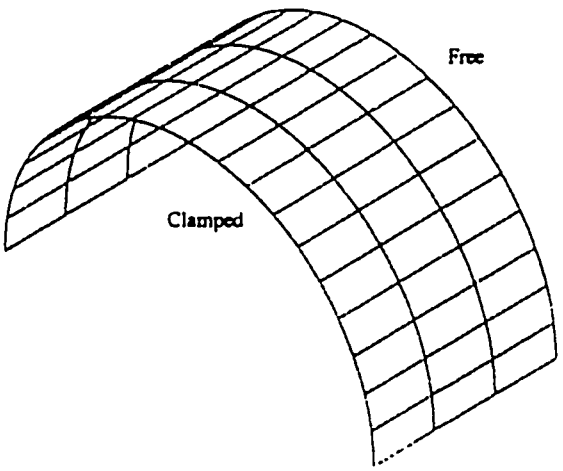

Figure 4.1: Finite element model of tank#1 (L/r =1.0).

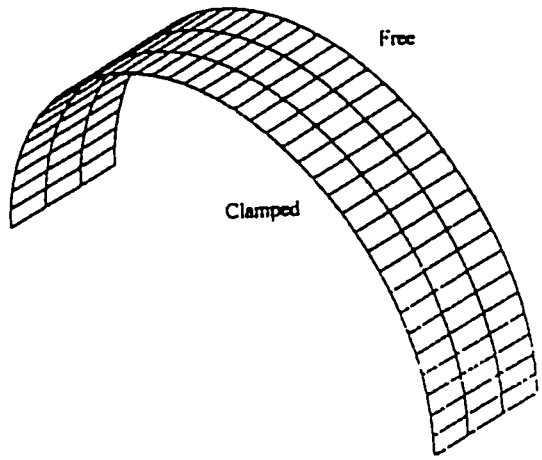

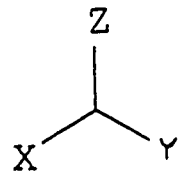

Figure 4.2: Finite element model of tank#2 (L/r =0.5)

Chapter 5

Validation

5.1 Geometry and Loading

The validity of the theory presented in Chap. 3 is partially checked through comparison with the FEM solution. The author has chosen two examples of broad tanks, for which the dimensionless functions $\alpha(x)$ in Eq. (3.2), are provided by Veletsos et al. [9,10].

The first tank is characterized by the following aspect ratios: $\frac{L}{r}=1.0$ and $\frac{r}{t}=1000.$ This tank is made from steel. Its material properties (E,ν) are given in Table 5.1. The second tank corresponds to the following geometric ratios: $\frac{L}{r}=0.5$ and $\frac{r}{t}=1000.$ This tank is also made from steel. The corresponding Young's modulus (E) and Poisson ratio (ν) are given in Table 5.1.

Empty tanks are examined in this chapter. Two kinds of horizontal loading are considered; external hydrostatic pressure and "hydrodynamic" pressure. Each of these pressures is multiplied by a factor of ten (10) in order to satisfy the following condition in ADINA [43]: " the smallest critical load (λ) should be greater than 1 and smaller than 500".

The theory, described in the chapters 3 and 4 is applied to these models. Results and discussion are presented in Sect. 5.3.

Table 5.1: Geometrical and material properties for tanks under examination

Tank #	L/r	r/t	Poisson ratio (ν)	Young's modulus (E) (MPa)
1	1.0	1000	0.3	207000
2	0.5	1000	0.3	207000

5.2 Convergence Check

In the analytical solution, the number of harmonics in the circumferential direction has a great influence on the convergence of the solution. This is shown in Table 5.2 . It has been found that sixteen (16) to twenty six (26) terms in the circumferential direction provide adequate convergence.

In the FEM solution, the number of elements in the axial and circumferential directions should be chosen carefully in order to obtain accurate results. The appropriate mesh is obtained when convergence is reached. Consequently, the analyst should refine the mesh until convergence is obtained. Convergence of the FEM results is shown in Table 5.3.

It can be seen from Table 5.3 and Figs. 5.1 that convergence is reached for tank # 1 when the critical load (λ) is equal to 13.55. Therefore, the appropriate mesh for the first tank consists of 3 elements in the axial direction and 20 elements in the circumferential direction.

For tank # 2, convergence is obtained when λ is equal to 21.93 (Figs. 5.2). Consequently, the appropriate mesh for the second tank consists of 3 elements in the axial direction and 40 elements in the circumferential direction.

It has been observed that the number of elements in the circumferential direction has the largest effect on the solution. This observation was reported also by Azar and Redekop [45] who used ADINA to study the ram bending of cylindrical pipes.

In the FEM solution the mesh depends significantly on the type of elements used and the number of nodes in each element. As example, if one solves the same problem using the plate elements or the 4-node shell elements (integration order=2x2x2), he must refine much more the corresponding mesh (the number of elements is much higher than in above cases). In the present study the use of the isoparametric 8-nodes shell elements with an integration order of 3x3x3 leads to an economical and accurate solution with relatively few elements [21].

Table 5.2: Effect of the number of harmonics in the circumferential direction (BUCBAN)

Number of Terms in the Circumferential Direction	Mode Number	Kind of Loading	Critical Load Factor for Tank # 1	Critical Load Factor for Tank # 2
8	1	Ext. Hydrost.	140.68	714.71
10	1	Ext. Hydrost.	41.30	268.31
12	1	Ext. Hydrost.	18.29	114.40
14	1	Ext. Hydrost.	13.13	56.36
16	1	Ext. Hydrost.	12.84	33.55
18	1	Ext. Hydrost.	12.84	25.07
20	1	Ext. Hydrost.	12.84	22.92
22	1	Ext. Hydrost.	12.84	22.92

Table 5.3: Convergence check for the FEM (external hydrostatic pressure)

Tank Number	L/r	Number of Elements in the Circumferential Direction	Number of Elements in the Longitudinal Direction	Critical Load Factor (ADINA)
1	1.0	16	3	14.19
1	1.0	18	3	13.77
1	1.0	19	3	13.64
1	1.0	20	3	13.55
1	1.0	21	3	13.55
1	1.0	22	3	13.55
1	1.0	20	2	16.4
1	1.0	20	4	13.55
1	1.0	22	6	13.55
1	1.0	24	9	13.55
2	0.5	28	3	24.73
2	0.5	32	3	24.63
2	0.5	36	3	24.20
2	0.5	38	3	23.10
2	0.5	40	3	21.93
2	0.5	44	8	21.93

5.3 Results and Discussion

Table 5.4 shows analytical and numerical results obtained for both tanks under lateral hydrostatic (external) and "hydrodynamic" pressures.

Table 5.4: Analytical and numerical results

Tank Number	Kind of Pressure	Critical Load Factor (BUCBAN)	Critical Load Factor (ADINA)	Solution Time(s) BUCBAN/ADINA	Percentage of Error(%) w.r.t. FEM Sol.
1	Ext. Hydrost.	12.84	13.55	321 / 1145.43	5.2
1	Hydrodynamic	38.25	36.26	413 / 2066.12	5.4
2	Ext. Hydrost.	22.92	21.93	362 / 1636.79	4.5
2	Hydrodynamic	56.80	60.05	540 / 5049.65	5.4

It is seen from Table 5.4 that results obtained from analytical and numerical analyses agree closely. The percentage of error measured with respect to FEM solution is approximately five percent (about the same percentage of error was found for other sizes of tanks in *Appendix B*). This indicates clearly that this method gives, as expected, an approximate solution for the problem. In fact, Galerkin's method usually doesn't provide an exact solution. It can be accurate only when boundary conditions are simple (example: simply-simply supported shell), which is not the case in the present study.

Error is due especially to the fact that an assumed displacement function is taken as the solution to the problem; this assumption is based on the experience and intuition of the analyst. It is not always easy to predict the exact shape of the displacement. The analyst should *feel the problem* in order to obtain a suitable function. The fact of not considering bending stresses and prebuckling deformations in the analysis has also some effects on the solution.

In the first stage of the analytical solution the smallest buckling load occurs at the first axial mode ($\hat{m}$=1). In the second stage, using the combination of two or three axial modes, the above listed values were obtained. The main goal of combining two or three axial modes is to obtain the *real or exact* first buckling mode. Results obtained after and before the superposition stage were very close. Therefore, the first buckling mode corresponds to the axial mode $\hat{m}$=1.

As mentioned in Sec. 2.1, tanks subjected to lateral loads can buckle into two modes: shear and bending. Shear buckling occurs usually at the top of the tank while bending buckling occurs near the base [13,46]. By looking to Figs. (5.4, 5.6, 5.8, 5.10), one can observe that most of the damages occur at the top of the tanks. Consequently, buckling is probably due to shear in this case. Results agree with those obtained by Nagashima et al. [13,21] who have found that shear buckling is dominant for short cylindrical shells.

In the FEM solution, only half of each tank was modeled because symmetrical buckling was expected. The real justification for expecting symmetrical buckling derives from the fact that geometry and loading are symmetric. In order to assure that buckling is symmetric the author has used a quarter tank model (Figs. 5.11, 5.12) to study the buckling of tanks under

external hydrostatic pressure. Results (Figs. 5.13-5.16) were identical to those obtained in the cases of halves of cylindrical shells (Figs. 5.3-5.10).

In *Appendix B* results are reported for other tanks. The same procedures were used and similar results were found. In fact, several researchers have used the above FEM model to study the buckling of tanks under lateral load. Kokubo et al. [21] have developed a special purpose FEM program. Their objective was to study the effects of four types of geometrical imperfections and combined loading (lateral load, bending,..) on cantilevered and simply supported tanks (short and tall). They have modeled halves of the cylinders using the 8-node isoparametric shell elements (Figs. 5.17-5.18). Nishino et al. [24] have used the FEM code 'FINAS' to study the buckling of liquid-filled thin-walled cylindrical tanks subjected to lateral excitation. They have modeled halves of the cylinders (Fig. 5.19). By looking to Fig. 5.19, one observes clearly that similar buckling modes were found in the present study (Figs. 5.4, 5.8). Natsiavas et al. [11] have used the FEM code ANSYS to study the seismic behavior of an unanchored liquid container. They have discretized half of the cylindrical tank by quadrilateral shell elements (Fig. 5.20). One of their objectives was to predict the possibility of any buckling failure at a given excitation level.

In reality, under dynamic action, loading becomes unsymmetric. This is due to several factors (rocking, sloshing motion,...).Therefore, nonsymmetrical buckling is often expected.

As mentioned by Nagashima et al. [13], the static approach is accurate as long as the study is made in the *medium range of frequency.* For high range of frequency, the analyst should expect higher percentage of error. Consequently, the present study can not cover dynamic problems involving high seismic acceleration.

In comparing results, consideration should be given to the major characteristics of the two methods. The analytical solution provides the option of finding buckling pressures for single specified modes or combination of modes. Accuracy depends on the simplicity of the specified buckling mode. In the present study, the first buckling mode (starting mode) is hard to predict. If the solution starts far from the *real* first buckling mode, results will be certainly wrong. This high degree of difficulty is due to the presence of the free edge. For this reason, constants in the displacement function should be adjusted according to the kind of loading. The number of degrees of freedom corresponds to the number of modes specified, and is usually quite low. The solution is thus computationally very economical (Table 5.4).

In the FEM there is no prior assumption made about the buckling mode. The number of degrees of freedom equals the number of unknown nodal displacements in the full domain, and is usually very large. The solution is thus computationally expensive (Table 5.4), but can accurately represent any general buckling mode. As well, solutions can readily be found for different boundary conditions.

Figure 5.1.a: Convergence of FEM Sol.
(Circumferential Direction; L/r=1.0)

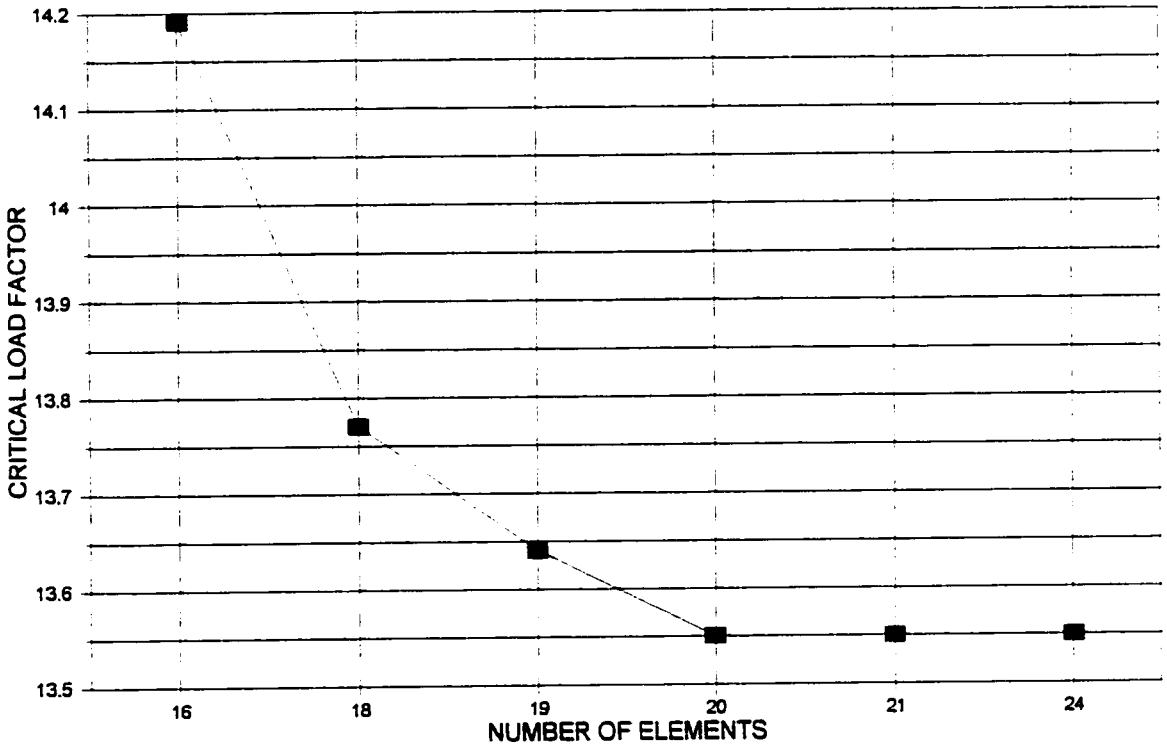

Figure 5.1.b: Convergence of FEM Sol.
(Axial Direction; L/r=1.0)

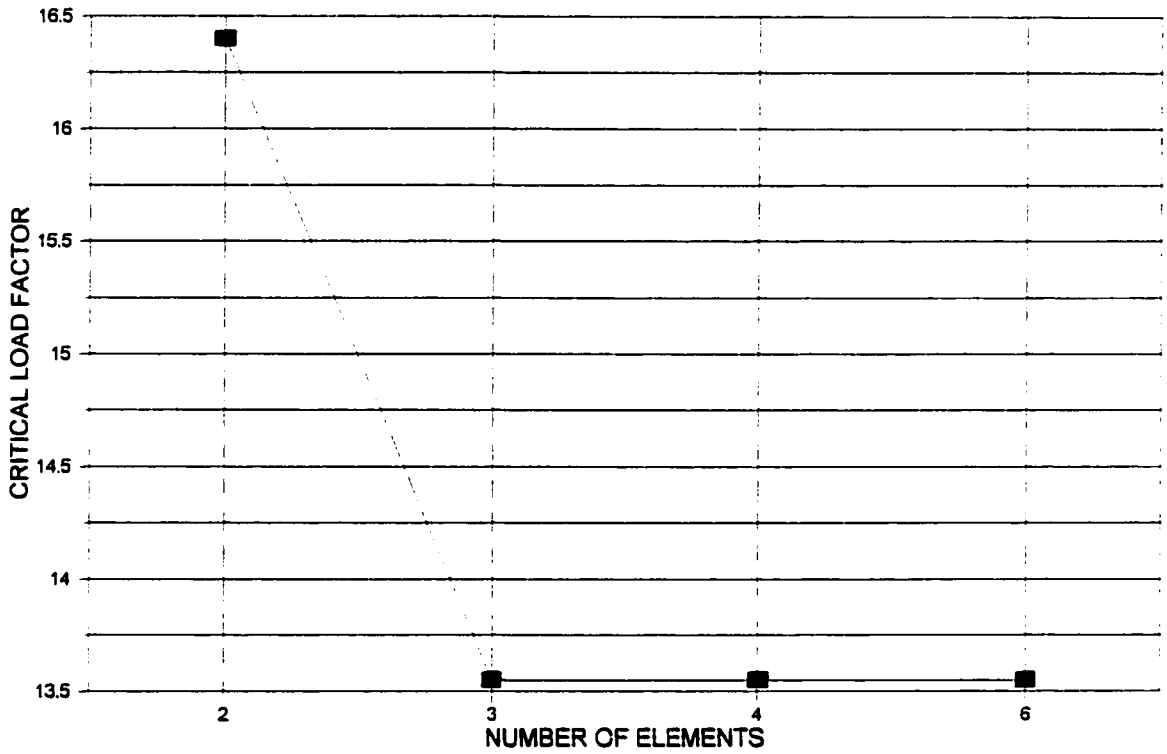

Figure 5.2.a: Convergence of FEM Sol.
(Circumferential Direction; L/r=0.5)

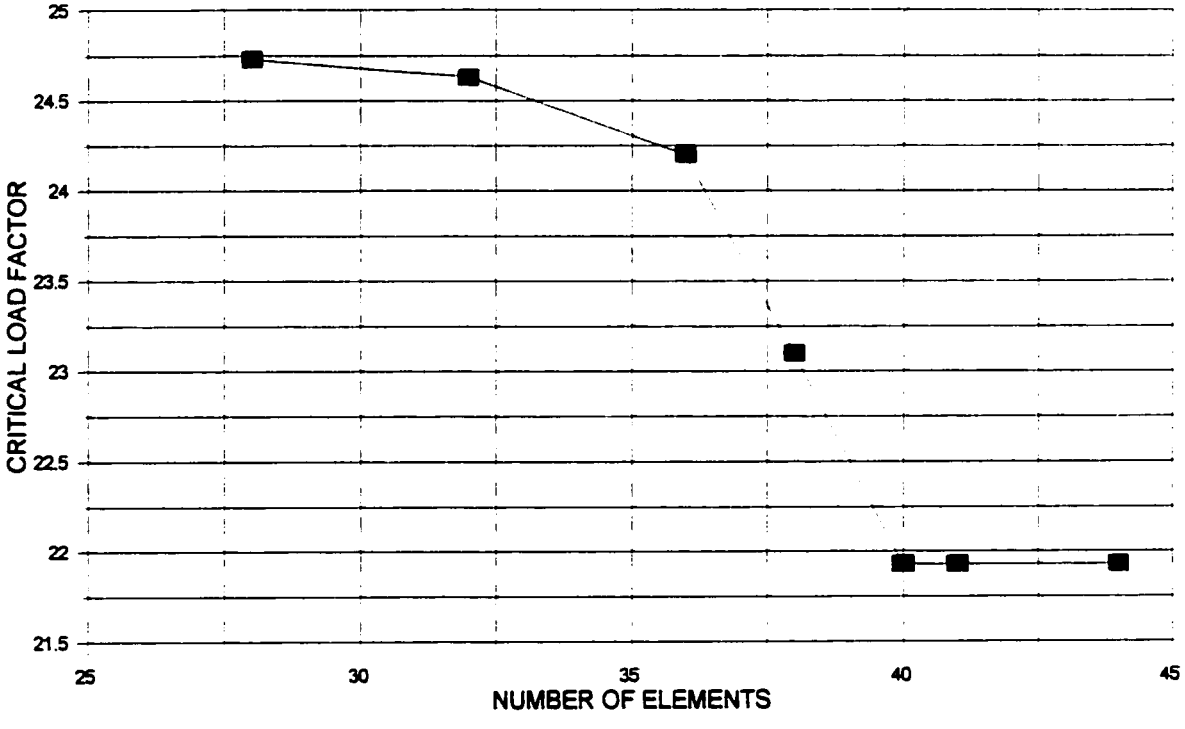

Figure 5.2.b: Convergence of FEM Sol.
(Axial Direction; L/r=0.5)

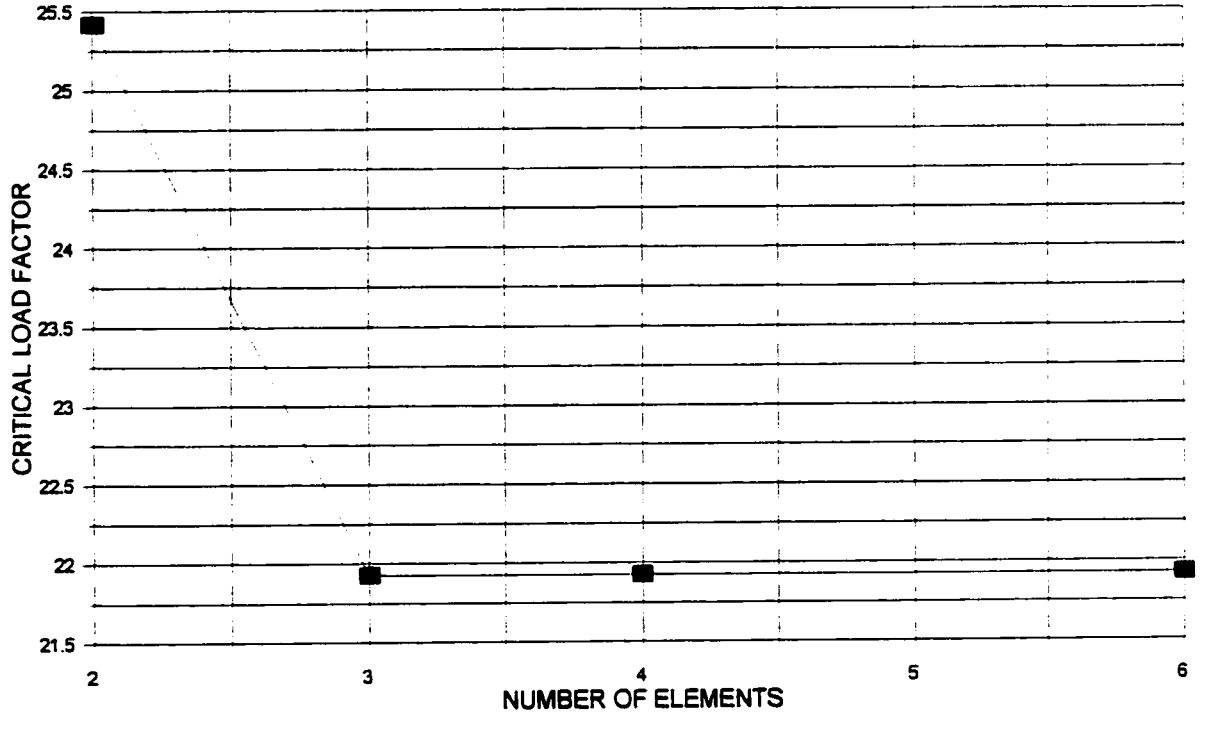

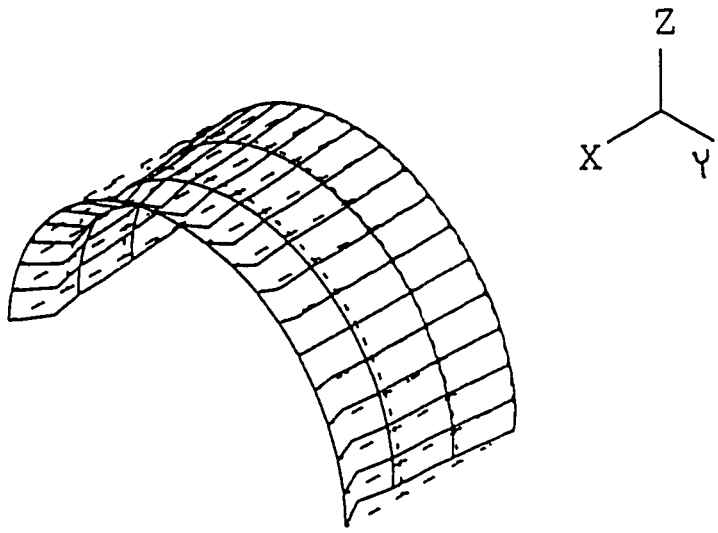

Figure 5.3: Deformed shape of tank#1 (L/r = 1.0; load=hydrostatic).

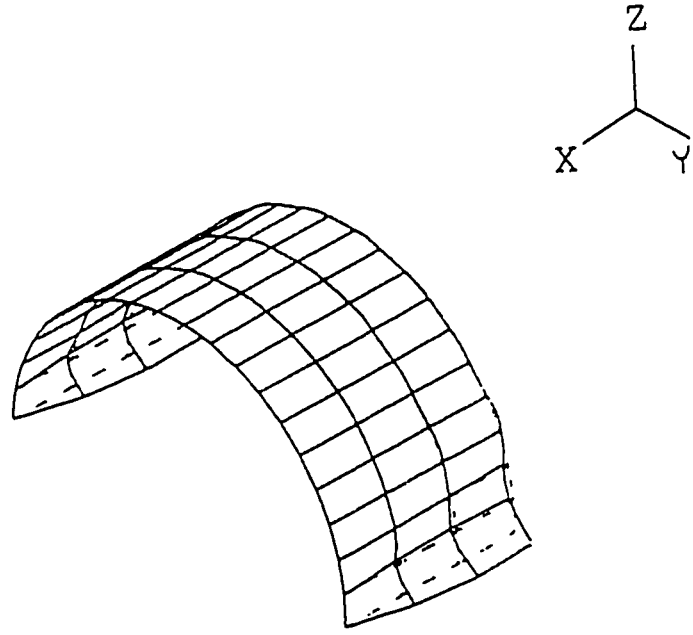

Figure 5.4: First buckling mode of tank#1 (L/r=1.0; load=hydrostatic).

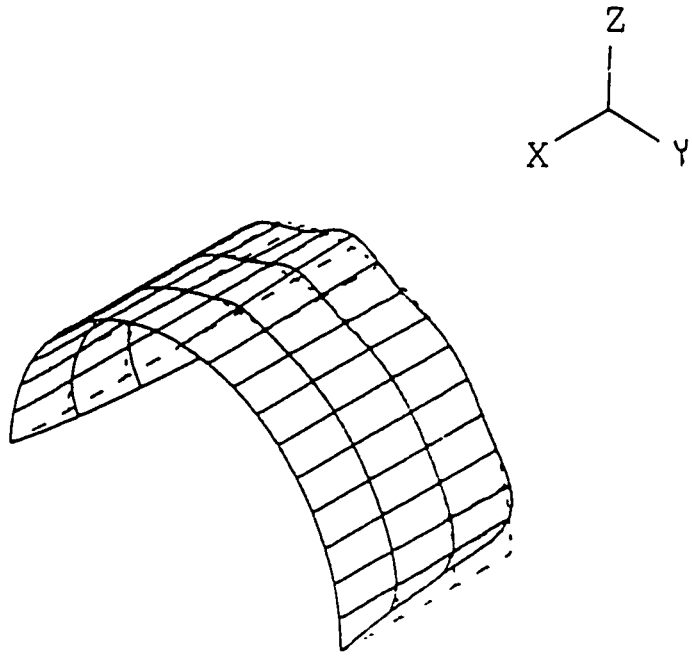

Figure 5.5: Deformed shape of tank#1 (L/r=1.0; load="hydrodynamic").

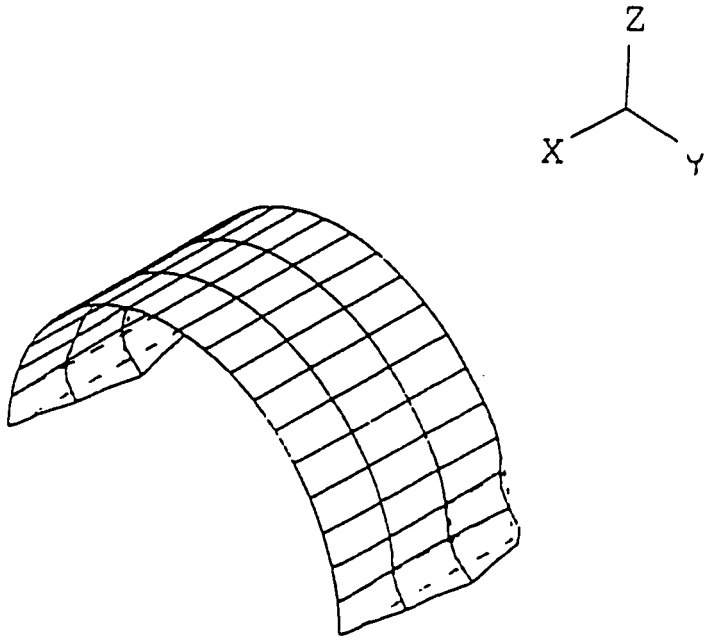

Figure 5.6: First buckling mode of tank#1 (L/r=1.0: load="hydrodynamic").

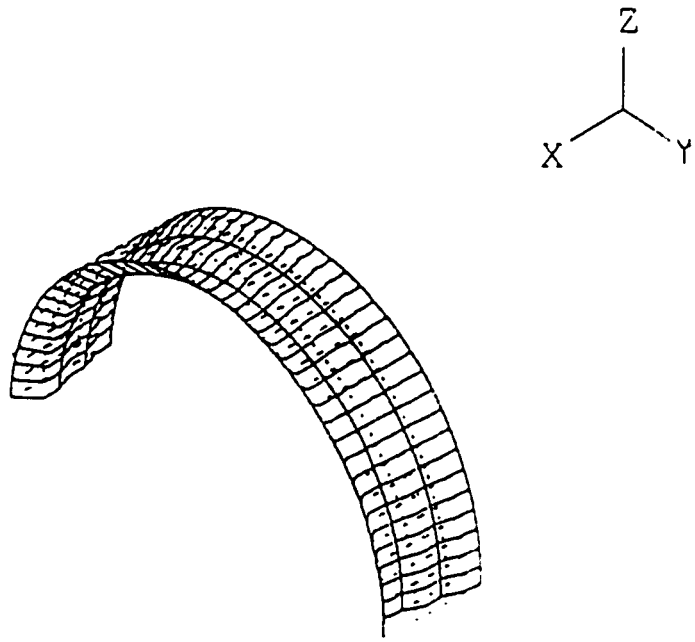

Figure 5.7: Deformed shape of tank#2 (L/r=0.5; load=hydrostatic).

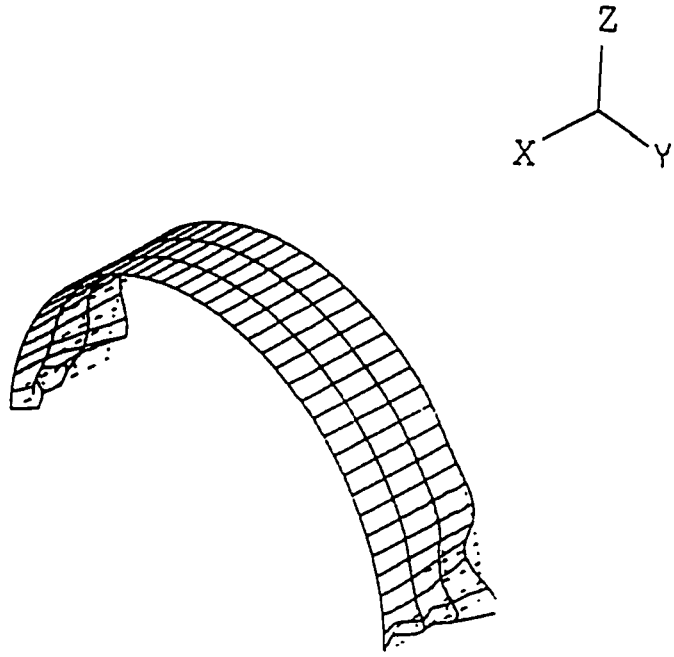

Figure 5.8: First buckling mode of tank#2 (L/r=0.5; load=hydrostatic).

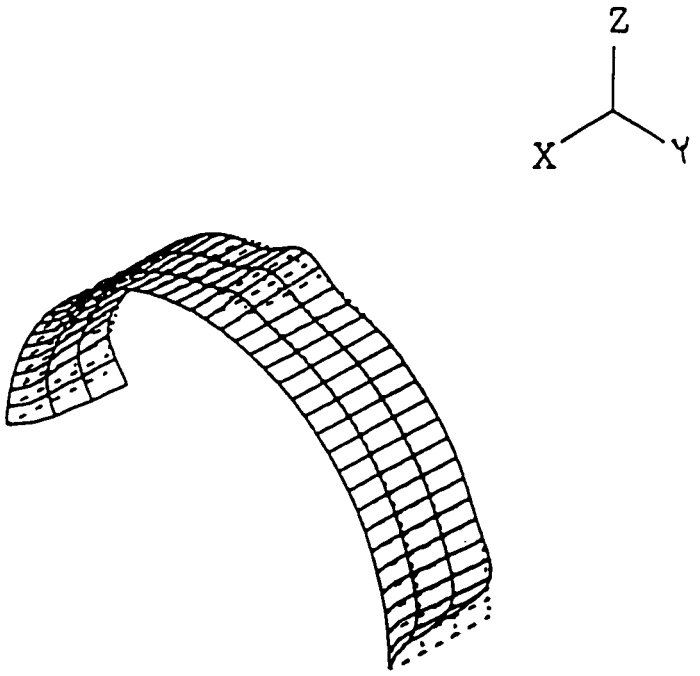

Figure 5.9: Deformed shape of tank#2 (L/r=0.5; load="hydrodynamic").

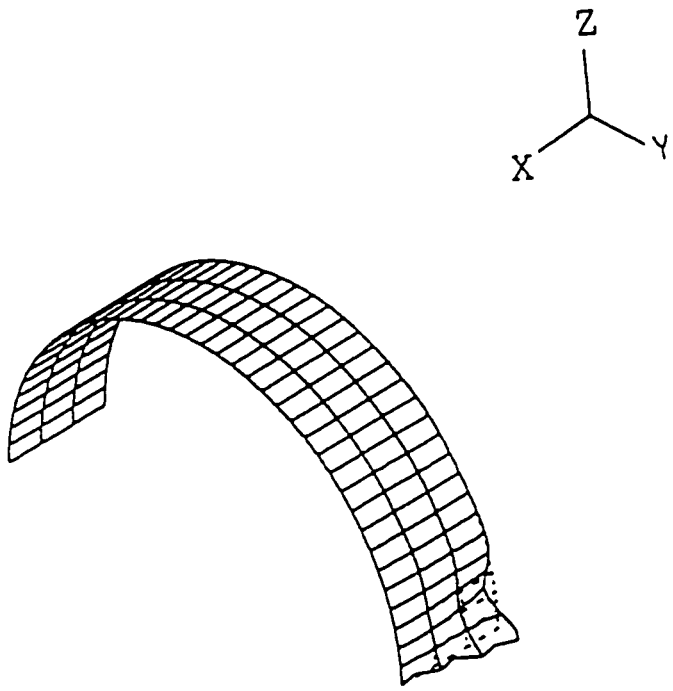

Figure 5.10: First buckling mode of tank#2 (L/r=0.5: load="hydrodynamic").

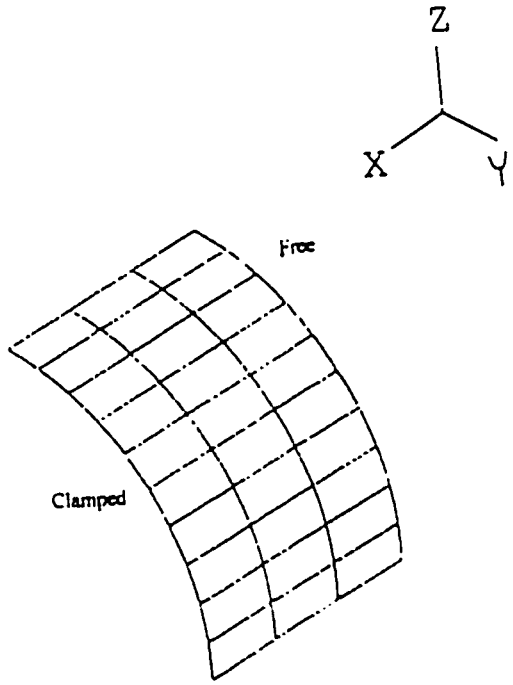

Figure 5.11: Finite element model of tank#1 (L/r=1.0; quarter of the tank is modeled).

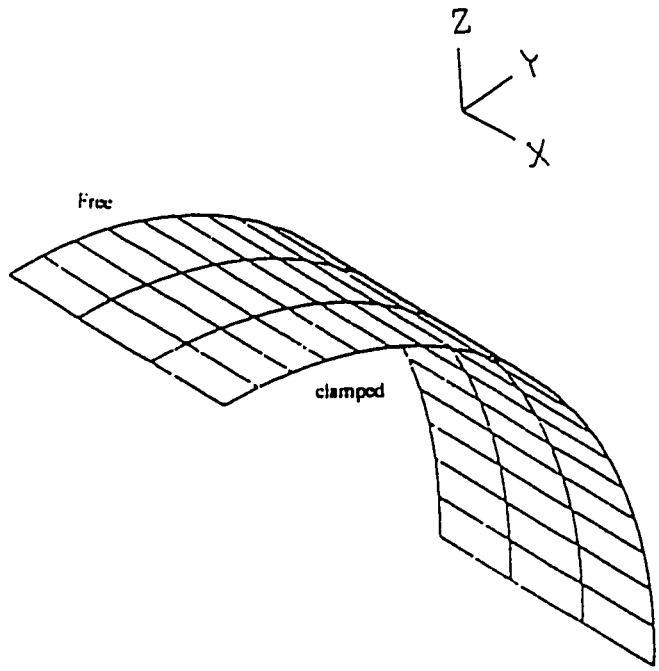

Figure 5.12: Finite element model of tank#2 (L/r=0.5; quarter of the tank is modeled).

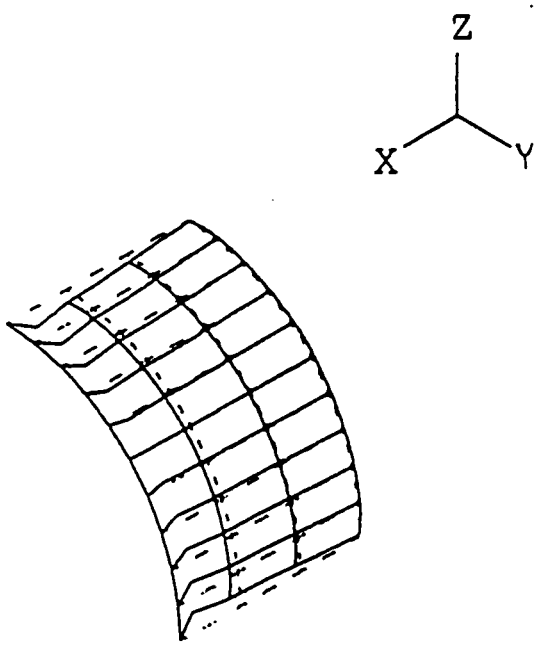

Figure 5.13: Deformed shape of tank#1 (L/r=1.0; load=hydrostatic; quarter of the tank is modeled).

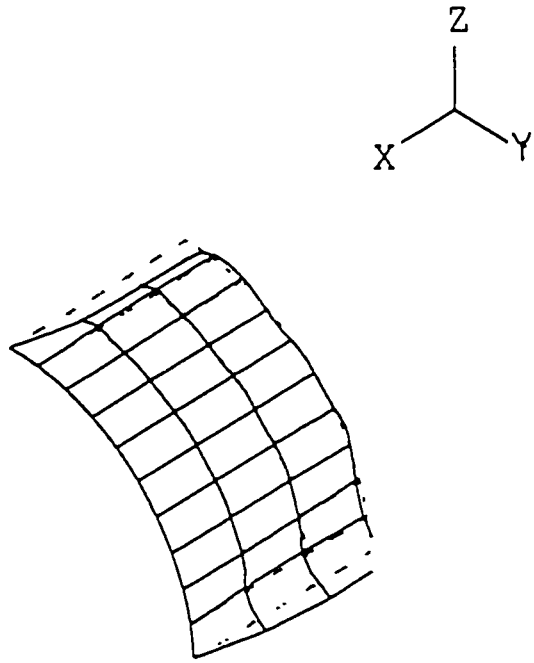

Figure 5.14: First buckling mode of tank#1 (L/r=1.0; load=hydrostatic; quarter of the tank is modeled)

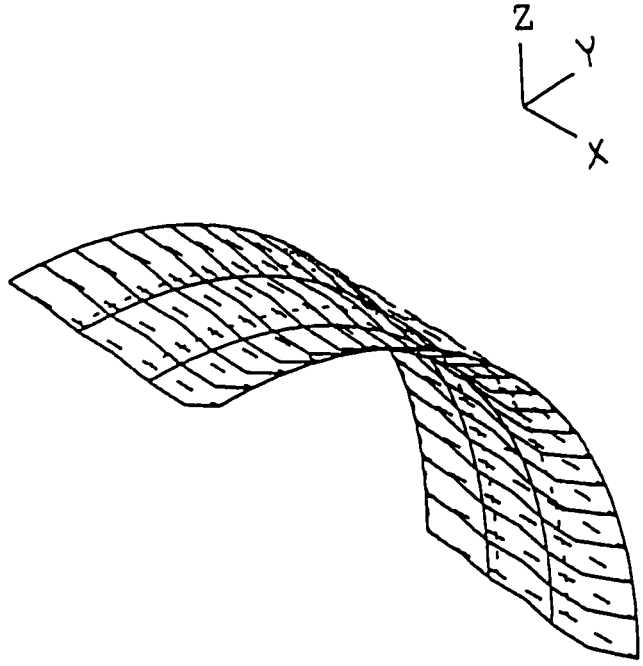

Figure 5.15: Deformed shape of tank#2 (L/r =0.5; load=hydrostatic; quarter of the tank is modeled).

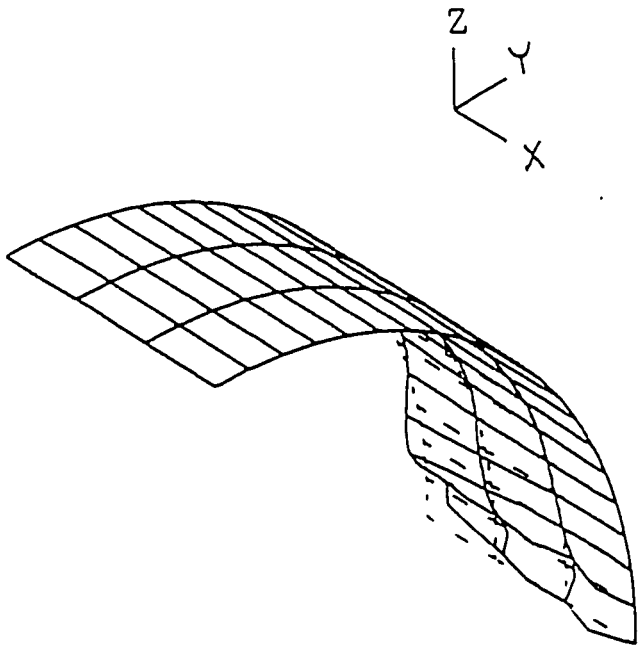

Figure 5.16 First buckling mode of tank#2 (L/r =0.5, load=hydrostatic, quarter of the tank is modeled)

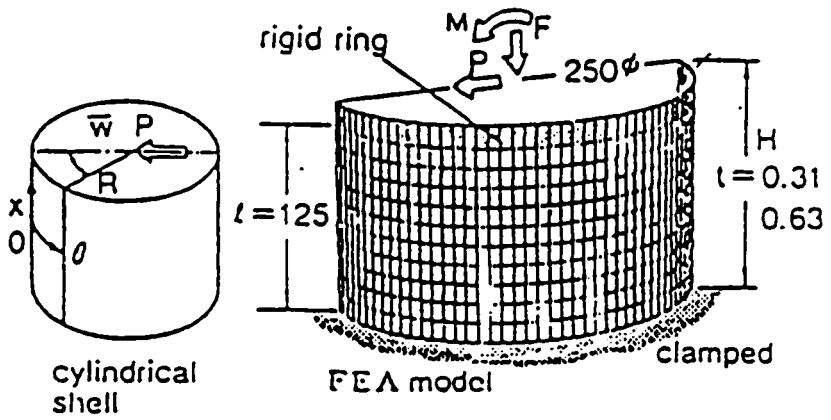

Figure 5.17: Finite element model of cylindrical shell [21].

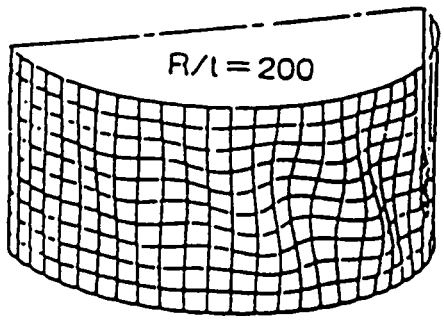

Figure 5.18: Shear mode obtained by FEM [21].

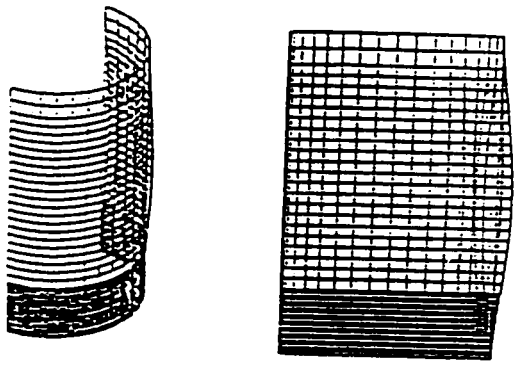

Figure 5.19: Shear buckling mode obtained by applying an external lateral pressure on the tank wall [24].

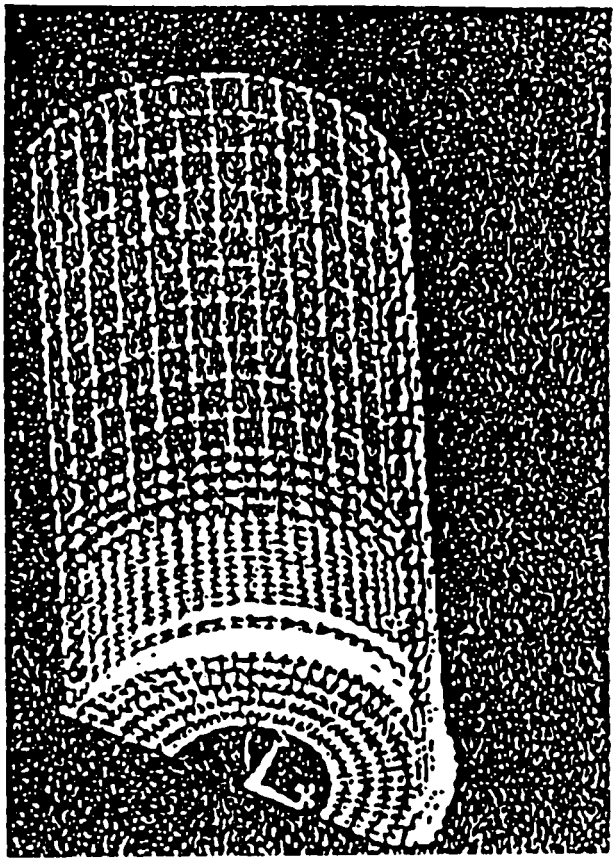

Figure 5.20: Finite element mesh of cylindrical shell [11].

Chapter 6

Practical Application

6.1 Geometry and Loading

Two practical models of broad, anchored, cylindrical tanks are examined in this chapter (Table 6.1). Tanks have been designed according to the standard AWWA D 100-84 [47].

The first tank is a steel model tank, of 16 m in diameter, 8 m high and 0.008 m in thickness. The second tank is also made from steel, with a radius of 15 m, a height of 7.5 m and a thickness of 0.015 m.

Both tanks filled with water are examined in this chapter. Consequently, effects of hydrostatic (internal) and "hydrodynamic" pressures are combined together for each tank. The membrane stresses caused by the "hydrodynamic" pressure are calculated at an acceleration G=0.3g.

The theory, described in the chapters 3 and 4 is applied to these models. The critical load factor is calculated with respect to the "hydrodynamic" pressure because the internal hydrostatic pressure does not cause buckling. Consequently, the sum of terms related to the membrane stresses caused by the internal hydrostatic pressure (Eq. 3.25) should be added to

the [A] matrix as shown in Eq. 3.27 (see Sect. 3.6.2). Results and discussion are presented in the next section.

Table 6.1: Geometry and loading

Tank Number	L(m)	r(m)	t(m)	E(MPa)	ν	Acceleration for "Hydrodynamic" pressure G
1	8.0	8.0	0.008	200000	0.3	0.3g
2	7.5	15	0.015	200000	0.3	0.3g

6.2 Results and Discussion

Analytical results are shown in Table 6.2 for these broad tanks. The critical load factor for tank#1 is equal to 6.4 while for tank#2 it is equal to 3.5. These results mean that both full tanks do not buckle at the above ground acceleration (0.3g). Therefore, the predicted critical ground acceleration for the first tank is equal to 1.9g while for the second it is equal to 1.1g .

Referring to some reports and experimental studies [4,14,46], the author has found that the values obtained for the critical accelerations are reasonable for this type of tank and loading. In the experimental study conducted by Niwa and Clough [14], some anchored tanks, filled with water, were tested on the University of California shaking table under a combination of horizontal and vertical accelerations. The motions were applied first with quite small peak accelerations, and the intensity was increased gradually in successive tests until damage was observed. Critical accelerations in the horizontal and vertical directions were found around

0.95g and 0.4g respectively. Therefore, the critical horizontal accelerations obtained in this section appear reasonable.

Lau et al. [4] have reported some observations regarding the effects of the 1989 Loma Prieta earthquake on some anchored tanks. The accelerations in the horizontal and vertical directions were recorded as 0.7g and 0.5g respectively. Only some of the anchored tanks suffered earthquake damage. This means that the average value for the critical horizontal acceleration is estimated to be at least equal to 1.0g (if the vertical acceleration is not considered).

Shih and Babcock [46] have studied experimentally the buckling of anchored oil storage model tanks (IP) under horizontal acceleration. The ground motion is simulated using three types of excitation. The acceleration spectrum of the base excitation varied between 0.5g and 5.0g. Most of the tanks, subjected to a base excitation less than 0.9g, did not buckle.

In fact, the analyst would expect to obtain by using an approximate static approach a higher critical acceleration than the one describing the real dynamic situation. This observation was reported by Niwa and Clough [14]. The present approximate solution is based on a static approach where several factors (sloshing motion, rocking motion, uplifting,...) were not considered. The consideration of some additional factors (Sect. 6.3) makes the solution more acceptable. Also one should remember that the static approach is only accurate for medium range of frequency [13].

It has been observed that the internal hydrostatic pressure affects strongly the solution. This hydrostatic pressure reduces enormously the effect of the "hydrodynamic" pressure (both tanks, subjected to a ground acceleration G=0.3g , buckle if they are empty). The same

observation was reported by Nagashima et al. [13], who found that the elevation of the water level intensifies dramatically the buckling resistance.

Table 6.2: Analytical results (BUCBAN)

Tank Number	Critical Load Factor (λ)
1	6.4
2	3.5

6.3 Practical Considerations

In the study of buckling of liquid storage tanks under earthquake motion, a number of factors have an influence on the solution. These factors include rocking motion, uplifting, vertical excitation, interaction between the base plate and the tank, interaction between the system and the ground, and sloshing motion. Each of these factors complicates significantly the problem. For this reason researchers have assumed that these factors are independent and have treated each phenomenon separately. But on the other hand, it is the combination of these factors which makes the problem realistic.

In order to understand the effects of the prelisted factors, one can refer to the following studies. The rocking problem has been studied analytically by Veletsos et al. [48] and Ishida et al. [17]. Results have shown that the rocking motion induces an overturning moment in the tank wall. This phenomenon is also related to the tank flexibility.

The uplifting problem has been studied by Malhotra et al. [2] and Ishida et al. [17]. They have reported that base uplifting may "significantly influence the dynamic response of tanks and lead to axial stresses in the tank wall". Axial stresses cause bending buckling (elephant

foot buckling or diamond-shaped buckling) [23]. Numerical methods have been used to solve this problem.

The effects of liquid sloshing have been studied analytically by Haroun et al. [49], Veletsos et al. [50] and Tang [51]. They have found that the sloshing motion increases stresses in the tank wall. The liquid sloshing is represented according to Veletsos by the *convective component*. This component can be neglected for relatively broad tanks [2].

The vertical acceleration has been considered by Veletsos et al. [52]. An analytical solution has been obtained for this problem. Results have shown that the vertical acceleration increases the axial membrane stresses in the tank wall. Therefore, according to Nagashima et al. [13], bending buckling is probable in this case.

Base plate/tank and soil/structure interactions have been analyzed by Auli et al. [18], Wunderlich et al. [25], Lau et al. [47], and Daysal et al. [53]. Numerical analyses (FEM) have been used to solve these problems. Researchers have found that these interactions introduce some nonlinearities in the problem and make the analysis much more complicated. Both interactions affect the dynamic response of the system.

In the present study, only the $\cos\theta$ mode has been considered in the "hydrodynamic" pressure. However, when a geometrically nonlinear theory of shells is used to analyze the dynamic response of broad tanks under earthquake motion, $\cos n\theta$ modes can have a significant influence on the membrane stresses near the base [8].

In future studies, one can consider in addition to the horizontal excitation the effects of the liquid sloshing and vertical acceleration. Attention should be paid to the formulation of the displacement function, which depends strongly on the boundary conditions.

Chapter 7

Conclusions

From the present study the following conclusions can be drawn.

- An approximate solution scheme based on the linearized Donnell's shell theory and Galerkin's approach has been developed to predict by static analysis the smallest buckling load factor of an anchored, full, broad, cylindrical liquid-storage tank under horizontal ground motion.
- Results obtained from this method agree with results from the FEM solution (ADINA). The percentage of error with respect to the FEM solution is around five percent; this is very acceptable for an approximate solution.
- The major advantage of this method is the saving in cost and time.
- This method can be used for different kinds of loading.
- The present study does not consider the prebuckling displacement, the initial bending stresses, the interaction between the base plate and the tank, the presence of an additional vertical acceleration, any possible rocking... . The consideration of some of these factors are recommended for future studies.

Bibliography

[1] Fisher, L., *Theory and Practice of Shell Structures,* Wilhelm Ernst & Sons, Berlin, 1968.

[2] Malhotra, P.K., and Veletsos, A.S. (1994), *Uplifting Response of an Unanchored Liquid Storage Tanks,* **Journal of Structural Engineering,** Vol. 120, No. 12, pp. 3525-3547.

[3] Bushnell, D. (1981), *Buckling of Shells- Pitfall for Designers*, **AIAA J.**, Vol. 19, No.9, pp. 1183-1226.

[4] Lau, D.T., Jablonski, A.M., Law, K.T., Pierre, J.R., and Tang, J.H.K. (1991), *Impact of the 1989 Loma Priesta Earthquake from a Canadian Perspective,* **6th Canadian Conference Earthquake Engineering,** Toronto.

[5] Jennings, P.C. (1971), *Engineering Features of the San Fernando Earthquake,* Report No. EERL 71-02, Caltech, Psadena, Calif., pp. 434-470.

[6] Manos, G.C., and Clough, R.W. (1985), *Tank Damage During the May 1983 Coalinga Earthquake,* **Earthquake Engineering Structural and Dynamics**, Vol. 13, pp. 449-466.

[7] Wozniak, R.S., and Mitchell, W.W. (1978), *Basis of Seismic Response Provisions for Welded Oil Storage Tanks*, **API Convention**, Toronto, Canada

[8] Zhou, M., Zheng, S., and Zhang, W. (1992), *Study on Elephant-Foot Buckling of Broad Liquid Storage Tanks by Nonlinear Theory of Shells*, **Computers and Structures**, Vol. 44, No. 4, pp. 783-788.

[9] Veletsos, A.S., Tang, Y., and Tang, H.T. (1992), *Dynamic Response of Flexibly Supported Liquid-Storage Tanks*, **J. Struct. Engrg.**, ASCE, Vol. 118, No. 1, pp. 264- 283.

[10] Veletsos, A.S., and Tang, Y. (1990), *Soil Structure Interaction Effects for Laterally Excited Liquid-Storage Tanks*, **J. Earthquake Engrg. and Struct. Dynamics**, Vol. 19, pp. 473-496.

[11] Natsiavas, S., Begley, C.J., and Peterson, P.J. (1996), *On the Seismic Behavior of Unanchored Liquid Containers*, **J. of Pressure Vessel Technology**, Vol. 118, pp. 257-264.

[12] Natsiavas, S., and Babcock, C.D. (1987), *Buckling at the Top of a Fluid-Filled Tank During Base Excitation*, **J. of Pressure Vessel Technology**, Vol. 109, pp. 374-380.

[13] Nagashima, H., Kokubo, K., Takayanagi, M., Saitoh, K., and Imaoka, T. (1987), *Experimental Study on the Dynamic Buckling of Cylindrical Tanks*, **JSME Int. J.**, Vol. 30, No. 263, pp. 737-746.

[14] Niwa, A., and Clough, R.W. (1982), *Buckling of Cylindrical Liquid - Storage Tanks Under Earthquake Loading*, **Earthquake Engrg. and Struct. Dynamics**, Vol. 10, pp. 107-122.

[15] Shih, C.F., and Babcock, C.D. (1980), *Scale Model Tests of a Fluid Filled Tank Under Harmonic Excitation*, ASME, Century 2 PVP Conference, 80-C2/PVP-66, San Francisco, California

[16] Manos, G.C. (1991), *Evaluation of the Earthquake Performance of Anchored Wine Tanks During the San Juan, Argentina, 1977 Earthquake*, **Earthquake Engrg. and Struct. Dynamics**, Vol. 20, pp. 1099-1114.

[17] Ishida, K., and Kobayashi, N.(1988), *An Effective Method of Analyzing Rocking Motion*

for Unanchored Cylindrical Tanks Including Uplift, **ASME J. of Pressure Vessel Tech nology**, Vol. 110, pp. 76-87.

[18] Auli, W., Fischer, F.D., and Rammerstofer, F.G. (1985), *Uplifting of Earthquake-Loaded Liquid-Filled Tanks*, 1985 PVP Conference, ASME, New Orleans, La. .

[19] Fujita, K. (1982), *Seismic Response Analysis of a Cylindrical Liquid-Storage Tank on an Elastic Foundation*, **Bulletin of Japan Society of Mechanical Engineers**, Vol. 25, pp. 1977-1984.

[20] Fisher, F.D., and Seeber, R. (1988), *Dynamic Response of Vertically Excited Liquid Storage Tanks Considering Liquid-Soil Interaction*, **Earthquake Engrg. and Struct. Dynamics**, Vol. 16, pp. 329-342.

[21] Kokubo, K., Nagashima, H., Takayanagi, M., and Mochizuki, A. (1993), *Analysis of Shear Buckling of Cylindrical Shells*, **JSME Int. J.**, Vol. 36, No. 3, pp. 259-266.

[22] Liu, W.K., Chen, Y.J., Tsukimori, K., and Uras, R.A. (1991), *Recent Advances in Dynamic Buckling Analysis of Liquid-Filled Shells*, **J. of Pressure Vessel Technology**, Vol. 113, pp. 314-320.

[23] Yi, W., and Natsiavas, S. (1992), *Seismic Response of Unanchored Fluid-Filled Tanks Using Finite Elements*, **J. of Pressure Vessel Technology**, Vol. 114, pp. 74 -79.

[24] Nishino, H., Kawamoto, Y., and Wada, H. (1996), *Dynamic Buckling Behavior of Liquid-Filled Thin-Walled Cylindrical Tanks*, **International Conference on Pressure Vessel Technology**, Vol. 2, pp. 23-34.

[25] Wunderlich, W., Schapertons, B., and Temme, C. (1994), *Dynamic Stability of Non-Linear Shell of Revolution Under Consideration of the Fluid-Soil-Structure Inter-*

action, **Int. J. for Numerical Methods in Engrg**, Vol. 37, pp. 2679-2697.

[26] Lu, S.Y. (1965), *Buckling of Cantilever Cylindrical Shell with a Transverse End Load*, **AIAA J.**, Vol. 3, No. 12, pp. 2350-2351.

[27] Shroeder, V.P. (1972), *Uber Stabilitat Der Querkrafbelasteten Dunnwandigen Kreiszylinderschale*, **AIAA J.**, Vol. 52, pp. 145-148.

[28] Galletly, G.D., and Bachut, J. (1983), *Buckling of a Cantilevered Cylindrical Shell Subjected to a Transverse Shearing Force at its Tip*, **Proceedings of the 3rd International Colloquium on Stability of Metal Structures**, Paris, Preliminary Report, CTICM, pp. 199-204.

[29] Galletly, G.D., and Bachut (1985), *Plastic Buckling of Short Vertical Cylindrical Shells Subjected to Horizontal Edge Shear Loads*, **J. of Pressure Vessel and Technology**, Vol. 107, pp. 101-106.

[30] Lorenz, R. (1911), *Die nichtachsensymmtrische Knickung dünwaniger Hohlzylinder*, **Phys. Z.**, Vol. 13, pp. 241-260

[31] Southwell, R.V. (1913), *On the Collapse of Tubes by External Pressure*, **Phil. Mag.**, Vol. 25, pp. 687-698.

[32] Von Mises, R.(1914), *Der Kritische Aussendruck Zylindrischer Rohre*, **Z. Ver. eutsch. Ing.**, Vol. 58, pp.750-755.

[33] Flügge, W. (1932), *Die Stabilität der Kreiszylinderschale*, **Ing.-Arch.**, Vol. 3, pp.463-506.

[34] Donnell, L.H. (1933), *Stability of Thin-Walled Tubes Under Torsion*, NACA Rep. 479

[35] Brosh, D.O., and Almroth, B.O., *Buckling of Bars, Plates and Shells*, McGraw-Hill, 1975.

[36] Tooth, A.S., and Fernandez, J.A. (1979), *A Study of the Buckling Behavior of Horizontally Supported Thin-Walled Cylindrical Storage Vessels Which Contain Fluid*, in Richards, T.H. and Stanley, P.(Eds.), **Stability Problems in Engineering Structures and Components**, Applied Science publishers, London, pp. 315-340.

[37] Huang, D., Redekop, D., and Xu, B. (1996), *Instability of a Cylindrical Shell Under Three-Point Bending*, **J. Thin-Walled Struct.**, Vol. 26, pp. 105-122.

[38] Yamaki, N., *Elastic Stability of Circular Cylindrical Shells*, North-Holland, Amesterdam, 1984.

[39] Finlayson, B.A., *The Method of Weighted Residuals and Variational Principles*, Academic Press, New York, 1972.

[40] Logan, D.L., *A First Course in the Finite Element Method*, 2nd ed., PWS-KENT, Boston, 1992.

[41] Grossi, R.O., and Laura, P.A.A. (1979), *Transverse Vibrations of Rectangular, Orthotropic Plates with One or Two Free Edges While the Remaining are Elastically Restrained Against Rotation*, **Ocean Engrg.**, Vol. 6, pp. 527-539.

[42] Grossi, R.O. (1987), *A Note on Boundary Conditions in the Study of Beams and Plates*, **J. of Sound and Vibration**, Vol. 124, No. 3, pp. 577-581.

[43] *ADINA- A Finite Element Program for Automatic Dynamic Incremental Nonlinear Analysis*, ADINA Engineering, 1981.

[44] Bathe, K.J., *Finite Element Procedures*, Prentice Hall, New Jersey, 1996.

[45] Redekop, D., and Azar, P. (1989), *Ram Bending of a Cylindrical Pipe in the Elastic Range*, **Int. J. of Pressure Vessel & Piping**, Vol. 37, pp. 307-320

[46] Shih, C.F., and Babcock, C.D. (1987), *Buckling of Oil Storage Tanks in SPPL Tank Farm During the 1979 Imperial Valley Earthquake*, **J. of Pressure Vessel Technology**, Vol. 109, pp. 249-255.

[47] Lau, D. T., and Zeng, X. (1995), *Nonlinear Behavior of Bottom Plate in Cylindrical Liquid Storage Tanks for Seismic Applications*, **Can. J. Civ. Engrg.**, Vol. 22, pp. 180-189.

[48] Veletsos, A.S, and Tang, Y. (1987), *Rocking Response of Liquid Storage Tanks*, **J. of Engrg. Mechanics**, Vol. 113, No. 11, pp. 1774-1761.

[49] Haroun, M. A., and Chen, W. (1988), *Seismic Large Amplitude Liquid Sloshing Theory*, **Proceeding of ASCE Structures Congress**, San Francisco, CA.

[50] Veletsos, A.S., and Shivakumar (1993), *Sloshing Response of Layered Liquids in Rigid Tanks*, **Earthquake Engrg. and Struct. Dynamics**, Vol. 22, pp. 801-821.

[51] Tang, Y. (1993), *Dynamic Response of Tank Containing Two Liquids*, **J. of Engrg. Mechanics**, Vol. 119, pp. 531-548.

[52] Veletsos, A.S., and Tang, Y. (1986), *Dynamics of Vertically Excited Liquids Storage Tanks*, **J. of Struct. Engrg.**, Vol. 112, pp. 1228-1246.

[53] Dayshal, H., and Nash, W.A. (1984), *Soil-Structure Interaction Effects on the Seismic Behavior of Cylindrical Liquid Storage Tanks*, **Proceedings, 8th World Conference**

on Earthquake Engineering, San Francisco, CA, Vol. 7, pp. 445-452.

[54] Lundquist, E.E. (1935), **NACA Tech.**, Note, No. 523.

[55] Flügge, W., *Stresses in Shells*, Second Edition, NewYork, Berlin, 1973.

[56] Shaaban, S.H., and Nash, W.A.(1976), *Finite Element Analysis of a Seismically Excited Cylindrical Storage Tank*, University of Massachusetts, Report No.GI 39644-3, Amherst Massachussetts.

[57] Haroun, M.A. (1980), *Dynamic Analyses of Liquid Storage Tanks*, Ph.D. thesis, Report No. EERL 80-04, Caltech, Pasadena, California.

[58] Manos, G.C., and Clough, R.W. (1982), *Further Study of the Earthquake Response of a Broad Cylindrical Liquid-Storage Tank Model*, Report No. UCB/EERC-89/07, Earthquake Engineering Research Center, University of California, Berkeley, California.

[59] Shih, C.F. (1981), *Failure of Liquid Storage Tanks Due to Earthquake Excitation*, Earthquake Engineering Research Laboratories, Caltech, Report No. EERL 81-04, Psadena, California.

[60] Paul, S. and Weingarten, V.I. (1961), *On the Buckling of Circular Cylindrical Shells Under Pure Bending*, **J. Appl. Mech.**, Vol. 28, pp.112-116.

[61] Calladine, C.R., *Theory of Shell Structures*, Cambridge University Press, 1983.

[62] Axelrad, E.L., *Theory of Flexible Shells*, North Holland, 1987.

[63] Narayan, R., *Shell Structures, Stability and Strength*, Elsevier Applied Science Publishers, London, 1985.

[64] Franklin, P., *An Introduction to Fourier Methods and the Laplace Transformation*, Dover Publications Inc., New York, 1958.

[65] Timoshenko, S.P, and Gere, J.M., *Theory of Elastic Stability*, McGraw-Hill, Toronto, 1961.

[66] Niordson, F.I., *Shell Theory*, North-Holland, New York, 1985.

[67] Bazart, Z.P., and Cedolin, L., *Stability of Structures*, Oxford, New York, 1991.

Appendix A

Definitions of terms used in equation (3.25)

$$I_{\hat{n}n} = \int_0^{2\pi} \cos\hat{n}\varphi \cos n\varphi d\varphi$$

$$I'_{\hat{n}n\bar{n}} = \int_0^{2\pi} \cos\hat{n}\varphi \cos(n-\bar{n})\varphi d\varphi$$

$$I''_{\hat{n}n\bar{n}} = \int_0^{2\pi} \cos\hat{n}\varphi \cos(n+\bar{n})\varphi d\varphi$$

$$J_{\hat{m}m} = \int_0^{\frac{L}{r}} \sin\mu_{\hat{m}}\varsigma \sin\mu_m\varsigma d\varsigma$$

$$J_{2\hat{m}m} = \int_0^{\frac{L}{r}} \sin 2\mu_{\hat{m}}\varsigma \sin\mu_m\varsigma d\varsigma$$

$$J_{3\hat{m}m} = \int_0^{\frac{L}{r}} \sin 3\mu_{\hat{m}}\varsigma \sin\mu_m\varsigma d\varsigma$$

$$J_{4\hat{m}m} = \int_0^{\frac{L}{r}} \sin 4\mu_{\hat{m}}\varsigma \sin\mu_m\varsigma d\varsigma$$

$$S_{\hat{m}} = \sin\frac{\hat{m}\pi}{2}$$

$$J_m = \int_0^{\frac{L}{r}} \sin\mu_m\varsigma d\varsigma$$

$$J_{\hat{m}2m} = \int_0^{\frac{L}{r}} \sin\mu_{\hat{m}}\varsigma \sin 2\mu_m\varsigma d\varsigma$$

$$J_{2\hat{m}2m} = \int_0^{\frac{L}{r_p}} \sin 2\mu_{\hat{m}}\varsigma \sin 2\mu_m \varsigma d\varsigma$$

$$J_{3\hat{m}2m} = \int_0^{\frac{L}{r_p}} \sin 3\mu_{\hat{m}}\varsigma \sin 2\mu_m \varsigma d\varsigma$$

$$J_{4\hat{m}2m} = \int_0^{\frac{L}{r_p}} \sin 4\mu_{\hat{m}}\varsigma \sin 2\mu_m \varsigma d\varsigma$$

$$J_{2m} = \int_0^{\frac{L}{r_p}} \sin 2\mu_m \varsigma d\varsigma$$

$$J_{\hat{m}3m} = \int_0^{\frac{L}{r_p}} \sin \mu_{\hat{m}}\varsigma \sin 3\mu_m \varsigma d\varsigma$$

$$J_{2\hat{m}3m} = \int_0^{\frac{L}{r_p}} \sin 2\mu_{\hat{m}}\varsigma \sin 3\mu_m \varsigma d\varsigma$$

$$J_{3\hat{m}3m} = \int_0^{\frac{L}{r_p}} \sin 3\mu_{\hat{m}}\varsigma \sin 3\mu_m \varsigma d\varsigma$$

$$J_{4\hat{m}3m} = \int_0^{\frac{L}{r_p}} \sin 4\mu_{\hat{m}}\varsigma \sin 3\mu_m \varsigma d\varsigma$$

$$J_{3m} = \int_0^{\frac{L}{r_p}} \sin 3\mu_m \varsigma d\varsigma$$

$$J_{\hat{m}4m} = \int_0^{\frac{L}{r_p}} \sin \mu_{\hat{m}}\varsigma \sin 4\mu_m \varsigma d\varsigma$$

$$J_{2\hat{m}4m} = \int_0^{\frac{L}{r_p}} \sin 2\mu_{\hat{m}}\varsigma \sin 4\mu_m \varsigma d\varsigma$$

$$J_{3\hat{m}4m} = \int_0^{\frac{L}{r}} \sin 3\mu_{\hat{m}}\varsigma \sin 4\mu_m \varsigma d\varsigma$$

$$J_{4\hat{m}4m} = \int_0^{\frac{L}{r}} \sin 4\mu_{\hat{m}}\varsigma \sin 4\mu_m \varsigma d\varsigma$$

$$J_{4m} = \int_0^{\frac{L}{r}} \sin 4\mu_m \varsigma d\varsigma$$

$$J_{\hat{m}} = \int_0^{\frac{L}{r}} \sin \mu_{\hat{m}}\varsigma d\varsigma$$

$$J_{2\hat{m}} = \int_0^{\frac{L}{r}} \sin 2\mu_{\hat{m}}\varsigma d\varsigma$$

$$J_{3\hat{m}} = \int_0^{\frac{L}{r}} \sin 3\mu_{\hat{m}}\varsigma d\varsigma$$

$$J_{4\hat{m}} = \int_0^{\frac{L}{r}} \sin 4\mu_{\hat{m}}\varsigma d\varsigma$$

$$\text{Xi} = \int_0^{\frac{L}{r}} d\varsigma$$

$$J'_{\hat{m}m\bar{m}} = \int_0^{\frac{L}{r}} \sin \mu_{\hat{m}}\varsigma \cos(\mu_{\bar{m}} - \mu_m)\varsigma d\varsigma$$

$$J''_{\hat{m}m\bar{m}} = \int_0^{\frac{L}{r}} \sin \mu_{\hat{m}}\varsigma \cos(\mu_{\bar{m}} + \mu_m)\varsigma d\varsigma$$

$$J'_{2\hat{m}m\bar{m}} = \int_0^{\frac{L}{r}} \sin 2\mu_{\hat{m}}\varsigma \cos(\mu_{\bar{m}} - \mu_m)\varsigma d\varsigma$$

$$J''_{2\hat{m}m\bar{m}} = \int_0^{\frac{L}{r}} \sin 2\mu_{\hat{m}}\varsigma \cos(\mu_{\bar{m}} + \mu_m)\varsigma d\varsigma$$

$$J'_{3\hat{m}m\bar{m}} = \int_0^{\frac{L}{r}} \sin 3\mu_{\hat{m}}\varsigma \cos(\mu_{\bar{m}} - \mu_m)\varsigma d\varsigma$$

$$J''_{3\hat{m}m\bar{m}} = \int_0^{\frac{L}{r}} \sin 3\mu_{\hat{m}}\varsigma \cos(\mu_{\bar{m}} + \mu_m)\varsigma d\varsigma$$

$$J'_{4\hat{m}m\bar{m}} = \int_0^{\frac{L}{r}} \sin 4\mu_{\hat{m}}\varsigma \cos(\mu_{\bar{m}} - \mu_m)\varsigma d\varsigma$$

$$J''_{4\hat{m}m\bar{m}} = \int_0^{\frac{L}{r}} \sin 4\mu_{\hat{m}}\varsigma \cos(\mu_{\bar{m}} + \mu_m)\varsigma d\varsigma$$

$$J'_{m\bar{m}} = \int_0^{\frac{L}{r}} \cos(\mu_{\bar{m}} - \mu_m)\varsigma d\varsigma$$

$$J''_{m\bar{m}} = \int_0^{\frac{L}{r}} \cos(\mu_{\bar{m}} + \mu_m)\varsigma d\varsigma$$

$$J'_{\hat{m}2m\bar{m}} = \int_0^{\frac{L}{r}} \sin\mu_{\hat{m}}\varsigma \cos(\mu_{\bar{m}} - 2\mu_m)\varsigma d\varsigma$$

$$J''_{\hat{m}2m\bar{m}} = \int_0^{\frac{L}{r}} \sin\mu_{\hat{m}}\varsigma \cos(\mu_{\bar{m}} + 2\mu_m)\varsigma d\varsigma$$

$$J'_{2\hat{m}2m\bar{m}} = \int_0^{\frac{L}{r}} \sin 2\mu_{\hat{m}}\varsigma \cos(\mu_{\bar{m}} - 2\mu_m)\varsigma d\varsigma$$

$$J''_{2\hat{m}2m\bar{m}} = \int_0^{\frac{L}{r}} \sin 2\mu_{\hat{m}}\varsigma \cos(\mu_{\bar{m}} + 2\mu_m)\varsigma d\varsigma$$

$$J'_{3\hat{m}2m\bar{m}} = \int_0^{\frac{L}{r}} \sin 3\mu_{\hat{m}}\varsigma \cos(\mu_{\bar{m}} - 2\mu_m)\varsigma d\varsigma$$

$$J''_{3\hat{m}2m\bar{m}} = \int_0^{\frac{L}{r}} \sin 3\mu_{\hat{m}}\varsigma \cos(\mu_{\bar{m}} + 2\mu_m)\varsigma d\varsigma$$

$$J'_{4\hat{m}2m\bar{m}} = \int_0^{\frac{L}{r}} \sin 4\mu_{\hat{m}}\varsigma \cos(\mu_{\bar{m}} - 2\mu_m)\varsigma d\varsigma$$

$$J''_{4\hat{m}2m\bar{m}} = \int_0^{\frac{L}{r}} \sin 4\mu_{\hat{m}}\varsigma \cos(\mu_{\bar{m}} + 2\mu_m)\varsigma d\varsigma$$

$$J'_{2m\bar{m}} = \int_0^{\frac{L}{r}} \cos(\mu_{\bar{m}} - 2\mu_m)\varsigma d\varsigma$$

$$J''_{2m\bar{m}} = \int_0^{\frac{L}{r}} \cos(\mu_{\bar{m}} + 2\mu_m)\varsigma d\varsigma$$

$$J'_{\hat{m}3m\bar{m}} = \int_0^{\frac{L}{r}} \sin\mu_{\hat{m}}\varsigma \cos(\mu_{\bar{m}} - 3\mu_m)\varsigma d\varsigma$$

$$J''_{\hat{m}3m\bar{m}} = \int_0^{\frac{L}{r}} \sin\mu_{\hat{m}}\varsigma \cos(\mu_{\bar{m}} + 3\mu_m)\varsigma d\varsigma$$

$$J'_{2\hat{m}3m\bar{m}} = \int_0^{\frac{L}{r}} \sin 2\mu_{\hat{m}}\varsigma \cos(\mu_{\bar{m}} - 3\mu_m)\varsigma d\varsigma$$

$$J''_{2\hat{m}3m\bar{m}} = \int_0^{\frac{L}{r}} \sin 2\mu_{\hat{m}}\varsigma \cos(\mu_{\bar{m}} + 3\mu_m)\varsigma d\varsigma$$

$$J'_{3\hat{m}3m\bar{m}} = \int_0^{\frac{L}{r}} \sin 3\mu_{\hat{m}}\varsigma \cos(\mu_{\bar{m}} - 3\mu_m)\varsigma d\varsigma$$

$$J''_{3\hat{m}3m\bar{m}} = \int_0^{\frac{L}{r}} \sin 3\mu_{\hat{m}}\varsigma \cos(\mu_{\bar{m}} + 3\mu_m)\varsigma d\varsigma$$

$$J'_{4\hat{m}3m\bar{m}} = \int_0^{\frac{L}{r}} \sin 4\mu_{\hat{m}}\varsigma \cos(\mu_{\bar{m}} - 3\mu_m)\varsigma d\varsigma$$

$$J''_{4\hat{m}3m\bar{m}} = \int_0^{\frac{L}{r}} \sin 4\mu_{\hat{m}}\varsigma \cos(\mu_{\bar{m}} + 3\mu_m)\varsigma d\varsigma$$

$$J'_{3m\bar{m}} = \int_0^{\frac{L}{r}} \cos(\mu_{\bar{m}} - 3\mu_m)\varsigma d\varsigma$$

$$J''_{3m\bar{m}} = \int_0^{\frac{L}{r}} \cos(\mu_{\bar{m}} + 3\mu_m)\varsigma d\varsigma$$

$$J'_{\hat{m}4m\bar{m}} = \int_0^{\frac{L}{r}} \sin\mu_{\hat{m}}\varsigma \cos(\mu_{\bar{m}} - 4\mu_m)\varsigma d\varsigma$$

$$J''_{\hat{m}4m\bar{m}} = \int_0^{\frac{L}{r}} \sin\mu_{\hat{m}}\varsigma \cos(\mu_{\bar{m}} + 4\mu_m)\varsigma d\varsigma$$

$$J'_{2\hat{m}4m\bar{m}} = \int_0^{\frac{L}{r}} \sin 2\mu_{\hat{m}}\varsigma \cos(\mu_{\bar{m}} - 4\mu_m)\varsigma d\varsigma$$

$$J''_{2\hat{m}4m\bar{m}} = \int_0^{\frac{L}{r}} \sin 2\mu_{\hat{m}}\varsigma \cos(\mu_{\bar{m}} + 4\mu_m)\varsigma d\varsigma$$

$$J'_{3\hat{m}4m\bar{m}} = \int_0^{\frac{L}{r}} \sin 3\mu_{\hat{m}}\varsigma \cos(\mu_{\bar{m}} - 4\mu_m)\varsigma d\varsigma$$

$$J''_{3\hat{m}4m\bar{m}} = \int_0^{\frac{L}{r}} \sin 3\mu_{\hat{m}}\varsigma \cos(\mu_{\bar{m}} + 4\mu_m)\varsigma d\varsigma$$

$$J'_{4\hat{m}4m\bar{m}} = \int_0^{\frac{L}{r}} \sin 4\mu_{\hat{m}}\varsigma \cos(\mu_{\bar{m}} - 4\mu_m)\varsigma d\varsigma$$

$$J''_{4\hat{m}4m\bar{m}} = \int_0^{\frac{L}{r}} \sin 4\mu_{\hat{m}}\varsigma \cos(\mu_{\bar{m}} + 4\mu_m)\varsigma d\varsigma$$

$$J'_{4m\bar{m}} = \int_0^{\frac{L}{r}} \cos(\mu_{\bar{m}} - 4\mu_m)\varsigma d\varsigma$$

$$J''_{4m\bar{m}} = \int_0^{\frac{L}{r}} \cos(\mu_{\bar{m}} + 4\mu_m)\varsigma d\varsigma$$

$$J_{\hat{m}\bar{m}} = \int_0^{\frac{L}{r}} \sin\mu_{\hat{m}}\varsigma \sin\mu_{\bar{m}}\varsigma d\varsigma$$

$$J_{2\hat{m}\bar{m}} = \int_0^{\frac{L}{r}} \sin 2\mu_{\hat{m}}\varsigma \sin\mu_{\bar{m}}\varsigma d\varsigma$$

$$J_{3\hat{m}\bar{m}} = \int_0^{\frac{L}{r}} \sin 3\mu_{\hat{m}}\varsigma \sin\mu_{\bar{m}}\varsigma d\varsigma$$

$$J_{4\hat{m}\bar{m}} = \int_0^{\frac{L}{r}} \sin 4\mu_{\hat{m}}\varsigma \sin\mu_{\bar{m}}\varsigma d\varsigma$$

$$J_{\bar{m}} = \int_0^{\frac{L}{r}} \sin\mu_{\bar{m}}\varsigma d\varsigma$$

$$K'_{\hat{m}m\bar{m}} = \int_0^{\frac{L}{r}} \sin\mu_{\hat{m}}\varsigma \sin(\mu_{\bar{m}} - \mu_m)\varsigma d\varsigma$$

$$K''_{\hat{m}m\bar{m}} = \int_0^{\frac{L}{r}} \sin\mu_{\hat{m}}\varsigma \sin(\mu_{\bar{m}} + \mu_m)\varsigma d\varsigma$$

$$K'_{2\hat{m}m\bar{m}} = \int_0^{\frac{L}{r}} \sin 2\mu_{\hat{m}}\varsigma \sin(\mu_{\bar{m}} - \mu_m)\varsigma d\varsigma$$

$$K''_{2\hat{m}m\bar{m}} = \int_0^{\frac{L}{r}} \sin 2\mu_{\hat{m}}\varsigma \sin(\mu_{\bar{m}} + \mu_m)\varsigma d\varsigma$$

$$K'_{3\hat{m}m\bar{m}} = \int_0^{\frac{L}{r}} \sin 3\mu_{\hat{m}}\varsigma \sin(\mu_{\bar{m}} - \mu_m)\varsigma d\varsigma$$

$$K''_{3\hat{m}m\bar{m}} = \int_0^{\frac{L}{r}} \sin 3\mu_{\hat{m}}\varsigma \sin(\mu_{\bar{m}} + \mu_m)\varsigma d\varsigma$$

$$K'_{4\hat{m}m\bar{m}} = \int_0^{\frac{L}{r}} \sin 4\mu_{\hat{m}}\varsigma \sin(\mu_{\bar{m}} - \mu_m)\varsigma d\varsigma$$

$$K''_{4\hat{m}m\bar{m}} = \int_0^{\frac{L}{r}} \sin 4\mu_{\hat{m}}\varsigma \sin(\mu_{\bar{m}} + \mu_m)\varsigma d\varsigma$$

$$K'_{m\bar{m}} = \int_0^{\frac{L}{r}} \sin(\mu_{\bar{m}} - \mu_m)\varsigma d\varsigma$$

$$K''_{m\bar{m}} = \int_0^{\frac{L}{r}} \sin(\mu_{\bar{m}} + \mu_m)\varsigma d\varsigma$$

$$K'_{\hat{m}2m\bar{m}} = \int_0^{\frac{L}{r}} \sin \mu_{\hat{m}}\varsigma \sin(\mu_{\bar{m}} - 2\mu_m)\varsigma d\varsigma$$

$$K''_{\hat{m}2m\bar{m}} = \int_0^{\frac{L}{r}} \sin \mu_{\hat{m}}\varsigma \sin(\mu_{\bar{m}} + 2\mu_m)\varsigma d\varsigma$$

$$K'_{2\hat{m}2m\bar{m}} = \int_0^{\frac{L}{r}} \sin 2\mu_{\hat{m}}\varsigma \sin(\mu_{\bar{m}} - 2\mu_m)\varsigma d\varsigma$$

$$K''_{2\hat{m}2m\bar{m}} = \int_0^{\frac{L}{r}} \sin 2\mu_{\hat{m}}\varsigma \sin(\mu_{\bar{m}} + 2\mu_m)\varsigma d\varsigma$$

$$K'_{3\hat{m}2m\bar{m}} = \int_0^{\frac{L}{r}} \sin 3\mu_{\hat{m}}\varsigma \sin(\mu_{\bar{m}} - 2\mu_m)\varsigma d\varsigma$$

$$K''_{3\hat{m}2m\bar{m}} = \int_0^{\frac{L}{r}} \sin 3\mu_{\hat{m}}\varsigma \sin(\mu_{\bar{m}} + 2\mu_m)\varsigma d\varsigma$$

$$K'_{4\hat{m}2m\bar{m}} = \int_0^{\frac{L}{r}} \sin 4\mu_{\hat{m}}\varsigma \sin(\mu_{\bar{m}} - 2\mu_m)\varsigma d\varsigma$$

$$K''_{4\hat{m}2m\bar{m}} = \int_0^{\frac{L}{r}} \sin 4\mu_{\hat{m}}\varsigma \sin(\mu_{\bar{m}} + 2\mu_m)\varsigma d\varsigma$$

$$K'_{2m\bar{m}} = \int_0^{\frac{L}{r}} \sin(\mu_{\bar{m}} - 2\mu_m)\varsigma d\varsigma$$

$$K''_{2m\bar{m}} = \int_0^{\frac{L}{r}} \sin(\mu_{\bar{m}} + 2\mu_m)\varsigma d\varsigma$$

$$K'_{\hat{m}3m\bar{m}} = \int_0^{\frac{L}{r}} \sin\mu_{\hat{m}}\varsigma \sin(\mu_{\bar{m}} - 3\mu_m)\varsigma d\varsigma$$

$$K''_{\hat{m}3m\bar{m}} = \int_0^{\frac{L}{r}} \sin\mu_{\hat{m}}\varsigma \sin(\mu_{\bar{m}} + 3\mu_m)\varsigma d\varsigma$$

$$K'_{2\hat{m}3m\bar{m}} = \int_0^{\frac{L}{r}} \sin 2\mu_{\hat{m}}\varsigma \sin(\mu_{\bar{m}} - 3\mu_m)\varsigma d\varsigma$$

$$K''_{2\hat{m}3m\bar{m}} = \int_0^{\frac{L}{r}} \sin 2\mu_{\hat{m}}\varsigma \sin(\mu_{\bar{m}} + 3\mu_m)\varsigma d\varsigma$$

$$K'_{3\hat{m}3m\bar{m}} = \int_0^{\frac{L}{r}} \sin 3\mu_{\hat{m}}\varsigma \sin(\mu_{\bar{m}} - 3\mu_m)\varsigma d\varsigma$$

$$K''_{3\hat{m}3m\bar{m}} = \int_0^{\frac{L}{r}} \sin 3\mu_{\hat{m}}\varsigma \sin(\mu_{\bar{m}} + 3\mu_m)\varsigma d\varsigma$$

$$K'_{4\hat{m}3m\bar{m}} = \int_0^{\frac{L}{r}} \sin 4\mu_{\hat{m}}\varsigma \sin(\mu_{\bar{m}} - 3\mu_m)\varsigma d\varsigma$$

$$K''_{4\hat{m}3m\bar{m}} = \int_0^{\frac{L}{r}} \sin 4\mu_{\hat{m}}\varsigma \sin(\mu_{\bar{m}} + 3\mu_m)\varsigma d\varsigma$$

$$K'_{3m\bar{m}} = \int_0^{\frac{L}{r}} \sin(\mu_{\bar{m}} - 3\mu_m)\varsigma d\varsigma$$

$$K''_{3m\bar{m}} = \int_0^{\frac{L}{r}} \sin(\mu_{\bar{m}} + 3\mu_m)\varsigma d\varsigma$$

$$K'_{\hat{m}4m\bar{m}} = \int_0^{\frac{L}{r}} \sin\mu_{\hat{m}}\varsigma \sin(\mu_{\bar{m}} - 4\mu_m)\varsigma d\varsigma$$

$$K''_{\hat{m}4m\bar{m}} = \int_0^{\frac{L}{r}} \sin\mu_{\hat{m}}\varsigma \sin(\mu_{\bar{m}} + 4\mu_m)\varsigma d\varsigma$$

$$K'_{2\hat{m}4m\bar{m}} = \int_0^{\frac{L}{r}} \sin 2\mu_{\hat{m}}\varsigma \sin(\mu_{\bar{m}} - 4\mu_m)\varsigma d\varsigma$$

$$K''_{2\hat{m}4m\bar{m}} = \int_0^{\frac{L}{r}} \sin 2\mu_{\hat{m}}\varsigma \sin(\mu_{\bar{m}} + 4\mu_m)\varsigma d\varsigma$$

$$K'_{3\hat{m}4m\bar{m}} = \int_0^{\frac{L}{r}} \sin 3\mu_{\hat{m}}\varsigma \sin(\mu_{\bar{m}} - 4\mu_m)\varsigma d\varsigma$$

$$K''_{3\hat{m}4m\bar{m}} = \int_0^{\frac{L}{r}} \sin 3\mu_{\hat{m}}\varsigma \sin(\mu_{\bar{m}} + 4\mu_m)\varsigma d\varsigma$$

$$K'_{4\hat{m}4m\bar{m}} = \int_0^{\frac{L}{r}} \sin 4\mu_{\hat{m}}\varsigma \sin(\mu_{\bar{m}} - 4\mu_m)\varsigma d\varsigma$$

$$K''_{4\hat{m}4m\bar{m}} = \int_0^{\frac{L}{r}} \sin 4\mu_{\hat{m}}\varsigma \sin(\mu_{\bar{m}} + 4\mu_m)\varsigma d\varsigma$$

$$K'_{4m\bar{m}} = \int_0^{\frac{L}{r}} \sin(\mu_{\bar{m}} - 4\mu_m)\varsigma d\varsigma$$

$$K''_{4m\bar{m}} = \int_0^{\frac{L}{r}} \sin(\mu_{\bar{m}} + 4\mu_m)\varsigma d\varsigma$$

Appendix B

Additional examples of anchored steel tanks are used to verify the theory of Chap. 3. Tanks, described by their aspect ratios (L/r, r/t) are subjected to external hydrostatic pressures. The critical load factor is calculated in each case.

L/r	t/r	BUCBAN	ADINA (quarter of the tank is modeled)	ADINA (half of the tank is modeled)	Percent. of Error w.r.t. FEM Sol.
2.0	0.001	17.02	16.32	16.32	4.2
1.5	0.001	29.85	29.00	29.00	2.9
1.25	0.01	111.64	116.66	116.66	4.3
0.75	0.01	261.91	272.12	272.12	3.8

Appendix C

Computer Program BUCBAN

```
C************************BUCBAN FORTRAN ***********************************

C     LAST MODIFICATION  -  JUNE 25 1997
C     TO STUDY THE  BUCKLING OF  BROAD, ANCHORED LIQUID STORAGE TANKS
C     UNDER HORIZONTAL GROUND MOTION .
C     THE LINEARISED DONNELL'S EQUATIONS ARE USED IN CONJUNCTION WITH
C     GALERKIN'S APPROACH.
C     RESULTED EIGENVALUE PROBLEM IS SOLVED USING THE INVERSE ITERATION METHOD.

      IMPLICIT DOUBLE PRECISION(A-H,O-Z)
      CHARACTER*7 THEO(1)
      COMMON/YY/R,XL,T,E,POI,PI,MINT,MHIM,NHIM,MLOI,MHII,NLOI,NHII,MT,KP
      COMMON/CODE/SAVE(20,3),MSAVE(20,2),NSAVE(4),MZ,NZ,SAVE1(20)
      COMMON/THEORY/IT,ISTAGE
      COMMON/ADD/X1,X2,X3,X4,X5
      DATA THEO/'DONNELL'/

C     MOST IS NUMBER OF SINGLE AXIAL MODE TRIALS - FIRST STAGE
C     MSPACE IS SPACING  BETWEEN AXIAL MODES - FIRST STAGE
C     MADD+1 IS NUMB OF AXIAL MODES IN SOLN  - SECOND STAGE

      DATA MOST/10/, MSPACE/10/, MADD/1/
C     X1,X2,X3,X4 and X5 ARE CONSTANTS FOR THE BUCKLING DISPLACEMENT FUNCTION
C     CHOOSE ANY VALUE FOR X2
      OPEN(UNIT=8,FILE='THESIS')
      IT=1
      CALL INFIX(1)
      WRITE(8,6) THEO(IT)
    6 FORMAT(//' STABILITY ANALYSIS USING: ',A,' THEORY'/)
      MINT=2
      CALL INFIX(2)
C     FIRST STAGE - SINGLE AXIAL MODE IN EACH TRIAL
      ISTAGE=1
      DO 10 MZ=1,MOST
      MLOI=1+(MZ-1)*MSPACE
      MHII=MLOI
      MSAVE(MZ,1)=MLOI
      MSAVE(MZ,2)=MHII
      WRITE(6,999) IT,MZ
  999 FORMAT(' CALCULATION STATUS REPORT - IT = ',I3,' MZ = ',I3)
      CALL COEFFM
      MM=NHII-NLOI+1
      CALL MAITER(MM)
   10 CONTINUE
C     SELECT AXIAL MODE WITH LOWEST CRITICAL LOAD
      HIRAT=99.D9
      MVALUE=999
      DO 20 MZ=1,MOST
      MVAL=1+(MZ-1)*MSPACE
      SAV=ABS(SAVE1(MZ))
      IF(SAV.GT.HIRAT) GO TO 20
      HIRAT=SAV
      MVALUE=MVAL
   20 CONTINUE
C     SECOND STAGE - COMBINATION OF AXIAL MODES
C     START WITH AXIAL MODE HAVING THE LOWEST CRITICAL LOAD
C     MATRIX SIZE IS (MADD+1)*(NHII-NLOI+1)
      ISTAGE=2
      MZ=MOST+1
      MLOI=MVALUE
      MHII=MVALUE+MADD*MINT
      NSAVE(1)=MLOI
      NSAVE(2)=MHII
      NSAVE(3)=NLOI-1
      NSAVE(4)=NHII-1
      CALL COEFFM
      MM=(MADD+1)*(NHII-NLOI+1)
      CALL MAITER(MM)
 1000 CONTINUE
      ROT=R/T
      ELOR=XL/R
      WRITE(8,16) ROT,ELOR,MHIM,NHIM
   16 FORMAT(//' RESULT SUMMARY'/
```

```
     1 ' R/T =', F7.2,' L/R =', F7.2,' MHIM = ',I2,' NHIM = ',I2/
     2                        ' ----------',
     3 '-------------------------------------------------'/
     4 '  MLOI MHII',15X,'DONNELL')
       DO 30 MZ=1,MOST
    30 WRITE(8,26) (MSAVE(MZ,J),J=1,2),SAVE1(MZ)
    26 FORMAT(1X,2I5,8X,D14.4)
       WRITE(8,36)                    SAVE1(MZ)
    36 FORMAT(/'  STAGE 2 RESULTS  ',D14.4)
       WRITE(8,46)  NSAVE(1),NSAVE(2)
    46 FORMAT('  STAGE 2 MLOI,MHII',7X,I3,',',I3)
       WRITE(8,56) NSAVE(3),NSAVE(4)
    56 FORMAT(/'  STA.1,2 NLOI,NHII',7X,I3,',',I3)
   959 CONTINUE
   963 STOP
       END
C*********************************************************************

       SUBROUTINE INFIX(IFUN)
C      INITIALIZE DATA
       IMPLICIT DOUBLE PRECISION(A-H,O-Z)
       COMMON/YY/R,XL,T,E,POI,PI,MINT,MHIM,NHIM,MLOI,MHII,NLOI,NHII,MT,KP
       COMMON/MATRIX/A1(3,61),B1(3,61),C1(3,61),B2(61),ROL,ACC,IND,RLOAD,
      1 G
       COMMON/HHH/AMN(40,40),BMN(40,40),CMN(40,40)
       IF(IFUN.GT.1) GO TO  500
       WRITE(8,6)
     6 FORMAT(/' STABILITY ANALYSIS OF A CYLINDRICAL SHELL ')
       WRITE(8,16) R,XL,T,E,POI
    16 FORMAT(/' SHELL GEOMETRIC AND MATERIAL PROPERTIES '/
      1  1X,' RADIUS           =',E12.5,2X,'MM'/
      2  1X,' LENGTH           =',E12.5,2X,'MM'/
      3  1X,' THICKNESS        =',E12.5,2X,'MM'/
      4  1X,' YOUNGS MODULUS   =',E12.5,2X,'MPA'/
      5  1X,' POISSON RATIO    =',E12.5  /)
       RETURN
C      INITIALISE THE MEMBRANE COEFFTS
       II=0
   500 DO 20 I=1,MHIM,2
       II=II+1
       DO 20 J=1,NHIM+1
       AMN(II,J)=.0D0
       BMN(II,J)=.0D0
    20 CMN(II,J)=.0D0
       CALL LOCLOD
       RETURN
       END
C*********************************************************************

       SUBROUTINE LOCLOD
       IMPLICIT DOUBLE PRECISION (A-H,O-Z)
C      MEMB. SOLUTION USING THE DEFINED WALL PRESSURE BY VELETSOS AND

C      TANG 'SOIL-STRUCTURE INTERACTION EFFECTS..'1990
       COMMON/YY/R,XL,T,E,POI,PI,MINT,MHIM,NHIM,MLOI,MHII,NLOI,NHII,MT,KP
       COMMON/MATRIX/A1(3,61),B1(3,61),C1(3,61),B2(61),ROL,ACC,IND,RLOAD,
      1 G
       COMMON/HHH/AMN(40,40),BMN(40,40),CMN(40,40)
       COMMON/THEORY/IT,ISTAGE
C      IND (INDICE)=1 FOR L/R=.5 AND IND=2 FOR L/R=1.0
       IND=1
       N=2
       NN=1
       MM=0
       DO 10 M=1,MHIM,2
       MM=MM+1
C      ADJUST THE MEMBRANE STRESSSES
       AMN(MM,N)=-1.0D0*A1(IND,M)*4.d0*ROL*G*(XL**2)/(PI**2)
       BMN(MM,NN)=0.0D0*B2(M)*ROL*ACC*R*XL
       BMN(MM,N)=-1.0D0*B1(IND,M)*ROL*G*(R**2)
10     CMN(MM,N)=-1.0D0*C1(IND,M)*2.d0*ROL*R*G*XL/PI
       NLOI=1
       NHII=26
       RETURN
```

```
      END
C*****************************************************************

      SUBROUTINE COEFFM
C     ROUTINE TO SET UP THE STABILITY MATRIX 'AMAT'
      IMPLICIT DOUBLE PRECISION (A-H,O-Z)
      COMMON/YY/R,XL,T,E,POI,PI,MINT,MHIM,NHIM,MLOI,MHII,NLOI,NHII,MT,KP
      COMMON/EEE/SMALL,AA(350,350),BB(350,350),BBB(350),XX(350)
      COMMON/ADD/X1,X2,X3,X4,X5
      PRINT*,'ARE YOU CONSIDERING THE COMBINATION OF BOTH HYDROST. AND'
      PRINT*,'HYDROD. PRESSURES ?. IF YES TYPE 1 IF NO TYPE 0.'
      READ*,SIGN
      PRINT*,'ARE YOU CONSIDERING INTERNAL HYDROSTATIC PRESSURE OR EXT.'
      PRINT*,'ONE?. IF INTERNAL TYPE 0 OTHERWISE TYPE 1'
      READ*,SIGNAL
C     CHOOSE ANY VALUE FOR X2
      X2=10.010D0
      X4=.5D0*X2
C     TAKE A FACTOR OF 1.0675 AND 1.0965 FOR EXT.HYDROSTATIC
C     PRESSURE AND HYDRODYNAMIC PRESSURE RESPECTIVELY.
      X3=(8.d0*X2+64.d0*X4)/28.d0
      X3=1.0965*X3
C     X3=X3*1.0675
      X1=(8.D0*X2+64.D0*X4-27.D0*X3)
      X5=X1-X3
C     EQUIVALENCES   MI,NI  =  MHAT,NHAT;    MJ,NJ  =  M,N
C     COEFFT PLACE MENT HORIZONTAL - ((MLO      (NLO-NHI)         MHI))
      KEQ=0
C     LOOP OVER MHAT TERMS  -  VERTICAL IN MATRIX
      DO 100 MI=MLOI,MHII,2
C     LOOP OVER NHAT TERMS  -  VERTICAL IN MATRIX
      DO 110 NI=NLOI,NHII
      NII=NI-1
      KEQ=KEQ+1
C     LOOP OVER M TERMS     -  HORIZONTAL IN MATRIX
      KCO=0
      DO 120 MJ=MLOI,MHII,2
C     LOOP OVER N TERMS     -  HORIZONTAL IN MATRIX
      DO 130 NJ=NLOI,NHII
      NJJ=NJ-1
      KCO=KCO+1
C     SET COEFFICIENTS FOR THE A AND B MATRICES
      CALL COFL(MI,MJ,NII,NJJ,COF)
      AA(KEQ,KCO)=COF
      CALL COFS(MI,NII,MJ,NJJ,SUM1,SUM2)
      IF((SUM2.EQ.0).AND.(SIGNAL.EQ.0).AND.(SIGN.EQ.0)) THEN
      PRINT*,'INTERNAL HYDROSTATIC PRESSURE DOES NOT CAUSE BUCKLING'
      STOP
      ENDIF
      BB(KEQ,KCO)=SUM2+SIGNAL*SUM1
      AA(KEQ,KCO)=AA(KEQ,KCO)-SUM1*(1-SIGNAL)
  130 CONTINUE
  120 CONTINUE
  110 CONTINUE
  100 CONTINUE
      MT=KEQ
  666 FORMAT(/' AA MATRIX FOR STABILITY ANALYSIS'//)
   66 FORMAT(1X,7D10.2)
 6666 FORMAT(/' BB MATRIX FOR STABILITY ANALYSIS'//)
  667 CONTINUE
      RETURN
      END
C*****************************************************************

      SUBROUTINE COFL(MI,MJ,NI,NJ,COF)
C     ROUTINE TO CALCULATE TERMS FOR THE A MATRIX
      IMPLICIT DOUBLE PRECISION (A-H,O-Z)
      COMMON/YY/R,XL,T,E,POI,PI,MINT,MHIM,NHIM,MLOI,MHII,NLOI,NHII,MT,KP
      COMMON/THEORY/IT,ISTAGE
      COMMON/MATRIX/A1(3,61),B1(3,61),C1(3,61),B2(61),ROL,ACC,IND,RLOAD,
     1 G
      COMMON/ADD/X1,X2,X3,X4,X5
      DIMENSION RLAM(10)
      DO 87 I=1,5
```

```
IF(I.EQ.1) THEN
MI1=MI
MJ1=MJ
SIGN=X1
ENDIF
IF(I.EQ.2) THEN
MI1=2*MI
MJ1=2*MJ
SIGN=-X2
ENDIF
IF(I.EQ.3) THEN
MI1=3*MI
MJ1=3*MJ
SIGN=X3
ENDIF
IF(I.EQ.4) THEN
MI1=4*MI
MJ1=4*MJ
SIGN=-X4
ENDIF
IF(I.EQ.5) THEN
SIGN=-X5*SIN(REAL(MI)*PI/2.D0)
ENDIF
EM=REAL(MJ)
EMI1=REAL(MI1)
EN=REAL(NJ)
AMU=.5D0*EM*PI*R/XL
AMUI=.5D0*EMI1*PI*R/XL
RKMI=-(1.D0/AMUI)*(COS(EMI1*PI/2.D0)-1.D0)
PRL=PI*R/XL
ADD=AMU*AMU+EN*EN
BRAC=ADD**4
BRAC1=(4.D0*AMU*AMU+EN*EN)**4
BRAC2=(16.D0*AMU*AMU+EN*EN)**4
BRAC3=(9.D0*AMU*AMU+EN*EN)**4
IF(NI.NE.NJ) THEN
RINN=0.0
ELSE
RINN=PI
IF(NI.EQ.0) RINN=2*PI
ENDIF
IF(MI1.NE.MJ1) THEN
RJMM=0.0
ELSE
RJMM=.5D0*XL/R
ENDIF
IF(I.EQ.1) THEN
SIN1=SIN((EMI1-2.D0*EM)*PI/2.D0)
SIN2=SIN((EMI1+2.D0*EM)*PI/2.D0)
RJ102=.5D0*((SIN1/(AMUI-2.D0*AMU))-(SIN2/(AMUI+2.D0*AMU)))
SIN3=SIN((EMI1-3.D0*EM)*PI/2.D0)
SIN4=SIN((EMI1+3.D0*EM)*PI/2.D0)
IF(AMUI.EQ.(3*AMU)) THEN
RJ103=.5D0*(XL/R - SIN4/(AMUI+3.D0*AMU))
ELSE
RJ103=.5D0*((SIN3/(AMUI-3.D0*AMU))-(SIN4/(AMUI+3.D0*AMU)))
ENDIF
SIN5=SIN((EMI1-4.D0*EM)*PI/2.D0)
SIN6=SIN((EMI1+4.D0*EM)*PI/2.D0)
RJ104=.5D0*((SIN5/(AMUI-4.D0*AMU))-(SIN6/(AMUI+4.D0*AMU)))
ENDIF
IF(I.EQ.2) THEN
SIN1=SIN((EMI1-EM)*PI/2.D0)
SIN2=SIN((EMI1+EM)*PI/2.D0)
SIN3=SIN((EMI1-4.D0*EM)*PI/2.D0)
SIN4=SIN((EMI1+4.D0*EM)*PI/2.D0)
SIN5=SIN((EMI1-3.D0*EM)*PI/2.D0)
SIN6=SIN((EMI1+3.D0*EM)*PI/2.D0)
RJ201=.5D0*(SIN1/(AMUI-AMU)-SIN2/(AMUI+AMU))
RJ203=.5D0*(SIN5/(AMUI-3.D0*AMU)-SIN6/(AMUI+3.D0*AMU))
RJ204=.5D0*(SIN3/(AMUI-4.D0*AMU)-SIN4/(AMUI+4.D0*AMU))
ENDIF
IF(I.EQ.3) THEN
SIN1=SIN((EMI1-EM)*PI/2.D0)
```

```
      SIN2=SIN((EMI1+EM)*PI/2.D0)
      SIN3=SIN((EMI1-2.D0*EM)*PI/2.D0)
      SIN4=SIN((EMI1+2.D0*EM)*PI/2.D0)
      SIN5=SIN((EMI1-4.D0*EM)*PI/2.D0)
      SIN6=SIN((EMI1+4.D0*EM)*PI/2.D0)
      IF(AMUI.EQ.AMU) THEN
      RJ301=.5D0*(XL/R -SIN2/(AMUI+AMU))
      ELSE
      RJ301=.5D0*(SIN1/(AMUI-AMU)-SIN2/(AMUI+AMU))
      ENDIF
      RJ302=.5D0*(SIN3/(AMUI-2.D0*AMU)-SIN4/(AMUI+2.D0*AMU))
      RJ304=.5D0*(SIN5/(AMUI-4.D0*AMU)-SIN6/(AMUI+4.D0*AMU))
      ENDIF
      IF(I.EQ.4) THEN
      SIN1=SIN((EMI1-EM)*PI/2.D0)
      SIN2=SIN((EMI1+EM)*PI/2.D0)
      SIN3=SIN((EMI1-2.D0*EM)*PI/2.D0)
      SIN4=SIN((EMI1+2.D0*EM)*PI/2.D0)
      SIN5=SIN((EMI1-3.D0*EM)*PI/2.D0)
      SIN6=SIN((EMI1+3.D0*EM)*PI/2.D0)
      RJ401=.5D0*(SIN1/(AMUI-AMU)-SIN2/(AMUI+AMU))
      RJ402=.5D0*(SIN3/(AMUI-2.D0*AMU)-SIN4/(AMUI+2.D0*AMU))
      RJ403=.5D0*(SIN5/(AMUI-3.D0*AMU)-SIN6/(AMUI+3.D0*AMU))
      ENDIF
      DR2=(E*T*T*T/(12.D0*(1.D0-POI*POI)*R*R))
      H1MN=X1*DR2*BRAC+X1*E*T*((AMU)**4)
      H2MN=-DR2*X2*BRAC1-16*X2*E*T*((AMU)**4)
      H3MN=X3*DR2*BRAC3+X3*81.D0*E*T*((AMU)**4)
      H4MN=-X4*DR2*BRAC2-X4*256.D0*E*T*((AMU)**4)
      H5MN=-X5*DR2*((EN)**8)*SIN(EM*PI/2.D0)
      IF(I.EQ.1) THEN
      COF1=SIGN*H1MN*RINN*RJMM+SIGN*H2MN*RINN*RJ102+
     1  SIGN*H3MN*RJ103*RINN+SIGN*H4MN*RJ104*RINN+SIGN*H5MN*RINN*RKMI
      ENDIF
      IF(I.EQ.2) THEN
      COF2=SIGN*H1MN*RJ201*RINN+SIGN*H2MN*RJMM*RINN+
     1  SIGN*H3MN*RJ203*RINN+SIGN*H4MN*RJ204*RINN+SIGN*H5MN*RINN*RKMI
      ENDIF
      IF(I.EQ.3) THEN
      COF3=SIGN*H1MN*RJ301*RINN+SIGN*H2MN*RJ302*RINN+
     1SIGN*RJMM*H3MN*RINN+SIGN*H4MN*RJ304*RINN+SIGN*H5MN*RINN*RKMI
      ENDIF
      IF(I.EQ.4) THEN
      COF4=SIGN*H1MN*RJ401*RINN+SIGN*H2MN*RJ402*RINN+
     1  SIGN*RJMM*H4MN*RINN+SIGN*H5MN*RINN*RKMI+
     1  SIGN*H3MN*RJ403*RINN
      ENDIF
      IF(I.EQ.5) THEN
      RJ001=1/AMU
      RJ002=-(1.D0/(2.D0*AMU))*(COS(EM*PI)-1.D0)
      RJ004=0.0
      RJ003=1.D0/(3.D0*AMU)
      XI=XL/R
      COF5=SIGN*H1MN*RJ001*RINN+SIGN*H2MN*RJ002*RINN+
     1 SIGN*H5MN*XI*RINN+SIGN*H3MN*RINN*RJ003
      ENDIF
 87   CONTINUE
      COF=COF1+COF2+COF3+COF4+COF5
      RETURN
      END
C ***************************************************************************

      SUBROUTINE COFS(MI,NI,MJ,NJ,SUM1,SUM2)
C     ROUTINE TO CALCULATE  TERMS OF THE B MATRIX
      IMPLICIT DOUBLE PRECISION (A-H,O-Z)
      COMMON/YY/R,XL,T,E,POI,PI,MINT,MHIM,NHIM,MLOI,MHII,NLOI,NHII,MT,KP
      COMMON/HHH/AMN(40,40),BMN(40,40),CMN(40,40)
      COMMON/THEORY/IT,ISTAGE
      COMMON/ADD/X1,X2,X3,X4,X5
      DIMENSION SUM1(6),SU(2,6)
      DATA TOL/1.D-05/
      DO 88 I=1,5
      IF(I.EQ.1) THEN
      MI1=MI
```

```
      SIGN=X1
      ENDIF
      IF(I.EQ.2) THEN
      MI1=2*MI
      SIGN=-X2
      ENDIF
      IF(I.EQ.3) THEN
      MI1=3*MI
      SIGN=X3
      ENDIF
      IF(I.EQ.4) THEN
      MI1=4*MI
      SIGN=-X4
      ENDIF
      IF(I.EQ.5) THEN
      SIGN=-X5*SIN(REAL(MI)*PI/2.D0)
      ENDIF
      EM=REAL(MJ)
      AMU=.5D0*EM*PI*R/XL
      AMU2=AMU*AMU
      EN=REAL(NJ)
      EN2=EN*EN
C     SUM CONTRIBUTIONS FROM THE TERMS OF THE MEMBRANE SOUTION
C     VARIATION OF NN=1,1 CORESPONDS TO HYDROSTATIC PRESSURE
C          "     "  NN=2,2      "        " HYDRODYNAMIC PRESSURE
C          "     "  NN=1,2      "        " COMBINATION OF BOTH PRESSURES
      DO 110 NN=1,NHIM+1
      NB=NN-1
      SUM=0.0D0
      MM=0
      DO 100 MB=1,MHIM,2
      CALL JINT(MI1,MJ,MB,ONEJM,TWOJM,ONEJ2M,TWOJ2M,ONEJ3M,TWOJ3M,
     1 ONEJ4M,TWOJ4M,RJMIMB,I)
      CALL KINT(MI1,MJ,MB,ONEKM,TWOKM,ONEK2M,TWOK2M,ONEK3M,TWOK3M,
     1 ONEK4M,TWOK4M,I)
      MM=MM+1
      AMUB=.5D0*REAL(MB)*PI*R/XL
      AMUB2=AMUB*AMUB
      CALL IINT(NI,NJ,NB,ONEI,TWOI)
      ENB=REAL(NB)
      A=AMN(MM,NN)
      B=BMN(MM,NN)
      C=CMN(MM,NN)
      ENMU2C=2.D0*EN*AMU*C
      ENDIF2=(EN-ENB)**2
      ENSUM2=(EN+ENB)**2
      EMDIF2=(AMU-AMUB)**2
      EMSUM2=(AMU+AMUB)**2
      EM2SU2=(2.D0*AMU+AMUB)**2
      EM2DI2=(2.D0*AMU-AMUB)**2
      EM4SU2=(4.D0*AMU+AMUB)**2
      EM4DI2=(4.D0*AMU-AMUB)**2
      EM3SU2=(3.D0*AMU+AMUB)**2
      EM3DI2=(3.D0*AMU-AMUB)**2

      DD1=-X1*(B*EN2+A*AMU2)
      DD2=X2*EN2*B+4.D0*X2*AMU2*A
      DD3=-X3*(EN2*B+9.D0*A*AMU2)
      DD4=X4*EN2*B+16.D0*AMU2*A*X4
      DD5=X5*EN2*SIN(EM*PI/2.D0)*B
      DD6=-2.D0*X1*EN*AMU*C
      DD7=4.D0*X2*EN*AMU*C
      DD8=-6.D0*X3*EN*AMU*C
      DD9=8.D0*X4*EN*AMU*C
      D11=.25D0*DD1*((EMDIF2+ENDIF2)**2)
      D12=.25D0*DD1*((EMDIF2+ENSUM2)**2)
      D13=-.25D0*DD1*((EMSUM2+ENDIF2)**2)
      D14=-.25D0*DD1*((EMSUM2+ENSUM2)**2)
      D21=.25D0*DD2*((EM2DI2+ENDIF2)**2)
      D22=.25D0*DD2*((EM2DI2+ENSUM2)**2)
      D23=-.25D0*DD2*((EM2SU2+ENDIF2)**2)
      D24=-.25D0*DD2*((EM2SU2+ENSUM2)**2)
      D31=.25D0*DD3*((EM3DI2+ENDIF2)**2)
      D32=.25D0*DD3*((EM3DI2+ENSUM2)**2)
```

```
      D33=-.25D0*DD3*((EM3SU2+ENDIF2)**2)
      D34=-.25D0*DD3*((EM3SU2+ENSUM2)**2)
      D41=.25D0*DD4*((EM4DI2+ENDIF2)**2)
      D42=.25D0*DD4*((EM4DI2+ENSUM2)**2)
      D43=-.25D0*DD4*((EM4SU2+ENDIF2)**2)
      D44=-.25D0*DD4*((EM4SU2+ENSUM2)**2)
      D51=.5D0*DD5*((AMUB2+ENDIF2)**2)
      D52=.5D0*DD5*((AMUB2+ENSUM2)**2)
      D61=.25D0*DD6*((EMDIF2+ENDIF2)**2)
      D62=-.25D0*DD6*((EMDIF2+ENSUM2)**2)
      D63=.25D0*DD6*((EMSUM2+ENDIF2)**2)
      D64=-.25D0*DD6*((EMSUM2+ENSUM2)**2)
      D71=.25D0*DD7*((EM2DI2+ENDIF2)**2)
      D72=-.25D0*DD7*((EM2DI2+ENSUM2)**2)
      D73=.25D0*DD7*((EM2SU2+ENDIF2)**2)
      D74=-.25D0*DD7*((EM2SU2+ENSUM2)**2)
      D81=.25D0*DD8*((EM3DI2+ENDIF2)**2)
      D82=-.25D0*DD8*((EM3DI2+ENSUM2)**2)
      D83=.25D0*DD8*((EM3SU2+ENDIF2)**2)
      D84=-.25D0*DD8*((EM3SU2+ENSUM2)**2)
      D91=.25D0*DD9*((EM4DI2+ENDIF2)**2)
      D92=-.25D0*DD9*((EM4DI2+ENSUM2)**2)
      D93=.25D0*DD9*((EM4SU2+ENDIF2)**2)
      D94=-.25D0*DD9*((EM4SU2+ENSUM2)**2)
   99 SUM=SUM+D11*ONEI*ONEJM+D12*ONEJM*TWOI+D13*TWOJM*ONEI+
     1 D14*TWOJM*TWOI+D21*ONEJ2M*ONEI+D22*ONEJ2M*TWOI+D23*TWOJ2M*ONEI+
     1 D24*TWOJ2M*TWOI+D41*ONEJ4M*ONEI+D42*ONEJ4M*TWOI+D43*TWOJ4M*ONEI+
     1 D44*TWOJ4M*TWOI+D51*RJMIMB*ONEI+D52*RJMIMB*TWOI+D31*ONEI*ONEJ3M+
     1 D32*ONEJ3M*TWOI+D33*TWOJ3M*ONEI+D34*TWOJ3M*TWOI+D61*ONEKM*ONEI+
     1 D62*ONEKM*TWOI+D63*TWOKM*ONEI+D64*TWOKM*TWOI+D71*ONEK2M*ONEI+
     1 D72*ONEK2M*TWOI+D73*TWOK2M*ONEI+D74*TWOK2M*TWOI+D91*ONEK4M*ONEI+
     1 D92*ONEK4M*TWOI+D93*TWOK4M*ONEI+D94*TWOK4M*TWOI+D81*ONEK3M*ONEI+
     1 D82*ONEK3M*TWOI+D83*TWOK3M*ONEI+D84*TWOK3M*TWOI
  100 CONTINUE
      SU(NN,I)=SUM
  110 CONTINUE
      SU(1,I)=SU(1,I)*SIGN
      SU(2,I)=SU(2,I)*SIGN
88    CONTINUE
      SUM1=SU(1,1)+SU(1,2)+SU(1,3)+SU(1,4)+SU(1,5)
      SUM2=SU(2,1)+SU(2,2)+SU(2,3)+SU(2,4)+SU(2,5)
      RETURN
      END

C*********************************************************************

      SUBROUTINE IINT(NI,NJ,NB,ONEI,TWOI)
C     COMPUTE THE TWO I INTEGRALS FOR THIS NI NJ NB SET
      IMPLICIT DOUBLE PRECISION(A-H,O-Z)
      COMMON/YY/R,XL,T,E,POI,PI,MINT,MHIM,NHIM,MLOI,MHII,NLOI,NHII,MT,KP
      DO 100 L=1,2
      NCOM=NJ-NB
      IF(L.EQ.2) NCOM=NJ+NB
      NSUM1=NI-NCOM
      NSUM2=NI+NCOM
      VAL=PI
      IF(NSUM1.EQ.0.AND.NSUM2.EQ.0) VAL=2.D0*PI
      IF(NSUM1.NE.0.AND.NSUM2.NE.0) VAL=.0D0
      IF(L.EQ.1) ONEI=VAL
  100 IF(L.EQ.2) TWOI=VAL
      RETURN
      END
C*********************************************************************

      SUBROUTINE JINT(MI,MJ,MB,ONEJM,TWOJM,ONEJ2M,TWOJ2M,ONEJ3M,TWOJ3M,
     1 ONEJ4M,TWOJ4M,RJMIMB,J)
C     COMPUTE THE TWO J INTEGRALS FOR THIS MI MJ MB SET
      IMPLICIT DOUBLE PRECISION(A-H,O-Z)
      COMMON/YY/R,XL,T,E,POI,PI,MINT,MHIM,NHIM,MLOI,MHII,NLOI,NHII,MT,KP
      DIMENSION VAL(2,4)
      AMUH=.5D0*REAL(MI)*PI*R/XL
      AMUH2=AMUH**2
      AMUB=.5D0*REAL(MB)*PI*R/XL
      DO 100 L=1,2
```

```
      DO 99 I=1,4
      IF(I.EQ.1) MJ1=MJ
      IF(I.EQ.2) MJ1=2*MJ
      IF(I.EQ.3) MJ1=3*MJ
      IF(I.EQ.4) MJ1=4*MJ
      RMCOM=MB-MJ1
      MCOM=MB-MJ1
      IF(L.EQ.2)THEN

      MCOM=MJ1+MB
      ENDIF
      AMUO=.5D0*REAL(MCOM)*PI*R/XL
      AMUO2=AMUO**2
      DIFMU=AMUH-AMUO
      SUMMU=AMUH+AMUO
      M1=MI-MCOM
      M2=MI+MCOM
      IF(J.LE.4) THEN
      IF((M1.NE.0).AND.(M2.NE.0)) THEN
      VAL(L,I)=.5D0*((-COS(M1*PI/2.D0)+1.D0)/DIFMU -
     1        (COS(M2*PI/2.D0)-1.D0)/SUMMU)
      ENDIF
      IF((M1.EQ.0).AND.(M2.NE.0)) THEN
      VAL(L,I)=-.5D0*(COS(M2*PI/2.D0)-1.D0)/SUMMU
      ENDIF
      IF((M1.NE.0).AND.(M2.EQ.0)) THEN
      VAL(L,I)=-.5D0*(COS(M1*PI/2.D0)-1.D0)/DIFMU
      ENDIF
      IF((M1.EQ.0).AND.(M2.EQ.0)) THEN
      VAL(L,I)=.0
      ENDIF
      ENDIF
      IF(J.EQ.5) THEN
      IF(MB.NE.MJ1) VAL(L,I)=SIN(REAL(MCOM)*PI/2.D0)/AMUO
      IF(MB.EQ.MJ1) VAL(L,I)=XL/R
      ENDIF
99    CONTINUE
100   CONTINUE
      ONEJM=VAL(1,1)
      ONEJ2M=VAL(1,2)
      ONEJ4M=VAL(1,4)
      ONEJ3M=VAL(1,3)
      TWOJM=VAL(2,1)
      TWOJ2M=VAL(2,2)
      TWOJ4M=VAL(2,4)
      TWOJ3M=VAL(2,3)
      IF(J.LE.4) THEN
      SIN1=SIN((MI-MB)*PI/2.D0)
      SIN2=SIN((MI+MB)*PI/2.D0)
      IF(MI.NE.MB) THEN
      RJMIMB=.5D0*(SIN1/(AMUH-AMUB) -SIN2/(AMUH+AMUB))
      ELSE
      RJMIMB=.5D0*(XL/R - SIN2/(AMUH+AMUB))
      ENDIF
      ENDIF
      IF(J.EQ.5) RJMIMB=1.D0/AMUB
      RETURN
      END
C*********************************************************************

      SUBROUTINE KINT(MI,MJ,MB,ONEKM,TWOKM,ONEK2M,TWOK2M,ONEK3M,TWOK3M,
     1  ONEK4M,TWOK4M,J)
C     COMPUTE THE K INTEGRAL FOR MI,MJ AND MB SET
      IMPLICIT DOUBLE PRECISION(A-H,O-Z)
      COMMON/YY/R,XL,T,E,POI,PI,MINT,MHIM,NHIM,MLOI,MHII,NLOI,NHII,MT,KP
      DIMENSION VAL(3,4)
      AMUH=.5D0*REAL(MI)*PI*R/XL
      DO 100 L=1,2
      DO 99  I=1,4
      IF(I.EQ.1) MJ1=MJ
      IF(I.EQ.2) MJ1=2*MJ
      IF(I.EQ.3) MJ1=3*MJ
      IF(I.EQ.4) MJ1=4*MJ
      RMCOM=MB-MJ1
```

```
      MCOM=MB-MJ1
      IF(L.EQ.2) THEN
      MCOM=MB+MJ1
      ENDIF
      AMUO=.5D0*REAL(MCOM)*PI*R/XL
      DIFMU=AMUH-AMUO
      SUMMU=AMUH+AMUO
      M1=MI-MCOM
      M2=MCOM+MI
      IF(J.LE.4) THEN
      IF((M1.NE.0).AND.(M2.NE.0)) THEN
      VAL(L,I)=.5D0*(SIN(M1*PI/2.D0)/DIFMU- SIN(M2*PI/2.D0)/SUMMU)
      ENDIF
      IF((M1.EQ.0).AND.(M2.NE.0)) THEN
      VAL(L,I)=.5D0*(XL/R - SIN(M2*PI/2.D0)/SUMMU)
      ENDIF
      IF((M1.NE.0).AND.(M2.EQ.0)) THEN
      VAL(L,I)=.5D0*(SIN(M1*PI/2.D0)/DIFMU- XL/R)
      ENDIF
      IF((M1.EQ.0).AND.(M2.EQ.0)) THEN
      VAL(L,I)=.0
      ENDIF
      ENDIF
      IF(J.EQ.5) THEN
      IF(MB.EQ.MJ1) VAL(L,I)=0.0
      IF(MB.NE.MJ1) VAL(L,I)=-(COS(REAL(MCOM)*PI/2.D0)-1)/AMUO
      ENDIF
99    CONTINUE
100   CONTINUE
      ONERM=VAL(1,1)
      ONER2M=VAL(1,2)
      ONER4M=VAL(1,4)
      ON2R3M=VAL(1,3)
      TWORM=VAL(2,1)
      TWOR2M=VAL(2,2)
      TWOR4M=VAL(2,4)
      TWOR3M=VAL(2,3)
      RETURN
      END
C*********************************************************************

      SUBROUTINE MAITER(N)
C     TO FIND THE SMALLEST EIGENVALUE USING MATRIX ITERATION METHOD
C     ERF. BATH       AX=LBX (GENERAL EIGENVALUE PROBLEM)
      IMPLICIT DOUBLE PRECISION(A-H,O-Z)
      COMMON/CODE/SAVE(20,3),MSAVE(20,2),NSAVE(4),MZ,NZ,SAVE1(20)
      COMMON/EEE/SMALL,AA(350,350),BB(350,350),BBB(350),XX(350)
      COMMON/ADD/X1,X2,X3,X4,X5,SIGNAL
      DIMENSION BBBO(350)
      DATA TOL/1.D-09/,NTRIAL/6000/
      MT=N
      ALAMO=.0D0
C     ASSUME MODE SHAPE FOR FIRST TRIAL
      XX(1)=1.D0
      DO 10 I=2,MT
10    XX(I)=XX(I-1)*.9D0
C     DO MATRIX REDUCTION OF THE AMAT MATRIX
      CALL MATRED(MT)
C     SET UP THE RHS
      DO 20 I=1,MT
      BBB(I)=.0D0
      DO 21 J=1,MT
21    BBB(I)=BBB(I)+BB(I,J)*XX(J)
20    BBBO(I)=BBB(I)
C     LOOP OVER MAXIMUM OF NTRIAL ITERATIONS
C     SOLVE FOR THE XK+1 USING BAKSUB
      K=1
970   CALL BAKSUB(MT)
C     SET UP THE YK+1- NONFACTORED
      DO 30  I=1,MT
      BBB(I)=.0D0
      DO 31 J=1,MT
31    BBB(I)=BBB(I)+BB(I,J)*XX(J)
30    CONTINUE
```

```
C     TOP AND BOTTOM OF RO FRACTION
      TOP=.0
      BOT=.0
      DO 40 I=1,MT
      TOP=TOP+XX(I)*BBBO(I)
   40 BOT=BOT+XX(I)*BBB(I)
      ALAM=TOP/BOT
C     CONVEGENCE CHECK
      DIF=DABS(ALAM-ALAMO)
      RAT=DIF/DABS(ALAM)
      IF(RAT.LE.TOL) THEN
      GO TO 900
      ENDIF
      K=K+1
      ALAMO=ALAM
      ROOT=DSQRT(DABS(BOT))
C     SET UP THE YK+1 - FACTOED
      DO 50 I=1,MT
      BBB(I)=BBB(I)/ROOT
   50 BBBO(I)=BBB(I)
      IF(K.LT.NTRIAL) THEN
      GO TO 970
      ENDIF
  900 CONTINUE
      SAVE1(MZ)=DABS(ALAM)
C     COMPUTE EIGENVECTOR
      SUM=.0D0
      DO 60 I=1,MT
   60 SUM=SUM+XX(I)*BBB(I)
      ROOT=DSQRT(DABS(SUM))
      DO 70 I=1,MT
   70 XX(I)=XX(I)/ROOT
      WRITE(8,16) K,ALAM
   16 FORMAT(/' MAITER SOL.',
     1  'ITERATIONS=',I5,'ROOT=',D11.4)
      WRITE(8,26) (XX(J),J=1,MT)
   26 FORMAT(' EIGENVECTOR'/(1X,6D11.3))
      RETURN
      END
C*****************************************************************

      SUBROUTINE MATRED(NEQ)
      IMPLICIT DOUBLE PRECISION(A-H,O-Z)
      COMMON/EEE/SMALL,AA(350,350),BB(350,350),BBB(350),XX(350)
      NEQM1=NEQ-1
C     MUST ZERO COLUMNS 1 TO IHI-1
      DO 10 IC=1,NEQM1
      D=1.D0/AA(IC,IC)
      ICP1=IC+1
C     MUST CHANGE EQUATIONS IC+1 TO NEQM1
      DO 11 IE=ICP1,NEQ
      FAC=AA(IE,IC)*D
C     MUST CHANGE COEFFICIENTS FROM IC+1 TO NEQM1
      DO 12 JC=ICP1,NEQ
   12 AA(IE,JC)=AA(IE,JC)-FAC*AA(IC,JC)
C     STORE FACTOR IN LOWER LEFT TRIANGLE
   11 AA(IE,IC)=FAC
   10 CONTINUE
      RETURN
      END
C*****************************************************************

      SUBROUTINE BAKSUB(NEQ)
      IMPLICIT DOUBLE PRECISION(A-H,O-Z)
      COMMON/EEE/SMALL,AA(350,350),BB(350,350),BBB(350),XX(350)
C     CHANGE RHS AS FOR A MATRIX REDUCTION
      NEQM1=NEQ-1
      DO 10 IC=1,NEQM1
      ICP1=IC+1
C     MUST CHANGE EQUATIONS IC+1 TO NEQM1
      DO 11 IE=ICP1,NEQ
      FAC=AA(IE,IC)
C     CHANGE RHS
   11 BBB(IE)=BBB(IE)-FAC*BBB(IC)
```

```
   10  CONTINUE
C      BACKSUBSTITUTION OF LAST UNKNOWNS
       XX(NEQ)=BBB(NEQ)/AA(NEQ,NEQ)
C      BACKSUBSTITUTION TO DETERMINE NEQM1 UNKNOWNS
       DO 20 I=1,NEQM1
       IE=NEQ-I
       JLO=NEQ-I
       SUM=.0
C      SUM THE QUANTITY TO BE DEDUCTED TERMS I TO NEQ
       DO 21 K=1,I
       JC=JLO+K
   21  SUM=SUM+AA(IE,JC)*XX(JC)
   20  XX(IE)=(BBB(IE)-SUM)/AA(IE,JLO)
       RETURN
       END

C-----------------------------------------------------------------------
       BLOCK DATA
       IMPLICIT DOUBLE PRECISION(A-H,O-Z)
       COMMON/YY/R,XL,T,E,POI,PI,MINT,MHIM,NHIM,MLOI,MHII,NLOI,NHII,MT,KP
       COMMON/MATRIX/A1(3,61),B1(3,61),C1(3,61),B2(61),ROL,ACC,IND,RLOAD,
      1 G
C      R=RADIUS  XL=LENGTH  T=THICKNESS  E=YOUNGS MOD  POI=POISS RATIO
       DATA R/15000.D0/, XL/7500.0D0/,T/15.00D0/,E/.207D06/,POI/.3D0/
       DATA MINT/0/, MHIM/59/,NHIM/1/,MLOI/0/,MHII/0/,NLOI/ 0/,NHII/ 0/
       DATA PI/3.1415926535897930/, MT/0/, KP/1/,ROL/1.0D-06/
       DATA ACC/9.81D0/, G/2.9430D0/
       END
```

IMAGE EVALUATION
TEST TARGET (QA-3)

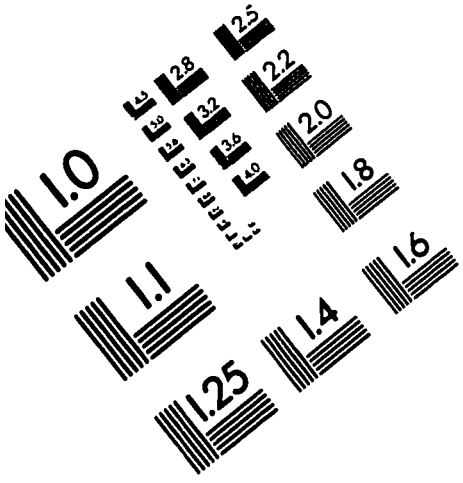

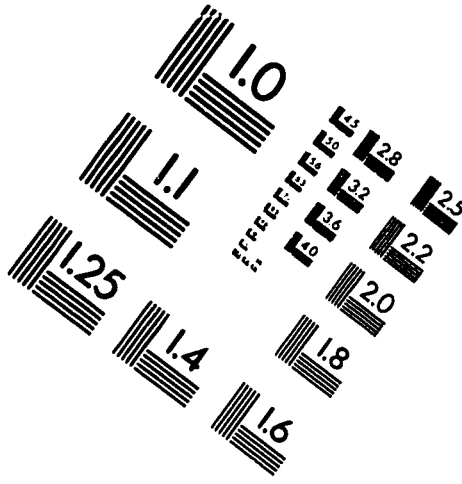

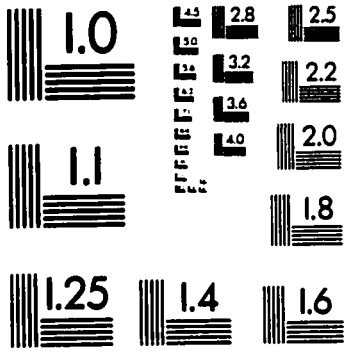

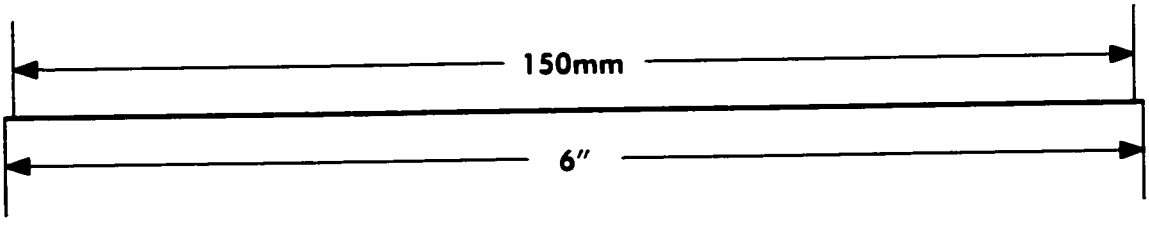

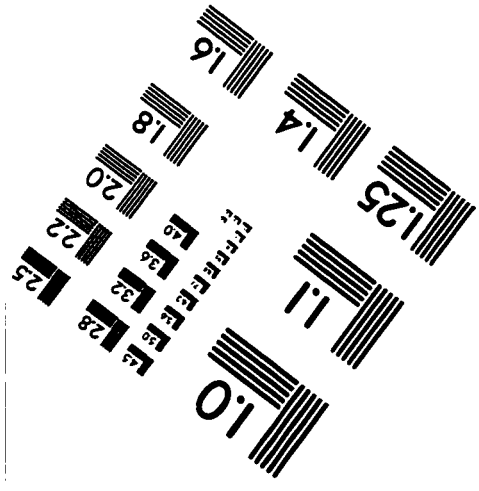

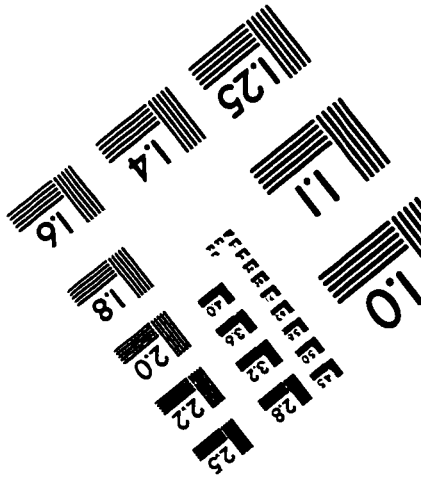

APPLIED IMAGE, Inc
1653 East Main Street
Rochester, NY 14609 USA
Phone: 716/482-0300
Fax: 716/288-5989